The dynamic status of actin in the regulation of environmental sensing and homeostatic control in *Saccharomyces cerevisiae*

Thesis submitted to the University of Kent for the Degree of Ph.D. in Biochemistry

Daniel G. J. Smethurst

Declaration

No part of this thesis has been submitted in support of an application for any degree or other qualification of the University of Kent, or any other University or Institution of learning

Daniel G.J. Smethurst
September 2014

Abstract

Actin is a highly conserved protein in eukaryotes which forms dynamic cytoskeletal structures. Rapid remodeling of actin filaments is important for the regulation of a broad range of critical cellular processes. The cytoskeleton is acutely responsive to stresses and there are multiple interactions between actin and signaling pathways, positioning it centrally to a cells ability to adapt and respond to their environment. Here I provide further evidence that a dynamic actin cytoskeleton regulates processes including endocytosis, mitochondrial respiration, and signal transduction. Results presented here show that actin is embedded in the signaling networks which control the responses to environmental change. Change to the dynamic status of actin modulates the activity of the transcription factor Ste12p which regulates both the mating and filamentous/invasive growth responses. The activity of these pathways are linked to cortical patch organisation, and our data suggests that there is crosstalk between multiple pathways. I propose that the links between actin dynamics and environmental sensing pathways leave it well positioned for a role as a biosensor. Actin dynamics is altered by changes in internal or external conditions, leading to adapted of cellular responses which may provide a protective function for a population.

Abbreviations

5-FOA	5-fluoroorotic acid
ADP	adenosine diphosphate
AntA	antimycin A
ATP	adenosine triphosphate
cAMP	cyclic adenosine monophosphate
CFW	calcofluor white
CP	capping protein
CWI	cell wall integrity
dH20	deionised water
DNA	deoxyribonucleic acid
DSB	double strand breaks
ECL	enhanced chemiluminescence
EDTA	ethylenediaminetetraacetic acid
ER	endoplasmic reticulum
ETS	electron transport system
F-actin	filamentous actin
FCCP	carbonylcyanide p-trifluoromethoxyphenylhydrazone
FRE	filamentation response element
G-actin	globular actin
GEF	guanosine exchange factor
GFP	green fluorescent protein
GO	gene ontology
GPCR	G-protein coupled receptor
GTP	guanosine triphosphate
HOG	high osmolarity glycerol
HR	homologous recombination
HU	hydroxyurea
Lat-A	latrunculin A
LiAc	lithium acetate
MAPK	mitogen activated protein kinase
MAPKK	mitogen activated protein kinase kinase
MAPKKK	mitogen activated protein kinase kinase kinase
MM	mismatch
MMS	methyl methanesulfonate
NADH	nicotinamide adenine dinucleotide
NES	nuclear export signal
NLS	nuclear localisation signal
OD	optical density
ORF	open reading frame
PAGE	polyacrylamide gel electrophoresis
PAK	p21-activated kinase
PCR	polymerase chain reaction
Pi	inorganic phosphate
PKA	protein kinase A
PM	perfect match
PRE	pheromone response element
PTP	permeability transition pore
PVDF	polyvinylidene fluoride

RMA	robust multi-array analysis
RNA	ribonucleic acid
ROS	reactive oxygen species
rpm	rotations per minute
SDS	sodium dodecyl sulfate
TCS	TEA consensus sequence
TE	Tris EDTA
TET	triethyltin
TF	transcription factor
TOR	target of rapamycin
UV	ultraviolet
WT	wild-type
YPD	yeast extract dextrose
YPG	yeast extract glycerol
YT	yeast extract tryptone

Table of Contents

1 Introduction

1.1 *S. cerevisiae* as a model organism

Since the advent of molecular biology in the mid-20th century, the budding yeast *Saccharomyces cerevisiae* has been used as an experimental model organism. In 1996 it was the first eukaryotic organism to have its entire annotated genomic sequence published (Goffeau et al. 1996) and has emerged as a cornerstone of research into the *Eukarya*. This is in part due to the relative ease with which the organism can be genetically manipulated, along with the conservation of many genes and pathways between yeast and man. To exploit this, the systematic deletion of almost every open reading frame (ORF) in the genome was carried out to create genome wide mutant libraries, which have been highly valuable in elucidating the functions of gene products. With these tools, high-throughput genome-scale experiments became possible, revealing connections between genes through phenotypic comparison and allowing identification of the components of cellular processes (Scherens & Goffeau 2004).

1.2 Actin and the cytoskeleton

Actin is a globular protein that polymerises to form filaments which compose the cytoskeleton, and is found in almost every eukaryotic cell. Over 70 years of research in the field has made it clear that eukaryotic cells possess a highly conserved and fundamental ability to assemble and remodel the actin cytoskeleton. The organisation of actin structures is tightly coordinated to regulate crucial cellular processes including endocytosis, cell morphology, and cell polarity. Multiple signaling

pathways and interacting proteins regulate the remodeling of actin structures, many of which are also highly conserved across eukaryotes. (Moseley & Goode 2006)

The actin protein was first isolated from muscle tissue extract by Straub in 1942 (Straub 1942), who subsequently reported that monomeric actin contained adenosine triphosphate (ATP) which was hydrolysed to adenosine diphosphate (ADP) and inorganic phosphate (Pi) during polymerisation. The amino acid sequence of rabbit muscle actin was determined in 1973, and it was noticed that the 374 residue sequence contained very few substitutions when compared to incomplete actin sequences from other organisms available at the time (Elzinga et al. 1973).

In 1990 atomic structure of actin monomers was published and was also used along with electron cryo-microscopy data to construct a model for the structure of actin filaments (Holmes et al. 1990; Kabsch et al. 1990). The monomer, termed G-actin, was shown to consist of two domains separated by the nucleotide binding site. Each of these domains is commonly further divided into two subdomains. The molecular structure of rabbit muscle G-actin is shown in Figure 1 with the residues of the nucleotide binding site highlighted. The ATPase binding pocket structure is also found in the functionally distinct hexokinase and Hsp70 families (Bork et al. 1992). This three-dimensional structure connects nucleotide binding to an interdomain hinge which is important for actin exchanging between the monomeric and polymerised states.

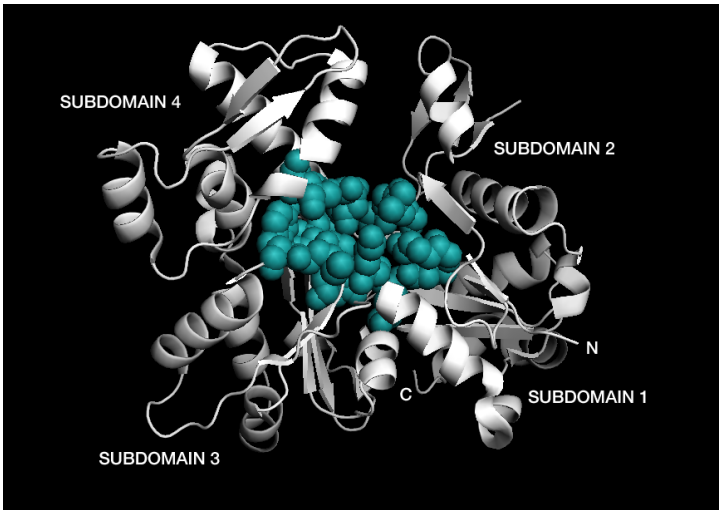

Figure 1. Structure of rabbit muscle G-actin. Residues involved in ATP binding site as reported by Kabsch et al. 1990 are highlighted as blue spheres and the C and N termini are labeled.

The filament, or F-actin, was found to consist of two intertwined helical strands which completed a full turn every 72nm, or 28 subunits. The nucleotide binding site cleft faces towards one end of the filament in all polymerised subunits, and this is termed the (-) end, or pointed end, while the opposite end is the (+) end, or barbed end. The (+) end is the major site of the addition of further subunits, while depolymerisation occurs preferentially at the (-) end.

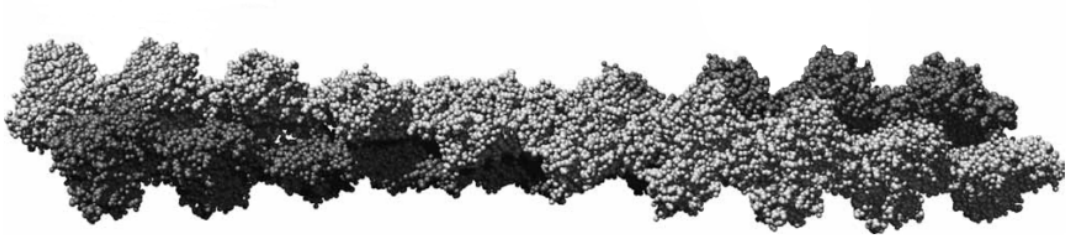

Figure 2. Model of F-actin structure modified from Spink et al. 2008 and based on electron cryo-microscopy data from Holmes et al. 2003.

1.2.1 Yeast actin

S. cerevisiae has served as a valuable model for research into the regulation of actin dynamics due to the conservation of the involved components and mechanisms. Prior to the sequencing of the yeast genome, much had already been discovered about the yeast cytoskeleton. Yeast actin was first isolated in 1980 (Water et al. 1980) and the single gene encoding it, *ACT1*, was identified two years later (Shortle et al. 1982).

The single actin gene in budding yeast made it possible for genetic approaches to be used to analyse the protein. The human genome encodes six isoforms of actin on separate genes, all of which share at least 93% amino acid identity with one another (Perrin & Ervasti 2010). The budding yeast actin isoform is 86% identical to human α smooth muscle actin (Amberg 1998).

1.2.1.1 Actin filament dynamics

The actin networks in eukaryotic cells are highly dynamic, with filaments being constantly disassembled and assembled from the available monomer pool (Pollard & Borisy 2003). The dynamic nature of actin filaments allows the generation of force in the direction of filament growth. The process is dependent on the binding and hydrolysis of ATP, and requires numerous conserved regulatory proteins.

The term treadmilling is applied to the cyclical process by which actin monomers are added to filaments, ATP is hydrolysed, and the monomers exit the filament and become reactivated by nucleotide exchange. Free monomers with ATP bound are added to the (+) end of a filament, and ATP is then hydrolysed to ADP and P_i. The phosphate is released while ADP remains bound to actin. ADP-bound actin can then

be released from the filament and undergoes nucleotide exchange, becoming re-charged with ATP, following which it is available to polymerise again (Moseley & Goode 2006). Treadmilling is fundamental to both the polarity of filaments and their dynamic properties.

De novo filament assembly begins with the formation of an actin trimer (Sept & McCammon 2001), and occurs at targeted sites driven by nucleation factors. In yeast these include the Arp2/3 complex and the formins Bnr1p and Bnr2p (Pollard 2007). The formins are responsible for de novo filament nucleation, where as the Arp2/3 complex nucleates filament assembly as branches on existing filaments.

Filament dynamics depends on both polymerisation and depolymerisation, and each of these processes involves multiple interacting proteins. Depolymerisation of filaments and filament severing are important to return monomers to the cytoplasmic pool. The essential gene *COF1* encodes the yeast cofilin protein, an actin-depolymerisation factor (ADF) which promotes filament depolymerisation and severing. Cofilin binds along filaments and to actin-ADP monomers (dos Remedios et al. 2003). An ADF homology (ADFH) domain is found in other actin regulators, the Arp2/3 regulator Abp1p (Quintero-monzon et al. 2005), and twinfilin, which consists of two adjacent ADFH domains (Lappalainen et al. 1998; Goode et al. 1998). The filament disassembly carried out by cofilin can be assisted by Srv2p, also referred to as the cyclase-associated protein (CAP), as well as Aip1p (Chaudhry et al. 2013).

Other interacting proteins associate with monomeric actin to facilitate a dynamic cytoskeleton. The role of profilin is in cooperation with that of cofilin in promoting filament turnover. While cofilin acts at the (-) end removing actin-ADP monomers, profilin binds monomeric actin near the interdomain hinge region and promotes the exchange of ADP to ATP, inhibits the hydrolysis of ATP and assists in adding monomers to the (+) end of filaments (Wolven et al. 2000; dos Remedios et al. 2003; Haarer et al. 1990)

Twinfilin interacts with ADP-actin monomers and is localised to sites of rapid turnover, including the cortical patches. Deletion of twinfilin results in uncontrolled filament growth suggesting that this protein has a role in sequestering monomers. It interacts with both cofilin and profilin, and requires the capping protein (CP) for localisation to the (+) end of filaments (Palmgren et al. 2001). CP is a heterodimer consisting of Cap1p and Cap2p, and also localises to cortical patches (Kim et al. 2004). Twinfilin also has a filament severing function which is inhibited by its interaction with capping protein (Moseley et al. 2006). CP appears to act to stabilise the entire filament by its interaction with the (+) end, preventing both dissociation and addition of subunits (Moseley & Goode 2006).

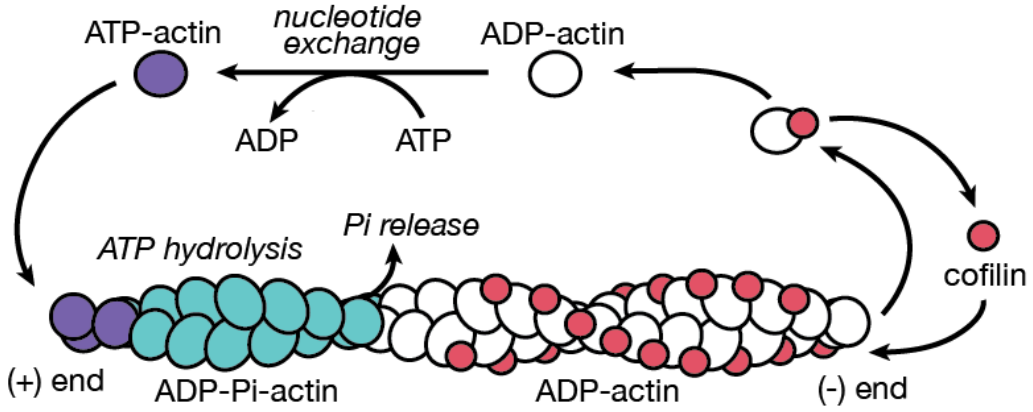

Figure 3. A simplified model of the actin treadmilling cycle. ATP-actin monomers bind at the (+) end of filaments, and subsequently the bound ATP is hydrolysed. The ADP-Pi-actin releases the Pi (inorganic phosphate) and undergoes a conformational change, facilitating an interaction with cofilin and dissociation from the filament at the (-) end. Free ADP-actin undergoes nucleotide exchange and reenters the cycle. Adapted from Moriyama & Yahara 2002.

Several drugs have proved valuable in laboratory studies into actin dynamics. Latrunculin-A (Lat-A) is a drug purified from the Red Sea sponge *Latrunculina magnificans* which interacts with and sequesters free G-actin (Morton et al. 2000). Its interaction with actin monomers depends on an interaction with aspartate 157 (Belmont, Patterson, et al. 1999) and is thought to inhibit nucleotide exchange. This interaction allows Lat-A to be used to effectively prevent filament polymerisation without affecting depolymerisation. Alternatively, cytochalasin-D has been used extensively but the effect is less specific, as it both induces depolymerisation and inhibits polymerisation (Casella et al. 1981).

Phalloidin is a cyclic peptide drug from the *Amanita phalloides* fungus which reduces depolymerisation of actin filaments, stabilising actin structures (Coluccio & Tilney 1984). The binding site consists of the residues glycine 158, aspartate 177 and arginine 179 (Drubin et al. 1993; Belmont, Patterson, et al. 1999). Modified phalloidin with fluorophore labels such as rhodamine are commonly used to visualise

F-actin structures. Jasplakinolide is another a cyclic peptide, isolated from the sea sponge *Jaspis johnstoni*, which stabilises the cytoskeleton. The stabilising effect of jasplakinolide on actin filaments has been reported as being greater than the effect of phalloidin (Visegrády et al. 2004).

1.2.2 Actin structures and functions

The distribution of actin within yeast cells was revealed in fluorescent microscopy studies using both labeled phalloidin and labeled anti-actin antibody (Adams & Pringle 1984; Kilmartin & Adams 1984). The organisation of actin filaments into two higher order structures, the cortical patches and polarised cables, was observed initially. The presence of a third transient higher order actin structure was observed but not definitively identified as the contractile cytokinetic ring for several years (Bi et al. 1998). More recently the presence of actin in the nucleus has been demonstrated, which is thought to consist primarily of G-actin or short oligomers (Olave et al. 2002).

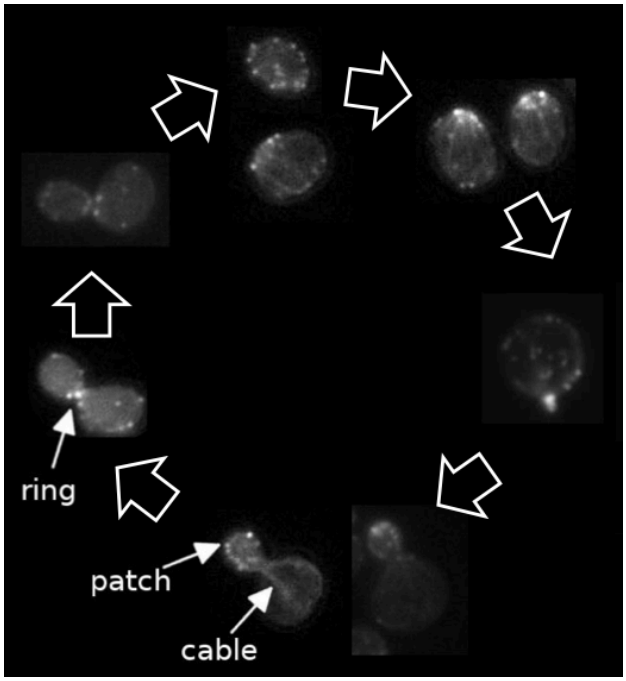

Figure 4. Actin higher order structures in *S. cerevisiae* stained with actin-phalloidin throughout the cell cycle. Cortical patches and cables are seen throughout while the contractile ring forms transiently during cytokinesis.

1.2.2.1 Cortical patches

Cortical patches are networks of branched actin filaments seen as small dots at the cell surface when actin is labeled. The plasma membrane at cortical patches appears as finger-like invaginations surrounded by actin filaments and associated actin regulatory proteins (Mulholland et al. 1999). Patches are motile and cluster at the site where a bud is emerging during cell division. Cortical patch motility is not dependent on actin dynamics, while the roles of the patches in endocytosis are highly dependent upon it (Belmont & Drubin 1998).

The cortical patches are now known to play a major role in endocytic processes. A functional actin cytoskeleton is required for endocytosis as shown in studies using both mutants and drugs which interfere with actin (Ayscough 2000; Wesp et al. 1997). Endocytosis allows the internalisation of external materials, and is also

important in maintaining the plasma membrane environment and recycling of membrane receptors. Cortical actin structures are therefore positioned at the interface between the cell and its immediate environment, and their function is crucial to environmental sensing and cellular responses.

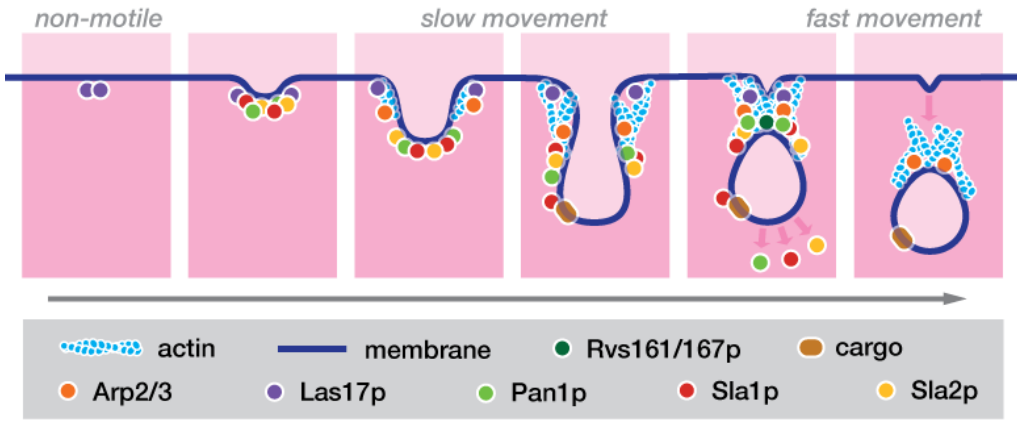

Figure 5. A model of cortical patch development during endocytosis, based on data and models in Kaksonen et al. 2003 and Ayscough 2005. Las17p arrives at the membrane early during patch development, followed by Pan1p, Sla1p and Sla2p. Activated Arp2/3 complex generates a branched actin network which provides the force for invagination. Sla1p interacts with cargo molecules in the membrane. Rvs161p and Rvs167p associate and assist with scission. Pan1p, Sla1p and Sla2p dissociate in the final stages and the new vesicle moves into the cell.

Endocytosis depends on complexes which form sequentially at the cortical patches. Real-time fluorescence microscopy has revealed distinct stages in patch assembly during endocytosis (Ayscough 2005). A simplified model of the patch assembly process is shown in Figure 5. The branched filaments of the cortical patches are under the regulation of the Arp2/3 complex. This complex includes seven highly conserved proteins including Arp2p, Arp3p, and Arc18p, and must be recruited and activated at the patches for actin polymerisation (Winter et al. 1997). Arp2/3 promotes the formation of a branched actin network (Engqvist-Goldstein & Drubin 2003).

The earliest component shown to arrive in the process is Las17p, the yeast homolog of the mammalian Wiskott-Aldrich syndrome protein WASP and a strong Arp2/3p activator (Feliciano & Di Pietro 2012; Ayscough 2005). Las17p localisation to patches depends on verprolin Vrp1p, a homolog of WASP-interacting protein (WIP) (Smith et al. 2001). Following this, Sla1p, Sla2p and Pan1p associate with the patch complex (Tang et al. 2000; Warren et al. 2002; Kaksonen et al. 2003). Abp1 associates with assembling patches as an actin network forms, and the patches become motile (Wesp et al. 1997). Actin polymerisation provides the driving force for the forming vesicle moving into the cell, and as the patch becomes highly motile, Sla1p, Sla2p and Pan1p dissociate (Kaksonen et al. 2003). The amphiphysin homologs Rvs161p and Rvs167p interact with actin and assist in vesicle scission, and as the vesicle moves into the cytoplasm, the actin network disassembles (Lombardi & Riezman 2001; Sivadon et al. 1997; Ayscough 2005).

SLA1 was identified from a screen for gene deletions which were lethal in combination with *ABP1* deletion (Holtzman et al. 1993), along with *SLA2* and the actin bundling gene *SAC6*. Sla1p associates with and regulates the dynamics of actin in cortical patches. It also has a role in localising Rho1p, a regulator of cell wall biosynthesis (Ayscough et al. 1999). Sla1p has known associations with three Arp2/3 activating proteins; Pan1p, Abp1p and Las17p (Warren et al. 2002). During endocytosis Sla1p can act as an adaptor. regulating the endocytic targeting of cargo such as the membrane receptors Ste2p, Ste3p and Wsc1p. This occurs via an interaction between Sla1p and NPFXD targeting motifs (Howard et al. 2002; Piao et al. 2007; Tan et al. 1996). Interestingly, Sla1p is also imported into the nucleus and this is was found to be required for its function in regulating endocytosis (Gardiner et

al. 2007). SH3 domains which are present in Sla1p mediate protein-protein interactions and are also found in Abp1p, Rvs167p, and the type I myosins (Rodal et al. 2003).

Yeast and mammalian endocytic processes are highly similar (Geli & Riezman 1998). The internalisation of yeast mating factor has been used as a model for receptor mediated endocytosis. The receptor Ste2p is positioned at the cell membrane to detect extracellular pheromone (also called mating factor), and upon binding the receptor and ligand become internalised (Dulić & Riezman 1990). Many mutant strains found to have defective pheromone internalisation are mutated in genes which interact with actin (Raths et al. 1993; Geli & Riezman 1996). Furthermore, cofilin mutants in which actin turnover is reduced fail to internalise endocytic vesicles (Lappalainen & Drubin 1997).

1.2.2.2 **Actin cables**

Actin cables are bundles of filaments which form an essential network in yeast cells used for the localisation and movement of vesicles and organelles. Cables are also crucial in defining cell polarity and are important in cell division for spindle positioning as well as moving elements between the mother and the emerging bud (Bretscher 2003). Actin cables are distributed randomly throughout cells in yeast when not dividing, and become oriented along the mother-bud axis during G1 phase (Adams & Pringle 1984). The assembly of a polarised cytoskeleton occurs following the establishment of a nascent bud site by the rho-GTPase Cdc42p and its guanine exchange factor (GEF) Cdc24p. Bem1p is also involved in these early events (Pruyne et al. 2004; Bose et al. 2001). The cables become anchored at the bud neck or nascent

bud site and extends out to the rest of the cell, with assembly taking place at the anchored end (Yang & Pon 2002).

Cdc42p activity is required for the activity of the formins in the nucleation of actin cables. The two closely related yeast formins, Bnr1p and Bni1p, are partially redundant with one another, as they can be deleted individually but loss of both is lethal. The formins directly interact with Cdc42p and another rho-GTPase Rho1, as well as actin and profilin to direct filament growth (Ozaki-Kuroda et al. 2001). The formation and maintenance of cables depends on several actin bundling factors, including the tropomyosins Tpm1p and Tpm2p, the fimbrin Sac6p, and may also involve Abp140p and the transgelin homolog Scp1p, which cross links filaments *in vitro.* Many of these actin bundling factors also play a role in stabilising actin in cortical patches (Yang & Pon 2002; Noma et al. 2011; Winder et al. 2003).

Transport along actin cables is achieved by the action of type V myosins. Vesicles have been shown to utilise myosin for transport along cables, as have organelles including as the vacuoles, ER, mitochondria, and nucleus (Hill et al. 1996; Pruyne et al. 2004; Fehrenbacher et al. 2004; Fehrenbacher et al. 2002; Schott et al. 2002). Mitochondria move in both anterograde and retrograde directions along the filament, either to retain organelles in the mother or distribute them to the emerging daughter bud (Boldogh & Pon 2006).

1.2.2.3 Cytokinetic ring

Cytokinesis is a fundamental cell process whereby cell components are partitioned and a single cell divides into two. In *S. cerevisiae* cell division is asymmetrical producing two cells of distinctly differing sizes. The process begins with the clustering of Cdc42p at the nascent bud site. This recruits the mitotic septins (Cdc3p, Cdc10p, Cdc11p, Cdc12p and Shs1p) which form a scaffold around which a contractile actomyosin ring assembles (Oh & Bi 2011). This is a complex process involving numerous components, including formins, type II and V myosins, tropomyosins and Rho1p (Wloka & Bi 2012). The branched actin filaments generated by Arp2/3 activity are not thought to be directly involved in the cytokinetic ring. However several Arp2/3 regulators which are involved in cortical patch assembly also contribute to cytokinetic ring assembly. These include Rvs167p and Vrp1p via an interaction with Hof1p (Nkosi et al. 2013).

The actomyosin ring contracts during cytokinesis in a manner which depends on actin filament depolymerisation, as shown by the loss of contractile force in cofilin mutants and jasplakinolide treated cells (Pinto et al. 2012). This is coupled with the formation of a chitinous septum by directed deposition of membranes, forming a physical barrier between the mother and daughter prior to the complete separation of the cells (Roncero & Sánchez 2010)

1.2.2.4 Nuclear actin

Fluorophore-labeled phalloidin staining does not indicate the presence of F-actin in the nucleus, but it is now accepted that there is a nuclear actin pool (Olave et al. 2002). The nature of nuclear actin function still remains to be fully revealed, but the

discovery of actin and actin-related proteins as components of chromatin remodeling complexes in yeast and other organisms has provided one answer. The NuA4 and INO80 complexes both contain actin and Arp4p, with Arp8p and Arp5p also found in INO80. The Swr1 complex also contains actin and Arp4p as well as Arp6p (Mizuguchi et al. 2004). A well conserved actin-Arp4p module appears to function within all three complexes (Kapoor et al. 2013). The SWI/SNF and RSC complexes do not contain actin but Arp7p and Arp9p are present in both (Sunada et al. 2005; Olave et al. 2002). The human SWI/SNF complex contains actin and Arp4p (BAF53), as do the human equivalents of INO80, SWR1 (SRCAP) and NuA4 (TIP60). It is thought that Arp7p/Arp9p represent a less conserved alternative to the actin-Arp4p module in these chromatin remodeling complexes (Bartholomew 2013).

The modulation of chromatin structure is an important process in genome regulation. Actin has also been show to bind and regulate the localisation of a transcriptional co-activator in mammalian cells (Vartiainen et al. 2007). Chromatin remodeling complexes such as INO80 are ATP-dependent, and it has been suggested that the conformational change in actin upon ATP hydrolysis modulate complex activity. The involvement of monomeric actin in control of the genome raises questions about how filament dynamics and modulation of the G-actin/F-actin ratios might affect chromatin remodeling and transcriptional regulation (Miralles & Visa 2006). Actin monomer binding proteins such as profilin, which can enter the nucleus, may play a role in regulating nuclear G-actin functions (Lederer et al. 2005).

1.2.3 The *act1-159* and *act1-157* mutations

A β-hairpin loop in subdomain 3 of actin contains the conserved motif of aspartic acid (Asp, D) 157, glycine (Gly, G) 158 and valine (Val, V) 159. The side chains of all three residues extend into the nucleotide binding site and are involved in binding the γ-phosphate of a bound ATP molecule. Val 159 is thought to act as the phosphate acceptor in the hydrolysis reaction (Kabsch & Holmes 1995). Following the hydrolysis of bound ATP to ADP the phosphate group is released from the filament as Pi. The release of Pi allows the conformational change of the monomer which destabilises the filament (Belmont, Orlova, et al. 1999; Korn et al. 1987). This is important in maintaining the polarised nature of the filament, as the (+) end where recently added monomers are ATP-bound remains stable while the (-) end is susceptible to depolymerisation.

Belmont & Drubin (1998) reported that yeast actin with a mutation of valine 159 to asparagine resulted in filaments which depolymerised around three times slower that of wild-type filaments. Three dimensional EM models of filaments revealed structural differences conferred by the V159N (*act1-159*) mutation. Incubation of wild-type filaments with BeF_4^- produces filaments consisting of BeF_3^--ADP-actin, a stable analog of ATP-actin or ADP-Pi actin. Despite having released Pi, the structure of *act1-159* filaments more closely resembled that of wild-type BeF_3^--ADP-actin filaments (Belmont, Orlova, et al. 1999) (Figure 6). Therefore the conformational change which normally follows the release of Pi does not occur in *act1-159* filaments. These filaments are described as being stabilised or having reduced dynamics. This *act1-159* has provided a useful tool for *in vivo* investigations into the roles of actin dynamics in cellular processes.

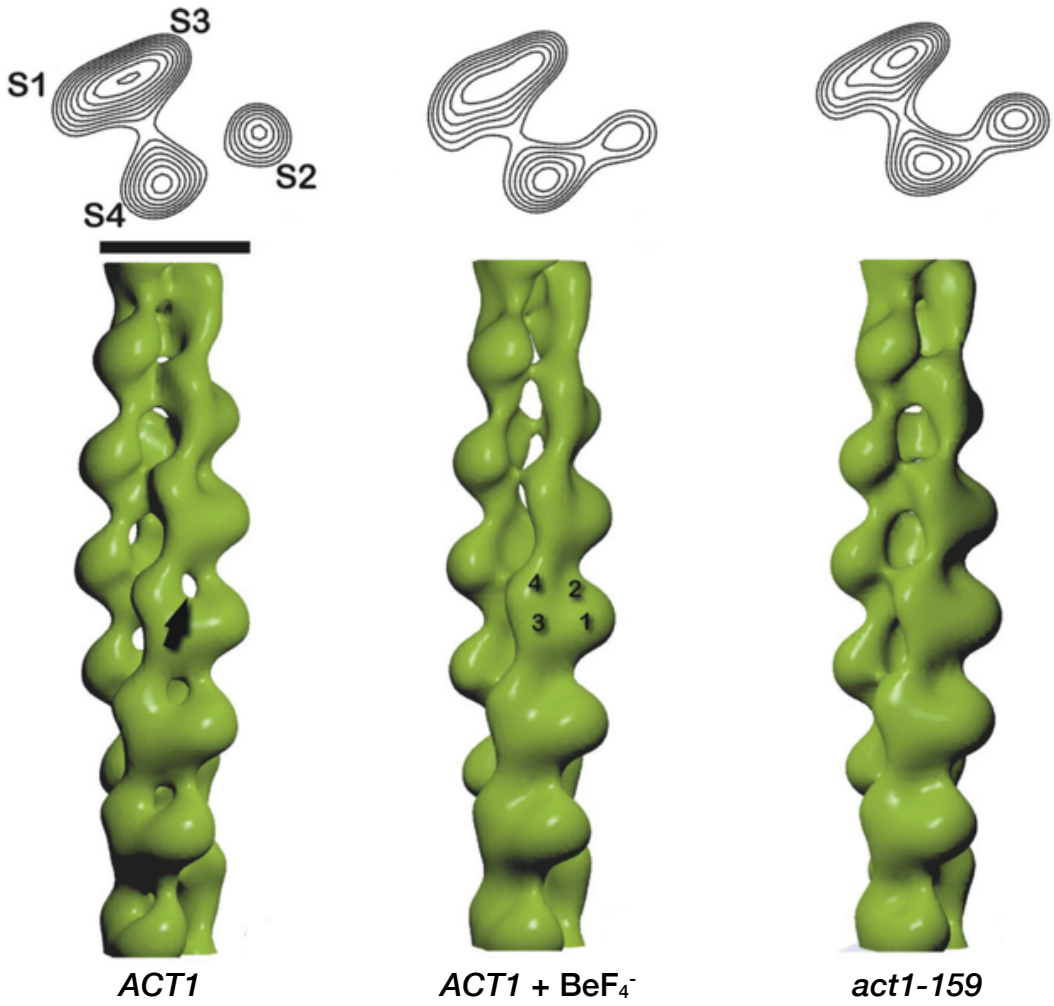

Figure 6. Cross sectional (top) and 3D surface reconstructions (bottom) of actin filaments (reproduced from Fig 5, Belmont et al. 1999). Subdomains are labeled (S1-4). Cross sectional images show the open nucleotide cleft in wild-type filaments as a gap in electron density between subdomains 2 and 4. The scale bar applies to the cross sections and represents 50Å. The open nucleotide cleft is also indicated by the black arrow in the surface view of a wild-type *ACT1* filament. The binding cleft is closed both when incubated with BeF_4^-, and when the V159N mutation is present in the actin gene.

The effects of the *act1-159* mutation on actin dynamics were characterised in several ways. Actin structures in *act1-159* cells resist Lat-A treatment for longer than wild-type, as Lat-A sequesters monomeric actin but does not increase depolymerisation rates. The cortical patches are larger in the mutant and the levels of F-actin are increased as a result of the stabilisation. Heterozygotes expressing both wild-type actin and *act1-159* show a semi-dominant effect of the mutant gene, with relatively

normal actin organisation but some larger cortical patches. This is due either to the assembly of some filaments entirely from mutant actin monomers, or filaments being assembled from a mixture of wild-type and mutant monomers (Belmont & Drubin 1998).

The act1-159 mutation is lethal in combination with profilin and cofilin mutations, demonstrating that the interactions between these proteins and the actin filament promote a functional dynamic cytoskeleton (Belmont & Drubin 1998). The mutation is also reported to increase the rate of nucleation, perhaps as a result of more stable actin trimer due to the reduced depolymerisation (Belmont, Orlova, et al. 1999).

The wider effects of reduced actin dynamics imposed by the *act1-159* mutation include reduced growth rates, sensitivity to high salt concentrations, severe defects in endocytosis (Belmont & Drubin 1998), and reduced lifespan. Severe mitochondrial effects are also reported, such as reduced mitochondrial membrane potential, and increased production of reactive oxygen species (ROS) (Gourlay et al. 2004). These mitochondrial effects are considered hallmarks of an apoptotic state and also represent some common phenotypes of aged yeast cells (Gourlay & Ayscough 2005a; Boldogh & Pon 2006).

Further +site-specific mutagenesis produced more actin alleles with single residue changes. Of particular interest was the mutation of residue 157 from Asp to Glu (D157E) (Belmont, Patterson, et al. 1999). This residue is close to Val 159 in both sequence and tertiary structure and appears to have a role in nucleotide binding. D157E conferred a resistance to Lat A *in vivo*, an inhibitor of nucleotide exchange.

The increased nucleotide exchange rate in act1-157 allows suppression of the defects caused by profilin mutations. Mutation of the actin-binding domain of profilin which causes cytoskeletal organisation defects were suppressed in the act1-157 mutant (Wolven et al. 2000). The D157E mutant (*act1-157*) might be considered in some ways as the inverse of the *act1-159* mutant, as it has increased rates of actin filament turnover. Additionally, ROS levels are decreased in this mutant when compared to wild-type cells (Gourlay et al. 2004). Aside from the increased nucleotide exchange rate and Lat A resistance, the mutant appears similar to the wild-type strain. A tendency for cells to have fewer actin structures was noted, although in a small number of cells more prominent cables were also observed (Belmont, Patterson, et al. 1999). In this study actin mutations are used to investigate the effects of altering actin dynamics upon cell signaling processes which connect cellular stress responses to the environment.

1.3 Actin and environmental sensing

A range of cell stresses induce a response from the actin cytoskeleton in *S. cerevisiae*. The reorganisation of actin structures can be brought about following insults including centrifugal force, heat shock, osmotic shock, nutrient restriction and oxidative stress (Chowdhury et al. 1992; Novick et al. 1989; Guo et al. 2009). Actin depolymerisation in *S. cerevisiae* is a specific response which can be induced by disruption of genes with no direct interaction with actin (Karpova et al. 2008). The recovery of actin dynamics following stress is dependent on MAPK signaling (Vilella et al. 2005). These observations indicate that cytoskeletal depolarisation under stress

is not a nonspecific effect, but rather that it is a controlled modulation of actin structures as an adaptive response to stress.

In support of this, it has been established that actin regulation is linked to yeast cell fates. Yeast cells undergo a controlled cell death in response to both chronological ageing and environmental stresses which has many of the features of apoptosis, including accumulation of ROS (Laun et al. 2001). Programs of apoptosis are initiated following insults including nutrient restriction, and oxidative stresses, genotoxic lesions and treatment with antifungal chemicals (Carmona-Gutierrez et al. 2010). It has been demonstrated that yeast cells with a stabilised cytoskeleton activate an apoptotic program that proceeds via an interaction between Srv2p/CAP and actin (Gourlay & Ayscough 2006). ROS can lead to reorganization of actin structures by oxidation of conserved cysteine residues, and acts to protect cells under stress (Farah et al. 2011). Therefore the actin cytoskeleton is embedded within adaptive responses to stress and as well as being the target of modulation, also participates in signaling pathways. The full extent to which cytoskeletal dynamics has an impact on signal transduction in the many pathways in which it has interactions remains to be shown.

The Rho GTPases represent a link between actin dynamics and cell signaling pathways. In particular Cdc42p has well documented roles in morphogenic processes including the formation of buds and mating projections, and is also an essential signaling component of the high osmolarity glycerol (HOG), mating and filamentous/invasive growth pathways. Control of morphogenesis depends in part on recycling Cdc42p via endocytosis, a process which itself is mediated by actin (Slaughter et al. 2009). A related Rho GTPase, Rho1p, also regulates actin

polymerisation through interactions with formins, as well as transducing signal in the cell wall integrity (CWI) pathway (Sit & Manser 2011).

Actin stabilisation by jasplakinolide and actin mutation has been shown to induce apoptosis in yeast cells (Gourlay et al. 2004; Franklin-Tong & Gourlay 2008). Conversely, mutations in actin and in actin regulatory proteins which result in increased dynamics can induce a stress response and promote extension of lifespan (Kotiadis et al. 2012; Gourlay et al. 2004). These data indicate that actin dynamics plays a role in the survival and adaptability of yeast cells.

1.3.1 Yeast signaling pathways

Actin is the target of numerous signaling pathways, and is also involved in the transduction of the signal in a variety of ways. The actin cytoskeleton interacts with components of all major yeast MAPK signaling cascades and the Ras/cAMP/PKA pathway. In this section the pathways are described with reference to the links to the cytoskeleton. A diagram of these signaling pathways is shown in Figure 7.

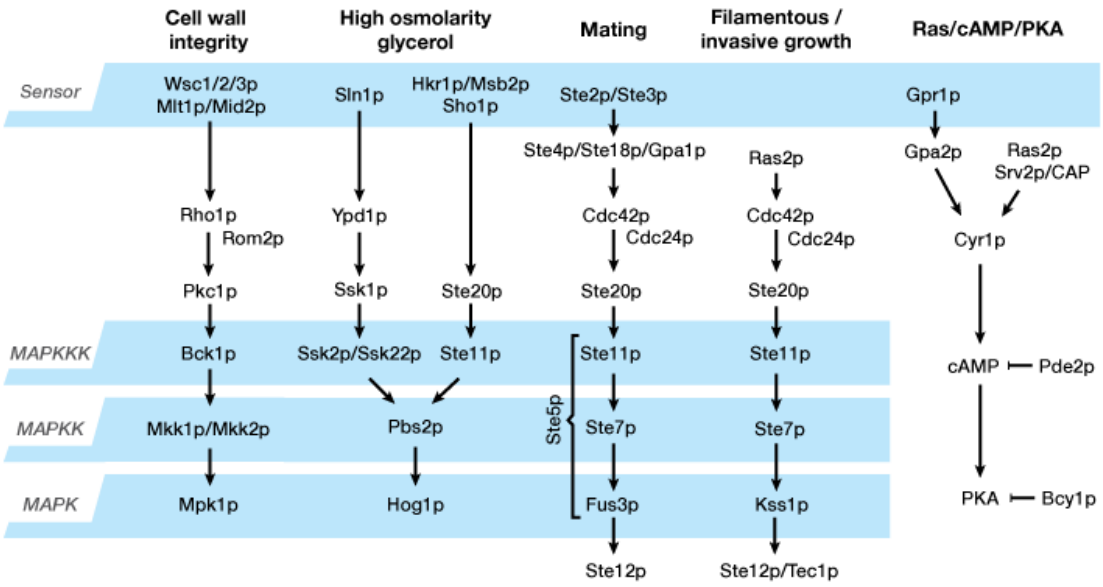

Figure 7. An overview of yeast MAPK and Ras/cAMP/PKA signal pathways described in section 1.3.1

The MAPK cascades, along with various activators and effectors, comprise a system of three sequentially activated kinases. A MAP kinase kinase kinase (MAPKKK) activates a MAP kinase kinase (MAPKK), which in turn activates a MAP kinase, which usually activates a transcription factor. Four major MAPK signaling cascades operate in *S. cerevisiae* in response to different environmental stimuli. The high osmolarity glycerol (HOG) pathway is activated during hypertonic stress and acts to increase glycerol levels. The cell wall integrity pathway (CWI) is activated under several conditions including low osmolarity, impairment of cell wall synthesis and heat stress. The mating pathway responds to pheromone secreted by yeast cells of the opposite mating type and induces cellular changes required for mating. During nutrient starvation (primarily nitrogen starvation) the filamentous/invasive growth pathway is activated. Additionally the Ras/cAMP/PKA pathway, while not a MAPK cascade, is closely linked with them and also responds to nutrient levels. Many of these pathways share components and all depend on membrane proteins and

culminate in the modulation of transcriptional programs (Herskowitz 1995; Staleva et al. 2004; Posas et al. 1998).

1.3.1.1 Mating response and filamentous/invasive growth pathways

The yeast mating pathway has served as a model for the eukaryotic signaling cascade, and is one of the most studied pathways involving a cellular response to an external stimulus. Yeast mating is dependent on the secretion of peptide mating factors, and the response to mating factors secreted by cells of the opposite haploid cell type. The response involves the expression of mating genes, morphological changes and a cell cycle arrest in the G1 phase (Herskowitz 1995). Cells of mating type a (*MAT***a**) secrete mating factor a, while mating type α (*MAT*α) cells secrete mating factor α. Extracellular mating factors secreted by potential mating partners first interacts at the membrane receptor. Each mating type expresses a different receptor gene, *STE2* in *MAT***a** cells and *STE3* in *MAT*α cells, both of which encode G-protein coupled receptors (GPCRs). Despite not exhibiting extensive sequence homology, these two receptors fulfill the same function of binding mating factor and transducing the signal via an identical intracellular pathway (Nakayama et al. 1987; Nakayama et al. 1985). As discussed in section 1.2.2.1, the GPCRs are recycled between the outer membrane and the vacuole in endocytic vesicles, and the receptors interact with Sla1p for targetting. Actin therefore regulates the mating pathway at the first step by influencing receptor localisation.

Mating factor binding to the GPCR receptor activates the associated intracellular heterotrimeric G-protein. The Gα subunit Gpa1p contains a guanine nucleotide

binding site, and when activated exchanges GDP for GTP. This exchange enables the Gβγ dimer, which consists of Ste4p and Ste18p, to transmit the signal to the MAPK pathway. Upon hydrolysis of bound GTP the G protein is inactivated (Klein et al. 2000). Release of the Gβγ dimer exposes binding sites on Ste4p while lipid moieties on Ste18p anchor the complex to the membrane (Bardwell 2004; Hirschman & Jenness 1999).

Ste4p mediates interactions which bring several components together and continue the signal transduction. Ste4p induces the binding of the membrane-anchored Rho GTPase Cdc42p with the PAK (p21-activated kinase) family kinase Ste20p, thereby activating Ste20p and localising it to the membrane. Cdc42p function requires its guanine nucleotide exchange factor Cdc24p (Simon et al. 1995; Lamson et al. 2002). Ste20p is known to interact with actin via Bem1p (Leeuw et al. 1995).

Concurrently, Ste5p interacts with Ste4p and becomes localised to the membrane. Ste5p is a large protein which acts a scaffold for three other components in the pathway. Ste11p is carried to the membrane with Ste5p where it comes into contact with Ste20p and becomes activated by phosphorylation. The Ste5p scaffold also binds the MAPKs Ste7p, and Fus3p. This forms the sequentially-activating MAPK module of the pathway, with Ste11p phosphorylating Ste7p, which in turn phosphorylates Fus3p (Elion 2001). Ste5p localisation is dependent on Bni1p-driven actin polymerisation, mediated by the Bni1p interaction with Rho1p, and possibly Cdc42p. While there is functional overlap between the two formins, Bnr1p cannot replace the role of Bni1p in localising Ste5p in *Δbni1* mutants. (Qi & Elion 2007).

Kss1p is a second MAPK which can act in the mating pathway and has partial functional overlap with Fus3p. Deletion of *FUS3* or *KSS1* does not prevent mating, while *fus3 kss1* double mutants are sterile (Elion et al. 1991). Fus3p and Kss1p share 56% amino acid sequence identity and both can be activated by Ste7p (Ma et al. 1995). While Fus3p appears to promote mating and inhibit invasive growth, the role of Kss1p in both pathways is less clear. As well as being able to transduce the mating signal in the absence of Fus3p, it can also promote recovery from pheromone induced cell cycle arrest, and in its unphosphorylated state also acts to inhibit the downstream transcription factor Ste12p (Courchesne et al. 1989; Roberts & Fink 1994; L. Bardwell et al. 1998). The dynamic localisation of Fus3p is important for its signaling functions, as membrane tethering causes hyperactivation, while the mating pathway becomes unresponsive when it is confined to the nucleus (Chen et al. 2010). Fus3p also phosphorylates Far1p, which activates cell cycle arrest and establishes the site of mating projection in the direction of the mating partner (Breitkreutz et al. 2001).

The regulation of gene expression for mating is controlled via the activity of Ste12p. This transcription factor is the target of Fus3p and Kss1p, and is activated by phosphorylation. Activation in response to pheromone involves Ste12p homomultimers, or heteromultimers with Mcm2p (Madhani & Fink 1998). Dig1p and Dig2p are negative Ste12p regulators which are partially redundant. Double mutants of *dig1* and *dig2* constitutively express the mating pathway-specific protein Fus1p as well as exhibiting invasive growth, indicating these proteins repress Ste12p driven transcription in both pathways in the absence of signaling (Bardwell et al. 1998; Gartner et al. 1992; Tedford et al. 1997). Mating factor induced Ste12p activity leads to differential expression of large numbers of genes, including components of

the pathway such as *STE2/STE3* and *FUS3* (Roberts 2000; Bardwell 2004). Genes required for fusion with mating partners are also expressed, including *FUS1* which has been used a reporter for mating pathway-specific expression (Posas et al. 1998). Fus3p also activates Far1p, a regulator of the cell cycle arrest in response to pheromone (Peter & Herskowitz 1994).

The promoters of mating genes contain pheromone response elements (PREs) with the sequence TGAAACA, which is the binding site of the transcription factor Ste12p (Hagen et al. 1991). Ste12p is also involved in the invasive growth response, in conjunction with another transcription factor, the TEA family protein Tec1p (Chou et al. 2006). Tec1p was originally identified as a regulator yeast transposon expression, and the Ty1 reporters have been a useful tool for investigating the expression of Ste12p-Tec1p complex targets (Mösch et al. 1996). The cooperative action of these two proteins involves binding at adjacent binding sites, the PRE described above and a Tec1p binding site with the TEA consensus sequence (TCS) CATTC(T/C). Together these two sequences constitute a filamentation response element (FRE) (Gancedo 2001). There is also evidence that Tec1p can mediate expression of some targets independently of Ste12p (Heise et al. 2010).

Although they have been shown to signal discretely from one another, much of the cascade upstream of Ste12p is shared with the filamentous/invasive growth pathway. Filamentous/invasive growth is the implementation of a growth program in budding yeast cells during nutrient limitation which is thought to be a foraging mechanism (Cullen & Sprague 2000). In diploid cells the pathway is used to form multicellular

pseudohyphae, while the pathway in haploid activates invasive growth (Mösch et al. 1999).

As well as the MAPK dependent activation of Ste12p/Tec1p complexes, regulation also comes through Ras/cAMP/PKA signaling, and crosstalk between the pathways occurs (Mösch et al. 1999; Vinod et al. 2008). In the MAPK pathway, Ras2p activates Cdc42p and the signal is transduced through the cascade via the sequential kinase activities of Ste20p, Ste11p, Ste7p and Kss1p, all of which are shared with the mating pathway. Despite the overlap in kinases between pathways, the scaffold Ste5p is required for mating but is not required for filamentous growth (Mösch et al. 1996).There is also a requirement for the 14-3-3 proteins Bmh1p and Bmh2p, which associate with Ste20 *in vivo* (Roberts et al. 1997). Fus3p inhibits the invasive growth pathway by phosphorylation of Tec1p, which targets it for ubiquitin-mediated degradation (Bao et al. 2004). In this pathway Kss1p works in an opposing role to Fus3p, promoting the activity of Tec1p (Brückner et al. 2004).

1.3.1.2 High osmolarity glycerol pathway

Yeast cells in high osmolarity environments induce the synthesis of glycerol so as to increase their internal osmolarity. This response is controlled by a signaling pathway connecting membrane osmosensor proteins to the MAPK Hog1p. Under osmotic stress, actin filaments rapidly disassemble, and can reassemble when the osmotic balance is reestablished (Yuzyuk et al. 2002).Two functionally redundant branches of the HOG pathway exist, referred to as the SHO1 and SLN1 branches, in reference to two membrane proteins which are active early during transduction of the signals (Hohmann 2002; Miermont et al. 2011).

Sho1p itself is no longer considered to be an osmosensor, but it has been suggested instead that it acts as an anchor for the putative osmosensors Hkr1p and Msb2p (Tatebayashi et al. 2007). Msb2p signaling has been shown to require the actin cytoskeleton and Bem1p, while Hkr1p does not (Tanaka et al. 2014). The Sho1p branch shares components with the mating and filamentous/invasive growth pathways, and Msb2p/Sho1p have been linked to activation of both pathways (Colombo et al. 2004; O'Rourke & Herskowitz 2002). As in the Ste12p targeting pathways, Cdc42p and Ste20p act together and activate the MAPK Ste11p at the membrane. The MAKK Pbs2p also becomes localised to the membrane and directly interacts with Sho1p in this process where it can be activated by Ste11p (Reiser et al. 2000; Raitt et al. 2000).

Sln1p itself is an osmosensor with cytoplasmic kinase activity (Reiser et al. 2003) and acts in a phosphorelay system, first by phosphorylating its own receiver domain. This phosphate is then transferred to Ypd1p and subsequently on to Ssk1p. Phosphorylated Ssk1p is inactive, and in this state the pathway does not signal further. Under high osmolarity conditions, the kinase activity of Sln1p is inhibited, leading to accumulation of active unphosphorylated Ssk1p. Active Ssk1p interacts with an inhibitory domain of the MAPKKKs Ssk2p ans Ssk22p, following which they autophosphorylate and become active (Posas et al. 1996; Posas & Saito 1998; Hohmann 2009). Ssk2p has a role in repolymerisation of actin following osmotic stress (Yuzyuk et al. 2002).

The two branches converge at the Pbs2p, which phosphorylates and activates the MAPK Hog1p (Maeda et al. 1995). Only upon phosphorylation is Hog1p transported into the nucleus, where it promotes a transcriptional program via numerous unrelated transcription factors including Sko1p, Msn2p/Msn4p, Hot1p and Rtg1p/Rtg3p (Maeda et al. 1995). In high osmolarity environments yeast cells undergo growth arrest and a rapid depolarisation of the cytoskeleton, and one function of HOG signaling is in regulating cytoskeleton repolarisation and the return to cell cycle progression (Chowdhury et al. 1992; Brewster & Gustin 1994; Gustin et al. 1998).

There is some overlap between the high osmolarity pathway and both Ste12p-mediated pathways. Sho1p has also been linked to activation of the mating pathway, as a number of cell wall integrity mutants were found to activate Fus1p expression by a mechanism involving Ste20p, Ste11p, Ste7p, Kss1p and Ste12p (Cullen et al. 2000). Sho1p has been shown to bind with the mating pathway regulated protein Fus1p, which may act to suppress Sho1p signaling to promote cell fusion (Nelson et al. 2004). Additionally, the HOG pathway and the CWI pathway respond to some of the same stress conditions and may operate in coordination to deliver a response (Rodríguez-Peña et al. 2010).

HOG signaling affects expression of proteins involved more general stress responses, including two heat shock proteins (HSPs), the chaperone Hsp104p and Hsp12, a small HSP is induced by several stress conditions (Rep et al. 1999; Varela et al. 1995).

1.3.1.3 Cell wall integrity pathway

Activation of the CWI pathway occurs in response to cell wall instability, which can occur due to environmental conditions including changes in osmolarity and temperature, as well events of cell growth and morphological change. The yeast cell wall consists of an inner layer composed of chitin and glucan polymers which forms a scaffold for the glycoprotein outer layer. The strength and elasticity of the cell wall provides protection against mechanical forces and against low osmolarity shock, which can cause cells to rapidly swell (Klis et al. 2006; Levin 2011).

Five cell surface proteins detect cell wall stress; Wsc1p, Wsc2p, Wsc3p, Mid2p and Mtl1p. All are structurally similar possessing a single transmembrane domain with a rigid periplasmic peptide thought to act as a mechanosensor (Verna et al. 1997; Philip & Levin 2001; Levin 2011). Distinct responses are associated with these receptors, with Mid2p being associated with cell wall remodeling in response to pheromone-induced morphological changes (Rajavel & Philip 1999). Distribution and recycling of Wsc1p is dependent on an interaction with Sla1p (Piao et al. 2007). Activation of the receptors leads to activation of the Rho GTPase Rho1p via its GEF Rom2p (Philip & Levin 2001).

Rho1p activity is integral to the CWI signal, and it also has a number of other functions. The signal transduction role of Rho1p is to activate protein kinase C (Pkc1p). The MAPK cascade following this involves the MAPKKK Bck1p, which activates the redundant MAPKKs Mkk1p and Mkk2p, resulting in the activation of the MAPK Mpk1p (Kamada et al. 1995; Levin 2005). Mpk1p (also called Slt2p) targets transcription factors including Rlm1p and Swi4p/Swi6p (Truman et al. 2009).

Other Rho1p roles include acting as a subunit of a glucan synthase complex which synthesises main cell wall polymer, and regulating the actin cytoskeleton via interactions with formins Bni1p and Bnr1p (Levin 2011). Rho1p is also linked to TOR signaling via Tor2p activation of Rom2p, and subsequent modulation of actin via Pkc1p (Schmidt et al. 1997; Helliwell et al. 1998). Many other pathways are involved in cross talk at different points in the CWI pathway, including Ras/cAMP/PKA and HOG pathways, enabling cell wall integrity to be maintained to a broad range of stress conditions (Fuchs & Mylonakis 2009; Rodríguez-Peña et al. 2010).

CWI signaling is activated when the cytoskeleton is depolarised, but this does not occur in the presence of osmotic support. This suggests that CWI responds to cytoskeleton depolarsation by the stress this applies to the cell wall (Harrison et al. 2001; Levin 2011).

1.3.1.4 Ras/cAMP/PKA pathway

While Ras2p has a role in the MAPK mediated filamentous/invasive growth pathway, it also signals independently via another pathway to coordinate cell growth, proliferation stress responses and mitochondrial activity with the availability of glucose (Thevelein & de Winde 1999). Activation of this pathway in the presence of glucose results in transcriptional and metabolic changes to the cell to promote the switch to fermentative rather than oxidative growth (Wang et al. 2004).

In the presence of glucose, the GTPase Ras2p exchanges GDP for GTP and associates with Srv2p/CAP. This complex leads to the activation of the adenylyl cyclase Cyr1p, which catalyses the production of the second messenger cyclic AMP (cAMP). Levels of cAMP are regulated by the phosphodiesterase Pde2p (and to a lesser extent Pde1p), converting it to AMP (Hu et al. 2010). Increased cAMP levels promotes the disassociation of the PKA inhibitor Bcy1p, and as a result PKA becomes active (Thevelein & de Winde 1999). PKA is a complex consisting of Tpk1p, Tpk2p and Tpk3p. PKA activity affects cell proliferation at least in part by promoting the export of Msn2p/Msn4p from the nucleus, and preventing the expression of the growth inhibitor Yak1 (Livas et al. 2011; Lee et al. 2011).

The source of Ras2p activation has proved difficult to identify but might involve intracellular acidification and the deactivation of Ras2p inhibitors Ira1p and Ira2p (Thevelein & de Winde 1999; Colombo et al. 1998). The GEF Cdc25p has been implicated in activating Ras2, but a Cdc25p activator which responds to a nutrient signal has not been identified (Colombo et al. 2004). Cyr1p can also be activated by a system involving the GPCR Gpr1 and the G protein subunit Gpa2. The increase in active GTP-Ras2p upon glucose addition is not dependent on the Gpr1/Gpa2 system, but full stimulation of cAMP synthesis requires input from both branches (Thevelein et al. 2005).

The Ras/cAMP/PKA has some level of regulation from both actin and MAPK components. Actin is linked to this pathway by its interaction with Srv2p/CAP, which binds both actin and Cyr1p. The pathway is hyperactivated when the cytoskeleton is stabilised, and this has been shown to be dependent on the G-actin binding region of

Srv2p/CAP. This hyperactivation leads to apoptosis, indicating that cytoskeletal dynamics are important in the response to environmental changes (Gourlay & Ayscough 2006). Cross-regulation of Ras/cAMP/PKA signaling occurs by interaction between the MAPKs Fus3p and Kss1p and Cdc25p, demonstrating another link to mating and filamentous/invasive growth pathways (Cherkasova et al. 2003).

1.4 Aims of the study

The dynamic state of the actin cytoskeleton is of key importance in many crucial cell processes. Actin is also embedded in numerous signaling pathways and its dynamic state can influence the ability of the cell to react to internal and external changes. Our lab has proposed previously that actin may have a role as a biosensor, monitoring the health of cells and their ability to maintain homeostasis, and providing a mechanism by which unhealthy cells can be removed from the population (Smethurst et al. 2013; Gourlay & Ayscough 2006). Here, I further investigate the role of actin dynamics in the maintenance of cellular homeostasis. I focus on how signaling pathways are affected by actin dynamics, and aim to elucidate the interactions between the cytoskeleton and these pathways which position actin centrally in the sensing and response to environmental change.

2 Materials & Methods

2.1 Water

Ultra pure deionised water (dH2O) was produced by Thermo Scientific Barnstead NanoPure Diamond system.

2.2 Sterilisation

Sterilisation of media, dH2O and other liquids was carried out at 121°C in a bench top Prestige Medical autoclave.

2.3 Growth conditions

Yeast cultures were grown either in rich media (YPD) or in minimal selective dropout (SD) media when maintaining plasmids. To make agar media Oxoid technical agar (Agar No. 3) was added to 1.5% prior to autoclaving.

2.3.1 Yeast media

YPD (200ml)

- 2g Oxoid Yeast Extract (1% w/v)
- 4g BD Bacto Peptone (2% w/v)
- Add water to volume of 190ml
- Autoclave
- Cool to 50-55°C
- Add 10ml sterilised 40% glucose in water (2% w/v)

YPG was made as YPD except with glycerol replacing the glucose at a final concentration of 2% v/v.

Selective drop-out media (200ml)

- 1.4g Formedium Yeast nitrogen base without amino acids
- 0.32g Formedium Complete supplement (CSM) dropout mixture containining required amino acids (or mass as indicated by manufacturer)
- Add water to volume of 190ml
- Autoclave
- Cool to 50-55°C
- Add 10ml sterilised 40% glucose in water (2% w/v)

2.3.2 E. coli media

YT (200ml)

- 3.2g BD Bacto Tryptone (1.6% w/v)
- 2g Oxoid Yeast Extract (1% w/v)
- 1g Fisher analytical grade NaCl (0.5% w/v)
- Add water to 200ml
- Autoclave

2.4 Strains and DNA

2.4.1 Yeast strains

Strain	Genotype	Source
CGY 769a	*MATα ura3-52, leu2-3,112, cry1, tub2- 201, ACT1::HIS3, his3Δ200*	(Belmont & Drubin 1998)
CGY 770a	*MAT**a** ura3-52, leu2-3,112, cry1, tub2- 201, ACT1::HIS3, his3Δ200*	(Belmont & Drubin 1998)
CGY 354	*MATα ura3-52, leu2-3,112, ade4, ade2, tub2-201, act1-157::HIS3, his3Δ200*	(Belmont, Patterson, et al. 1999)
CGY 339	*MATα ura3-52, leu2-3,112, ade4, ade2, tub2-201, act1-159::HIS3, his3Δ200*	(Belmont & Drubin 1998)
CGY 340	*MAT**a** ura3-52, leu2-3,112, ade4, ade2, tub2-201, act1-159::HIS3, his3Δ200*	(Belmont & Drubin 1998)
CGY638	*MAT**a** his3Δ1 leu2Δ met15Δ ura3Δ Δcox4::HIS*	(Leadsham & Gourlay 2010)

CGY862b	*MAT***a** *his3Δ1 leu2Δ met15Δ ura3Δ cox4d-1::HIS3*	(Leadsham et al. 2013)
CGY862d	*MAT***a** *his3Δ1 leu2Δ met15Δ ura3Δ cox4d-2::HIS3*	(Leadsham et al. 2013)
CGY 470	*MAT***a** *ACT1::HIS3 bar1Δ::LYS2 his3Δ200 ura3-52 lys2-801 leu2-3 112 ade2*	(Whitacre et al. 2001)
CGY 441	*MAT***a** *act1-105::HIS3 bar1Δ::LYS2 his3Δ200 ura3-52 lys2-801 leu2-3 112 ade2*	(Whitacre et al. 2001)
CGY 442	*MAT***a** *act1-119::HIS3 bar1Δ::LYS2 his3Δ200 ura3-52 lys2-801 leu2-3 112 ade2*	(Whitacre et al. 2001)
CGY 443	*MAT***a** *act1-120::HIS3 bar1Δ::LYS2 his3Δ200 ura3-52 lys2-801 leu2-3 112 ade2*	(Whitacre et al. 2001)
CGY 444	*MAT***a** *act1-124::HIS3 bar1Δ::LYS2 his3Δ200 ura3-52 lys2-801 leu2-3 112 ade2*	(Whitacre et al. 2001)
CGY 445	*MAT***a** *act1-122::HIS3 bar1Δ::LYS2 his3Δ200 ura3-52 lys2-801 leu2-3 112 ade2*	(Whitacre et al. 2001)
CGY 446	*MAT***a** *act1-125::HIS3 bar1Δ::LYS2 his3Δ200 ura3-52 lys2-801 leu2-3 112 ade2*	(Whitacre et al. 2001)
CGY 447	*MAT***a** *act1-129::HIS3 bar1Δ::LYS2 his3Δ200 ura3-52 lys2-801 leu2-3 112 ade2*	(Whitacre et al. 2001)
CGY 448	*MAT***a** *act1-20::HIS3 bar1Δ::LYS2 his3Δ200 ura3-52 lys2-801 leu2-3 112 ade2*	(Whitacre et al. 2001)
CGY 449	*MAT***a** *act1-3::HIS3 bar1Δ::LYS2 his3Δ200 ura3-52 lys2-801 leu2-3 112 ade2*	(Whitacre et al. 2001)
CGY 450	*MAT***a** *act1-117::HIS3 bar1Δ::LYS2 his3Δ200 ura3-52 lys2-801 leu2-3 112 ade2*	(Whitacre et al. 2001)
CGY 451	*MAT***a** *act1-135::HIS3 bar1Δ::LYS2 his3Δ200 ura3-52 lys2-801 leu2-3 112 ade2*	(Whitacre et al. 2001)
CGY 452	*MAT***a** *act1-104::HIS3 bar1Δ::LYS2 his3Δ200 ura3-52 lys2-801 leu2-3 112 ade2*	(Whitacre et al. 2001)
CGY 453	*MAT***a** *act1-113::HIS3 bar1Δ::LYS2 his3Δ200 ura3-52 lys2-801 leu2-3 112 ade2*	(Whitacre et al. 2001)
CGY 454	*MAT***a** *act1-111::HIS3 bar1Δ::LYS2 his3Δ200 ura3-52 lys2-801 leu2-3 112 ade2*	(Whitacre et al. 2001)
CGY 455	*MAT***a** *act1-4::HIS3 bar1Δ::LYS2 his3Δ200 ura3-52 lys2-801 leu2-3 112 ade2*	(Whitacre et al. 2001)
CGY 997	*MAT***a** *Δpdr5::TRP1, Δsnq2::hisG, ura3- 52, his3-Δ200 leu2-Δ1, trp1-Δ63, lys2-801 ade2-101*	(Ayscough 2000)
CGY 370	*his3Δ1, leu2Δ, ura3Δ, met15Δ*	(Heeren et al. 2004)
CGY 371	*his3Δ1, leu2Δ, ura3Δ, met15Δ, Δras2::KanMx*	(Heeren et al. 2004)
CGY 372	*his3Δ1, leu2Δ, ura3Δ, met15Δ, RAS2(ala18,val19)*	(Heeren et al. 2004)
BY4741	*MAT***a** *his3Δ1 leu2Δ0 met15Δ0 ura3Δ0*	(Brachmann et al. 1998)
Δrad52	BY4741	*MAT***a** knockout collection
Δabp140	BY4741	*MAT***a** knockout collection
Δacf4	BY4741	*MAT***a** knockout collection
Δaim21	BY4741	*MAT***a** knockout collection
Δaim3	BY4741	*MAT***a** knockout collection
Δaim7	BY4741	*MAT***a** knockout collection
Δaip1	BY4741	*MAT***a** knockout collection
Δadp1	BY4741	*MAT***a** knockout collection
Δarc18	BY4741	*MAT***a** knockout collection
Δark1	BY4741	*MAT***a** knockout collection

Δarp1	BY4741	*MAT**a*** knockout collection
Δarp5	BY4741	*MAT**a*** knockout collection
Δarp6	BY4741	*MAT**a*** knockout collection
Δarp8	BY4741	*MAT**a*** knockout collection
Δbag7	BY4741	*MAT**a*** knockout collection
Δbbc1	BY4741	*MAT**a*** knockout collection
Δbit2	BY4741	*MAT**a*** knockout collection
Δbit61	BY4741	*MAT**a*** knockout collection
Δbni1	BY4741	*MAT**a*** knockout collection
Δbnr1	BY4741	*MAT**a*** knockout collection
Δbsp1	BY4741	*MAT**a*** knockout collection
Δbud6	BY4741	*MAT**a*** knockout collection
Δbzz1	BY4741	*MAT**a*** knockout collection
Δcap1	BY4741	*MAT**a*** knockout collection
Δcap2	BY4741	*MAT**a*** knockout collection
Δcrn1	BY4741	*MAT**a*** knockout collection
Δcyk3	BY4741	*MAT**a*** knockout collection
Δend3	BY4741	*MAT**a*** knockout collection
Δent1	BY4741	*MAT**a*** knockout collection
Δent2	BY4741	*MAT**a*** knockout collection
Δgea1	BY4741	*MAT**a*** knockout collection
Δgip3	BY4741	*MAT**a*** knockout collection
Δjnm1	BY4741	*MAT**a*** knockout collection
Δlsb6	BY4741	*MAT**a*** knockout collection
Δmsb3	BY4741	*MAT**a*** knockout collection
Δmyo4	BY4741	*MAT**a*** knockout collection
Δplp1	BY4741	*MAT**a*** knockout collection
Δrgd1	BY4741	*MAT**a*** knockout collection
Δrvs167	BY4741	*MAT**a*** knockout collection
Δsac6	BY4741	*MAT**a*** knockout collection
Δsac7	BY4741	*MAT**a*** knockout collection
Δscp1	BY4741	*MAT**a*** knockout collection
Δsiw14	BY4741	*MAT**a*** knockout collection
Δsla1	BY4741	*MAT**a*** knockout collection
Δslo1	BY4741	*MAT**a*** knockout collection
Δspa2	BY4741	*MAT**a*** knockout collection
Δtpm2	BY4741	*MAT**a*** knockout collection
Δtsc11	BY4741	*MAT**a*** knockout collection
Δtwf1	BY4741	*MAT**a*** knockout collection
Δvrp1	BY4741	*MAT**a*** knockout collection
Δyke2	BY4741	*MAT**a*** knockout collection
Δysc84	BY4741	*MAT**a*** knockout collection
CGY 384	*ura3-52, his3D200, leu2-3,112, lys2-801, COF1::LEU2*	(Lappalainen & Drubin 1997)
CGY 388	*ura3-52, his3D200, leu2-3,112, lys2-801, cof1-7::LEU2*	(Lappalainen & Drubin 1997)
	ura3-52, his3D200, leu2-3,112, lys2-801, cof1-7::LEU2Δpor1::kan	Corte-Real Lab
	ura3-52, his3D200, leu2-3,112, lys2-801, COF1::LEU2 Δpor1::kan	Corte-Real Lab

Table 1. Yeast strains used in the study

2.4.2 *E. coli* strains

Strain	Genotype
DH5α	*F-deoR endA1 relA1 gyrA96 hsdT17(rk- mk+) phoA supE44 thi-1 Δ(lacZYA-argF)U169 ϕ80δlacZΔM15*

Table 2. *E. coli* strains used in the study

2.4.3 Plasmids

Strain	Description	Source
pCG 162	pRS316 + SEC63-GFP URA3 CEN	(Fehrenbacher et al. 2002)
pCG 46	pYX142-mtGFP	(Westermann & Neupert 2000)
pCG 394	BHUM212, FRE(Ty1)::CYC1::LacZ URA3	(Mösch et al. 1999)
pCG 525	FRE(Ty1)::CYC1::LacZ LEU2	(L Bardwell et al. 1998)
pCG 124	pAG425GPD-ccdB, Gateway expression vector, LEU2, 2μ	Invitrogen
pCG 550	pRS315 STE3-GFP CEN LEU	
pCG 479	CIT2-lacZ URA	(Giannattasio et al. 2005)
pCG 515	pRS315 FUS1-luciferase CEN LEU2	(Ayscough et al. 1999)
pCG 82	pKA51/pRS313 SLA1	(Ayscough et al. 1999)
pCG 88	pRS313 empty	(Ayscough et al. 1999)
pCG 83	pRS313 SLA1-ΔGap1+SH3#3	(Ayscough et al. 1999)
pCG 84	pRS313 SLA1-ΔSH3#1+2	(Ayscough et al. 1999)
pCG 85	pRS313 SLA1-ΔGap2	(Ayscough et al. 1999)
pCG 117	pRS313 SLA1-PSRP	(Ayscough et al. 1999)
pCG 118	pRS313 SLA1-ΔGap1	(Ayscough et al. 1999)
pCG 119	pRS313 SLA1-Δall SH3	(Ayscough et al. 1999)
pCG 538	pKA470/pRS313 mutated SLA1ΔHis3 (Δ518-574) part SHD1 CEN HIS	Ayscough Lab
pCG 539	pKA470/pRS313 mutated SLA1ΔHis3 (Δ518-737) SHD1+SHD2 CEN HIS	Ayscough Lab
pCG 542	pKA486/pRS313 mutated SLA1ΔHD2, HIS3 (Δ632-737) CEN HIS	Ayscough Lab
pCG 67	pRS316 SLA1	Ayscough Lab
pCG 92	pRS 316 empty	
pCG 537	pRS316 SLA1 with first NLS mutangenised CEN URA	Ayscough Lab
pCG 498	pRS416 URA3 CEN Hog1p-GFP	(Ferrigno et al. 1998)
pCG 347	Active Ras2p GFP	(Leadsham et al. 2009)
pCG 194	YEP13_52 (PDE2+promoter) LEU2	(Gourlay & Ayscough 2005b)
pCG 393	YEp13 empty LEU2	(Gourlay & Ayscough 2005b)

Table 3. Plasmids used in the study

2.4.4 Oligonucleotide primers

Primer	5' to 3' sequence
STE12 LoxP Knock out Forward	TCAGGTTGCATCTGGAAGGTTTTTATCGGACCTTCGA TTGGTATCGCATAGGCCACTAGTGGATCTG
STE12 LoxP Knock out Reverse	ATGAAAGTCCAAATAACCAATAGTAGAACAGAGGAAA TCTTAAAACAGCTGAAGCTTCGTACGC
FUS3 LoxP Knock out Forward	ATGCCAAAGAGAATTGTATACAATATATCCAGTGACTT CCAGTTGCAGCTGAAGCTTCGTACGC
FUS3 LoxP Knock out Reverse	CTAACTAAATATTTCGTTCCAAATGAGTTTCTTGAGGT CTTTCGTGCATAGGCCACTAGTGGATCTG

Table 4. Oligonucleotide primers used in the study

2.5 Yeast genetics techniques

2.5.1 Yeast transformation

Exogenous DNA was transformed into yeast cells by the lithium acetate method as follows. Yeast cells were grown overnight in liquid media and 1ml of the cell suspension was transferred to a 1.5ml microcentrifuge tube and pelleted in a bench centrifuge at 4000rpm for 4 minutes. The supernatant was discarded and the pellet resuspended in 0.5ml TE buffer at pH 8. The cells were pelleted as previously and resuspended in 0.5ml of 0.1M lithium acetate (LiAc) in TE at pH 8. Cells were then pelleted again and resuspended in 0.1ml of 0.1M lithium acetate (LiAc) in TE at pH 8. To this suspension 15µl of single stranded carrier DNA (boiled salmon sperm DNA, 10mg/ml) was added and the mixture was vortexed briefly. An appropriate quantity of DNA was then added, usually 2µl of mini prep plasmid, and the mixture was vortexed briefly. 0.7ml of 40% polyethylene glycol (PEG) in 0.1M LiAc in TE was added and the mixture was vortexed briefly. The microcentrifuge tube was then incubated at room temperature for 1 hour with rotation. Following this the cells were heat shocked at 42°C for 15 minutes. Cells were pelleted by centrifugation as previously and resuspended in 0.2ml of sterile H_20. The suspension was then decanted

onto dry agar plates with appropriate selective media and incubated at 30°C for at least 2 days until colonies were visible.

In the case of deletion cassette transformations, the protocol was altered so as to use cells in log growth phase. Overnight cultures were subcultured to an OD of 0.1 and grown to an OD of 0.5-0.7 before being used in the transformation. The cells were then transformed as above either with 15µl of unconcentrated PCR product or 2µl of concentrated product.

2.5.2 Generation of rho^0 petites

Method from (Fox et al. 1991) cited by (Heeren et al. 2004). Strains were grown overnight to stationary phase in YPD containing 25µg/ml of ethidium bromide. From this culture a second was inoculated in the same medium and grown overnight to stationary phase. The culture was streaked out to single colonies on YPD agar plates and these were subsequently checked for loss of functional mitochondria by growth on YPG.

2.5.3 Generation yeast knock outs using loxP deletion cassettes

Method from (Gueldener et al. 2002). To delete a gene, first a DNA cassette must be produced which will recombine with specific regions of the genome in order to disrupt the sequence of the target gene and insert a marker gene. A number of plasmids described in Gueldener et al. 2002 provide marker genes flanked by loxP sequences. A pair of PCR primers were designed which included the sequence of either 19 or 22 nucleotides adjacent to the loxP sequence and a further 45 nucleotide sequence from the beginning and end of the target gene. A PCR reaction using these

primers was then carried out in which the marker gene plasmid is used as the template DNA. This generated a DNA cassette containing the selection marker of choice, flanked by both loxP sites and specific sequences corresponding to the start and end of the target gene. Upon transformation of this DNA element into yeast cells, a recombination event should occur due to the 45 nucleotide sequences at either end of the cassette, resulting in the marker gene and loxP sites replacing the target gene. A diagram of the process is shown in Figure 8. A schematic diagram.

Successful disruption of the target gene allows the transformed yeast to grow on media selective for the marker gene. To confirm the marker gene had been inserted in the correct locus, colonies growing on selective medium were subjected to colony PCR. The primers used in this reaction consisted of a target gene specific primer with the sequence of a region adjacent to the target gene, and a deletion cassette specific primer, thereby producing a fragment of a defined size if the cassette was correctly inserted.

If necessary the loxP system allows for the removal of the marker gene by transformation with a URA selectable plasmid expressing Cre recombinase, resulting in recombination between loxP sites. The Cre recombinase plasmid can then be lost by growing cultures in nonselective media and then plating to single colonies on medium containing 5-FOA.

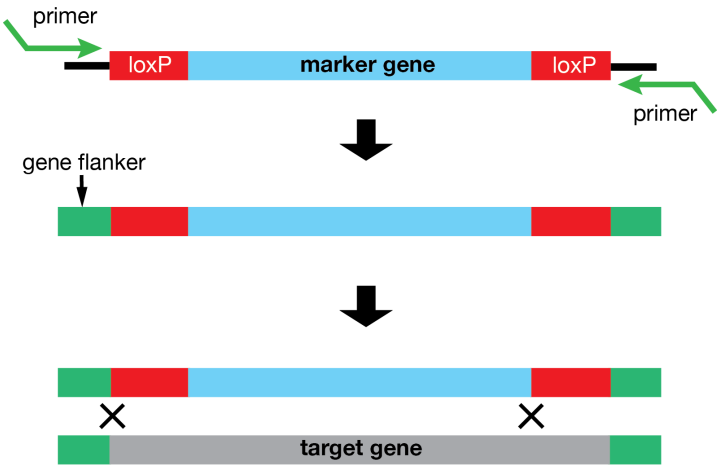

Figure 8. A schematic diagram showing the key steps in generating loxP cassettes for disrupting a target gene

2.5.4 Sporulation of diploids

Haploid yeast strains of opposite mating types were patched together onto YPD agar and grown overnight to mate. Cells were then patched to double drop-out minimal medium to select for diploids. For example, when mating a mat α strain which can synthesise histidine but is an adenine auxotroph with a mat a strain which can synthesise adenine but is a histidine auxotroph, selective media lacking both histidine and adenine will ensure only mated diploids will grow.

Diploid cells were transferred to pre-sporulation medium (0.8% Oxoid yeast extract, 0.3% Difco peptone, 10% glucose, 1M sorbitol, 1.5% Oxoid technical agar) and incubated at 30°C for 1-2 days. Cells were then transferred to sporulation medium (1% potassium acetate, 0.1% Oxoid yeast extract, 0.05% glucose, 1M sorbitol, 1.5% Oxoid technical agar) for 5-15 days until four-spored asci (tetrads) could be observed under the microscope.

2.5.5 Tetrad dissection

Following sporulation, colonies were picked from the sporulation agar plates and suspended in 50µl of cold 1mg/ml lyticase in sterile water. The suspension was incubated at room temperature for 8 to 15 minutes to digest the spore coat. 3µl aliquots were taken at several points during the digestion and ejected onto the edge of a dry YPD agar plate. Using a dissection microscope (MSM 400, Singer Instruments) cells from the aliquots were observed and asci containing four spores were identified. These were dissected using the integrated micromanipulator and positioned on the plate to allow them to grow into separate colonies. The plate was incubated at 30°C for 3 days or until colonies were visible.

2.6 Molecular biology techniques

2.6.1 Agarose gel electrophoresis

Agarose was dissolved in TAE by heating in a microwave and stirring until the liquid was clear. Normally the agarose was made at 0.8% for larger (1-10kb) DNA fragments, with higher percentages up to 1.5% to better resolve smaller fragments. The liquid was allowed to cool to around 60°C before ethidium bromide (10mg/ml) was added at 0.0167µl/ml (0.5µl in a 30ml minigel). The liquid was inverted several times to mix and poured slowly into the gel tray, and an appropriately sized comb was inserted. The gel was left to set for 30-60 minutes.

When set, the comb was removed and TAE was poured in to the tank to submerge the gel. An appropriate DNA marker was loaded in the first well (usually Promega 1kb DNA ladder G57511) and 6x loading buffer containing bromophenol blue was mixed

1 in 6 with the DNA samples, which were then pipetted into subsequent wells. The tank was then connected to a power pack with the anode connected at the same side as the wells, and the cathode at the opposite end. A voltage of 80V was applied to the tank for 30-60minutes. When sufficient migration had occurred as shown by the position of the visible bromophenol blue front, the tank was disconnected and the DNA visualised with UV light.

2.6.2 Extraction of DNA from agarose

When DNA fragments separated by agarose gel electrophoresis were to be extracted for further use, a QIAquick Gel Extraction Kit (Qiagen) was used according to the supplied protocol for use with a microcentrifuge.

2.6.3 Purification of plasmids

YT supplemented with an appropriate antibiotic (ampicillin or kanamycin) was inoculated with a colony of *E. coli* containing the desired plasmid and grown overnight at 37°C with shaking. 1ml of culture was centrifuged at 13000rpm for 30s to pellet cells and the supernatant was discarded by decanting. Plasmid DNA was extracted from cells using a QIAprep Spin Miniprep Kit (Qiagen) by following the supplied protocol.

2.6.4 Quantification of nucleic acid samples

A Spectrostar Nano UV/Vis spectrum absorbance microplate reader (BMG Labtech) was used with the LVis microdrop plate to analyse the concentration of nucleic acid in a 2μl sample.

2.6.5 *E. coli* transformation

A 50μl aliquot of frozen competent DH5α *E. coli* cell suspension was thawed on ice and mixed gently. A volume of plasmid solution containing at least 20ng of DNA and not exceeding 2.5μl was added and mixed gently by tapping the tube. The suspension was incubated on ice for 1 hour and then placed at 42°C for 90 seconds. 200μl of YT was added and the suspension was incubated with shaking at 37°C for 30 minutes. The suspension was then plated onto YT agar containing appropriate antibiotic to select for transformants and incubated overnight at 37°C.

2.6.6 Restriction enzyme digestion of DNA

Enzymatic scission of DNA at specific sequences was carried out using various restriction endonucleases from Roche, Promega and New England Biolabs. The manufacturers supplied appropriate buffers and recommended protocols which were adhered to with some variations. Typically 1μg of DNA was added to 2.5μl of 10x buffer as supplied and 1 unit of the restriction endonuclease. The reaction mixture was made up to 25μl with sterile dH_2O and incubated at the appropriate temperature for the enzyme (usually 37°C). Incubation times varied from 1 to 24 hours depending on enzyme activity. Depending on the outcome, reactions were repeated with changes made to amounts of each component or incubation times to improve digestion.

2.6.7 Polymerase Chain Reaction (PCR)

Polymerase chain reaction (PCR) was used to amplify DNA sequences for numerous purposes including generating knockout cassettes and genome analysis. The reaction depends on a thermostable polymerase from the bacterium *Thermus aquaticus*, referred to as Taq pol. Increased temperature is used to separate double stranded

DNA, and then a lower temperature is used to allow annealing of single strands. Oligonucleotide primers are included in the reaction which will anneal to the template DNA and from which Taq pol will synthesise a complimentary strand in a 5' to 3' direction at a third intermediate temperature. The new strands synthesised in this process can then act as template strands as the temperature cycle is repeated, resulting in amplification of the target sequence.

A basic PCR reaction in a thermocycler was used for most reactions with denaturation steps at 94°C, annealing steps at 52°C and elongation steps at 72°C. This consisted of an initial 5 minute denaturation step, followed by a repeating loop of 1 minute at 94°C, 1 minute at 52°C and 2.5 minutes at 72°C. This loop repeated 30 times before a final 10 minute elongation step at 72°C. The heating profile of the reaction was modified on occasion, for example by decreasing the length of the elongation step to increase the preference for shorter fragments.

A typical 100µl reaction mix used for amplification of a deletion cassette is given in Table 5. Taq polymerase, PCR buffer, MgCl2 and dNTPs were supplied by Invitrogen. Primers were synthesised by Eurofins MWG Operon.

Reagent	Volume (µl)
10x PCR buffer (without MgCl2)	10µl
MgCl2 (50mM)	4µl
forward primer (100µM)	1µl
reverse primer (100µM)	1µl
dNTPs (10mM)	2µl
Taq pol (5 units/µl)	0.8µl
template DNA (~150ng/µl)	1µl
dH2O	80.2µl

Table 5. Typical PCR reaction mixture

2.6.8 Phenol/chloroform/isoamyl alcohol concentration of DNA

The DNA sample was made up to 500µl with sterile dH_2O and an equal volume of phenol:chloroform:isoamyl alcohol (25:24:1) was added. This solvent mixture is non-polar and has a higher density than water, so that organic material dissolves in the lower layer while polar nucleic acids remain in the aqueous upper layer. The mixture was vortexed for 1 minute and centrifuged at full speed in a bench microcentrifuge for 1 minute. Taking care not to carry over any of the organic phase, the aqueous phase was removed to a clean microcentrifuge tube. The volume of the aqueous phase was determined and a 0.1 volume of 3M sodium acetate (pH 5.2) was added and mixed well. A 0.6 volume of isopropanol was added and mixed well. The tube was incubated at -18°C overnight. The following day, the tube was centrifuged at full speed for 10 minutes to pellet the precipitated DNA. The supernatant was removed and the pellet washed with 1ml of 70% ethanol. The tube was centrifuged for 10 minutes at full speed, and the supernatant discarded. The tube was then left open until any remaining ethanol had evaporated , and the DNA was resuspended in TE.

2.6.9 Whole cell protein extraction for SDS PAGE

Protein samples for use in polyacrylamide gel electrophoresis were prepared according to the method described in (von der Haar 2007). The concentration of cells in a culture was counted under a microscope using a haemocytometer. The volume containing a defined number of cells (typically between 0.5×10^8 and 2×10^8) was harvested by centrifugation for 4 minutes at 1200g. For log cultures at an OD_{600} of 0.5 this was around 10ml. Alternatively if the electrophoretic analysis was not to be quantitative, the cell number was estimated from the optical density. Harvested cells were resuspended in 200µl of lysis buffer (0.1M NaOH, 0.05M EDTA, 2% w/v SDS,

2% v/v β-mercaptoethanol) and incubated at 90°C for 10 minutes. 5µl of 4M acetic acid was added and the sample was vortexed for 30 seconds before incubating at 90°C for 10 minutes. 50µl of loading buffer (0.25M Tris-HCl pH6.8, 50% glycerol, 0.05% bromophenol blue) was added and the sample was centrifuged for 1 minute at 13000rpm in a bench microcentrifuge before use. Alternatively the sample may have been frozen following addition of loading buffer for use at a later date.

2.6.10 Polyacrylamide gel electrophoresis

Polyacrylamide gels were cast with two layers; an upper stacking layer and a lower resolving layer. These gel layers were made in 50ml falcon tubes by mixing components as in Table 6.

Reagent	Resolving gel	Stacking gel
Acrylamide 40% (BIORAD)	2ml	0.375ml
1.5M Tris (pH8.8), 0.4% SDS	2ml	-
0.5M Tris (pH6.8), 0.4% SDS	-	0.75ml
dH20	4ml	1.875ml
TEMED (BIORAD)	5µl	3.5µl
APS (BIORAD) 10%	35µl	35µl

Table 6. Polyacrylamide gel layer recipe

APS was freshly dissolved in water at 10% w/v. Gel cassettes were prepared consisting of two glass plates with a rubber gasket to seal the sides and bottom held together by a clamp on either side. First the resolving layer would be made, mixed by inversion, and poured into the gel cassette. 1ml of isopropanol was pipetted on top to flatten the surface and the gel was allowed to set for at least an hour. The isopropanol was poured off and the stacking layer was made, mixed by inversion and poured on top. A comb was inserted to form the wells and the gel was left to set for at least 30 minutes. The comb and gasket were then carefully removed and the cassette was placed in a gel tank and sealed against the central column. TGS was poured in to submerge the wells, and protein samples in loading buffer were pipetted in along with

a well containing protein marker (ColorPlus marker P7709S). The electrodes were connected to a power pack and a voltage of 90V was applied until the bromophenol blue front was seen to enter the resolving layer, upon which the voltage was increased to 120V, and the gel was run until sufficient separation could be assumed. The tank was the disconnected from the power pack and the cassette removed.

2.6.11 Semi-dry transfer to PVDF

A polyacryamide gel containing protein samples separated by electrophoresis was removed from the cassette and the stacking layer was removed and discarded. The Resolving layer was carefully removed and placed in transfer buffer (0.0029% w/v glycine, 0.0058% w/v Tris base, 0.00004% w/v SDS, 20% v/v methanol). PVDF Western blotting membrane was cut to the size of the gel and wet thoroughly in methanol and then placed in transfer buffer for 10 minutes. Two pieces of blotting paper were cut to the same size and soaked in transfer buffer. One of the pieces of blotting paper was placed on the anode plate of a Trans-Blot Semi-Dry Transfer Cell (BIORAD), followed by the PVDF membrane, the polyacrylamide gel, and the second piece of blotting paper. The cathode plate was placed on top and connected to a power pack. A voltage of 25V was applied to the apparatus for 15 minutes.

2.6.12 ECL detection

Following semi-dry transfer, the PVDF membrane was placed in blocking buffer (5% w/v dried milk powder (Marvel) in PBST (PBS containing 0.2% Tween-20)) and incubated at room temperature for 45 minutes with shaking. The membrane was then briefly rinsed in PBST twice, followed by a 15 minute wash and two 5 minute washes. PBST was then removed and blocking buffer containing the required HRp-

conjugated antibody at the appropriate dilution was added, and the membrane was shaken at room temperature for 20-30 minutes. The membrane was then washed twice in PBST briefly followed by a 15 minute wash and three 5 minute washes, and finally was left in PBST.

In a dark room, ECL solutions (Table 7) were mixed in equal proportions. The PBST was poured off the membrane and the mixed ECL solution was added and shaken for 1 minute. The membrane was then removed and placed in a clear plastic sleeve. A sheet of film (Hyperfilm ECL, Amersham) was exposed to the membrane for varying lengths of time depending on signal intensity, ranging from a few seconds to 10 minutes. Leaving the membrane under light for several minutes before exposing the film was also used to reduce excessively intense signals. After exposing the film, it was developed using a Compact X4 Automatic Processor (Xograph Healthcare).

Reagent	Stock concentration	Solution I	Solution II
Luminol	250 mM	1 ml	-
p-coumaric acid	90 mM	0.44 ml	-
TRIS. HCl (pH8.5)	1 M	10 ml	10 ml
H_2O_2	30%	-	64 µl
H_2O	-	Up to 100 ml	Up to 100 ml

Table 7. Reagents for ECL solution

2.7 Phenotypic analysis

2.7.1 Microscopy

Fluorescence microscopy was carried out using an Olympus IX81 inverted research microscope. Images were captured through a Hamamatsu photonics C4742 digital camera, with light excitation from an Olympus MT20 illumination system. Olympus CellR imaging software was used to control the apparatus. Images were taken at 100x magnification using automatic contrast adjustment unless otherwise stated in the

figure legend. The numerical apertures of the 60x and 100x objectives were 1.35 and 1.40 respectively.

2.7.1.1 Fluorescent proteins

Cells expressing proteins fused to green fluorescent protein (GFP) were used to observe localisation. An excitation wavelength of 488nm was used and viewed at an emission wavelength of 509nm using filters on the microscope stage.

2.7.1.2 Calcofluor white staining

Cultures in log growth phase were incubated in 25μM calcofluor white at room temperature for 5 minutes before being place on a microscope slide and viewed under the microscope.

2.7.1.3 Actin-phalloidin staining

134ul of 37% formaldehyde was added to 1ml of a log yeast culture in a microcentrifuge tube and incubated at room temperature for 30 minutes to 1 hour. The tube was then centrifuged at 4000rpm for 4 minutes in a bench microcentrifuge and the pellet washed twice in PBS containing BSA (1mg/ml) and TX-100 (0.1%). The pellet was resuspended in 40ul of the same solution and 1ul of rhodamine phalloidin in methanol was added. The tube was incubated in the dark at room temperature for 30 minutes. The cells were then washed twice in PBS containing BSA (1mg/ml) and 3ul was spotted onto microscope slides and viewed under a fluorescence microscope.

2.7.2 Growth analysis in multiwell plates

Overnight cultures were grown in 3-5ml volumes in the appropriate medium. The cell density of each culture was determined by the OD_{600} and cultures were diluted to a density OD_{600} of 0.1 in Greiner Bio-one 24-well cell culture plates. Cultures were grown in a Spectrostar Nano plate readers (BMG Labtech). Standard instrument settings are given in Table 8.

Parameter	Value
Cycle time (sec)	1800
Flashes per well	3
Excitiation	600
Shaking frequency (rpm)	400
Shaking mode	double orbital
Additional shaking time before each cycle (s)	30
Target temperature (°C)	30

Table 8. Spectrostar Nano settings for growth analysis

2.7.2.1 Growth data analysis

All data obtained from plate reader was blank corrected before further analysis. Data was displayed on a graph with a log Y axis. Data was rearranged and saved as a .csv file and loaded in R. Maximum growth rates were calculated over 7 data points (3.5 hrs) using an R script (https://www.princeton.edu/genomics/botstein/protocols).

2.7.3 Spot assays

Plates with the appropriate agar medium were dried in a drying oven for 15-30 minutes. The optical density of cultures was measured and diluted to an OD_{600} of 0.1 in 500µl (unless otherwise stated) in a sterile autoclaved steel multiwell plate. If a 1/10 dilution series was to be used, the culture was then diluted in adjacent wells by pipetting 50µl into 450µl of H_20. Uniform volumes of cultures were transferred to the dried agar plates by submerging flat-bottomed steel pins into the wells and then

placing on the agar. Once dried the plates were inverted and incubated at 30°C for at least 2 days until colonies were visible.

2.7.4 *lacZ* reporter assays

2.7.4.1 β-galactosidase liquid culture assay

Reagents are described in Table 9. Cells transformed with a *lacZ* plasmid were grown overnight in selective media and then subcultured to an OD_{600} of 0.1 and grown to an OD_{600} of 0.5. In a 1.5ml microcentrifuge tube, 100µl of culture was added to 500µl of Z buffer and incubated at 30°C for 30 minutes. 150µl of ONPG solution was added and samples were shaken by hand to start the reaction. After sufficient colour was visible in the solutions, 400µl of 1.5M Na_2CO_3 was added to stop the reaction. Samples were centrifuged for 30s at 16000g and absorbance measured at 420nm and 550nm.

Reagent	Description
Z buffer	60mM Na_2HPO_4, 40mM NaH_2PO_4, 10mM KCl, 1mM Mg_2SO_4, 50mM β-mercaptoethanol (β-mercaptoethanol added directly before use)
ONPG	4mg/ml in water, made directly before use

Table 9. Reagents for β-galactosidase assay

The following formula was used to calculate the Miller units values, where t is the reaction time and v is the volume assayed.

$$1 \text{ Miller unit} = 1000 * \frac{(Abs_{420} - (1.75 * Abs_{550}))}{(t * v * Abs_{600})}$$

2.7.4.2 X-gal colony assay

Selective agar media containing X-gal was made as described in 2.3.1, except that the volume was made up to 170ml instead of 200ml before autoclaving. After

autoclaving, the media was cooled to 50°C in a water bath. 400µl of 20mg/ml X-gal in N,N-dimethylformamide (DMF) was added, along with 20ml of potassium phosphate buffer (1M, pH7) and 10ml glucose (40%). Plates were poured and allowed to set and kept at 4°C protected from light. Cultures were spotted to X-gal agar as described in section 2.7.3.

2.7.5 Firefly luciferase reporter assay

Overnight cultures expressing a firefly luciferase construct were grown in selective media, and subcultured for growth to log phase. PLB and Dual Glo Luciferase buffer were placed at room temperature 30 minutes before beginning assay. When cultures were at OD_{600} of around 0.5, they were diluted to a matching cell density and 20ul of each added to the wells of an opaque white 96 well microtitre plate containing 20ul of PLB. To this 40ul of Dual Glo Luciferase buffer containing the luciferase substrate was added and the plate was incubated with shaking at room temperature for 10 minutes. Luminescence was measured using Spectrostar Nano plate readers (BMG Labtech).

2.7.6 High resolution respirometry

The measurements of the consumption of O_2 from mitochondria were made using an Oroboros O2K Oxygraph High Resolution Respirometer. The apparatus was controlled using Oroboros DatLab 4 software, which also performed subsequent data analysis. The respirometer was calibrated as described in the manufacturer's documentation before each assay. Cells subcultured from an overnight culture and grown to log phase were counted with a hameocytometer and diluted to a concentration of 3.5×10^6 cells/ml. This cell suspension was placed into the

respirometer and the chambers were sealed. Triethiltyn bromide (TET) (Sigma), Carbonylcyanide p- trifluoromethoxyphenylhydrazone (FCCP) (Fluka), and Antimycin A (AntA) (Sigma) were added by injection through chamber inlets. The concentrations used are shown in Table 10.

Drug	Final concentration (mM)
TET	0.2
FCCP	0.012
AntA	0.002

Table 10. Concentrations of drugs used in respirometry

2.8 Transcript expression profiling

Samples for microarray analysis were prepared from cultures grown in selective media to log growth phase, and pelleted by centrifugation. Frozen samples were delivered to Source Bioscience (http://www.lifesciences.sourcebioscience.com/) for total RNA isolation. Following isolation, RNA sample quality was assessed to confirm that OD 260/280 ratios were greater than 1.9 and samples displayed two distinct ribosomal peaks in a fluorescence spectrum, with a 28s/18s peak ratio close to 2.0.

2.8.1 Affymetrix Yeast 2.0 GeneChip

The Affymetrix Yeast 2.0 GeneChip was used, which contains probes for detection and hybridisation of transcripts from *S. cerevisiae.* There is a total of 5,744 probe sets for 5,841 genes of the 5,845 genes present in *S. cerevisiae*. Further information is available from the product data sheet (http://www.affymetrix.com/support). Isolated RNA samples were hybridised with the chip according to manufacturer instructions and scanned to produce the raw data CEL files.

2.8.2 Microarray analysis tools

Analysis of microarray data and quality control assessments were performed with two pieces of software. Affymetrix Expression Console (version 1.3.1) was used to perform principal component analysis and to visualise probe intensity on the chip layout.

The *affylmGUI* package was run using R (version 3.1.0) to generate MA and volcano plots and to differential expression data from raw CEL file data. This is a graphical user interface which implements the *limma* linear modeling approach (Smyth 2005).

3 Transcript expression profile analysis of mutants with altered cytoskeletal dynamics

3.1 Chapter introduction

Reduced actin dynamics is associated with a large number and variety of phenotypes (Eitzen et al. 2002; Ayscough & Drubin 1998; Belmont, Patterson, et al. 1999; Gourlay et al. 2004). These include those associated with actin-regulated processes, such as endocytic and morphological defects, as well as other which are less easily explained such as increased generation of ROS and increased transcriptional accuracy (unpublished data). Investigation into the *act1-157* mutation which increases filament turnover rates suggested that cells expressing this isoform have increased rates of endocytosis and reduced ROS levels (Gourlay et al. 2004; Belmont, Patterson, et al. 1999). Additionally, previous work from our lab utilised a microarray study to investigate causes of phenotypes observed in mutants of the actin filament depolymerising protein cofilin (V. N. Kotiadis et al. 2012). This revealed links between cytoskeletal dynamics and cellular stress response pathways which I was interested in investigating further.

To investigate how yeast cells modulate RNA transcription programs in response to changes in the dynamic status of the actin cytoskeleton, I carried out a microarray study comparing mutants with altered actin dynamics to a strain with wild-type actin. Observations from the altered transcription profiles were then used as the basis to design further experiments into how actin dynamics is related to the numerous interesting phenotypes observed in these actin mutants.

High-density oligonucleotide expression arrays, or microarrays, produce large amounts of data about the RNA transcript expression patterns, and are widely used in biological research (Wu et al. 2004). These large data sets can reveal how genetic differences affect biological pathways and are useful for generating hypotheses to explain how genotype relates to phenotypic observations.

The arrays used in this study were the GeneChip Yeast Genome 2.0 Array (Affymetrix). This array contains 11 probe pairs per probe set, with each probe consisting of a 25 bp oligonucleotide. The Yeast 2 array detects RNA transcripts for 5841 of 5845 *S. cerevisiae* genes. Each probe pair includes a perfect match (PM) and mismatch (MM) probe. The PM probe is a DNA sequence complimentary to a region of the transcript, while the MM probe is the same DNA sequence but with the central base altered. This allows for differentiation between specific and non-specific binding during hybridization with the sample. Upon scanning the arrays, a value is obtained for each probe which is a measure of the amount of hybridization that has taken place. These values must be adjusted to account for both any optical noise and the differences between signal at PM and MM probes (Wu et al. 2004).

3.2 Sample preparation

The strains used in this study were first described in Belmont & Drubin 1998 and Belmont et al. 1999. The mutations were constructed by oligonucleotide-directed mutagenesis as described in Wertman et al. 1992, and confirmed in the final haploid strain by sequencing the region containing the mutation.

Total RNA extracts were prepared as described in Chapter 2. All strains used in this study were transformed with an empty LEU plasmid vector to allow the wild-type to be used in another study which is not discussed here. Cultures were grown overnight in –LEU SD media, inoculated into fresh media and grown to log phase (OD_{600} = 0.5) before RNA was extracted and sent for processing. The genotypes of each sample and the filenames of the raw data file are shown in Table 11.

Genotype	CEL file name
ACT1, mat α	769A124_A.CEL 769A124_C.CEL 769A124_D.CEL
act1-159, mat α	339_5998.CEL 339_5999.CEL 339_6000.CEL
act1-157, mat α	13B124_B.CEL 13B124_C.CEL 13B124_D.CEL

Table 11. Sample identities used in microarray study

3.3 Probe summarisation

Probe summarization algorithms are used to perform background correction, normalise the data and summarise the multiple probe level values. Normalisation is the process by which the non-biological variation in data is minimised in order to make multiple array data sets comparable. Summarisation involves combining the 11 probe pairs to give a single expression value for the genes represented by each probeset. Systematic variation can occur for various reasons including differences in RNA purity or labeling efficiency. The robust multi-array average (RMA) method described in (Irizarry et al. 2003) was used in this study. The background correction is performed is a non-linear correction based on the distribution of PM values within a single chip. Quantile normalisation is used in the RMA algorithm, and the values are summarised to an expression value with a median polishing model fitting method.

3.4 Quality assessment and control

Several data quality metrics were used to assess the validity of the data and to identify any unexpected variations in the summarised probe data before continuing to further analysis. Two programs were used for this; Affymetrix Expression Console (version 1.3.1), and R (version 3.1.0) running the *affylmGUI* package which implements the *limma* linear modeling approach (Smyth 2005).

3.4.1 Probe intensity

The probe cell intensities were viewed using Affymetrix Expression Console, which displays the raw data intensities arranged by their position on the array chip. Comparison of these images was used to determine if any of the arrays were damaged or if there are any major intensity issues on regions of the chip. Intensity is indicated by colour, with the darkest blue indicating the lowest intensity and white indicating the highest intensity. An example of one of these images is shown in Figure 9. All samples produced very similar probe intensity images indicating no major issues with the chip intensity.

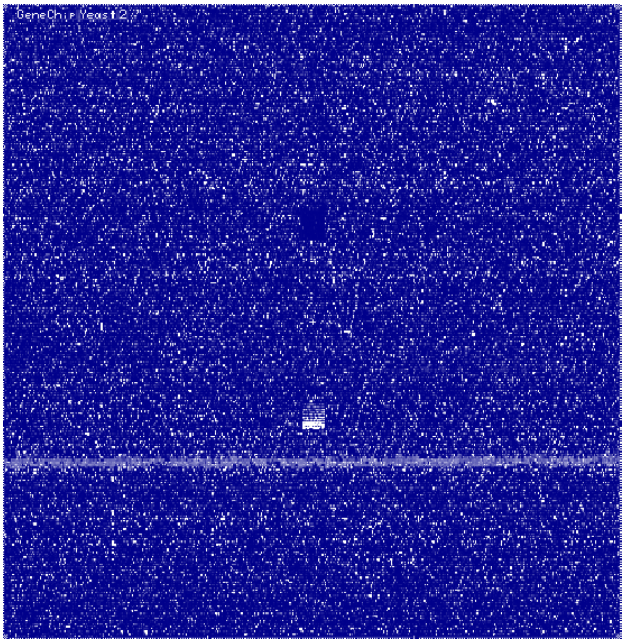

Figure 9. Probe intensity view of sample 769A124_A.CEL

3.4.2 Intensity distribution

Boxplots were used to show the intensity distribution of each sample prior to and following RMA normalisation. This plot is used to compare the probe intensities between arrays, and can indicate arrays that are particularly different from the others and also indicate if this is corrected by normalisation. The boxplots in Figure 10 and Figure 11 show that normalised data have similar intensity distributions, and variation between samples has been minimised by the RMA algorithm. The central line in the box represents the median value, and the whiskers indicate the range of values not considered outliers.

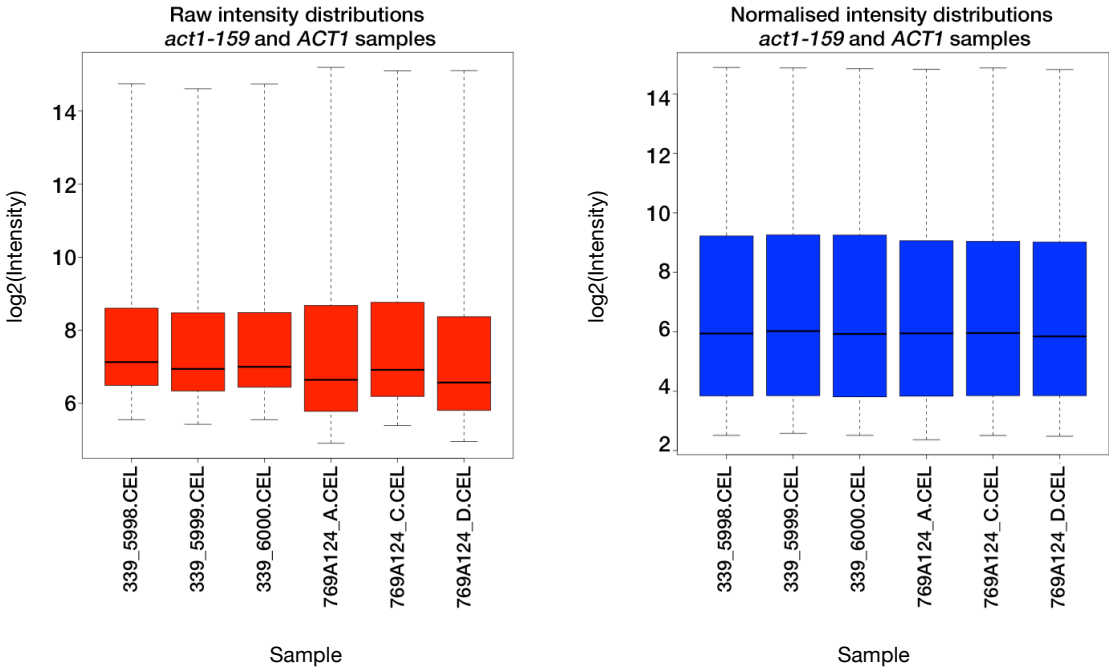

Figure 10. Intensity box blots for raw and normalised data from *act1-159* and *ACT1* samples.

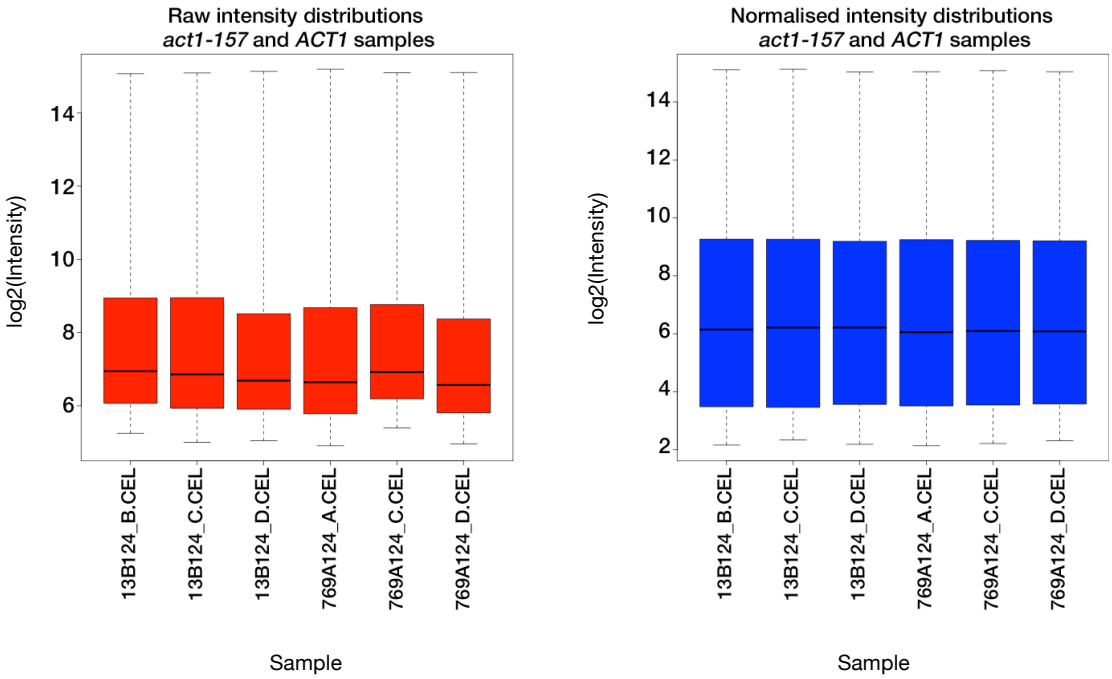

Figure 11. Intensity box blots for raw and normalised data from *act1-157* and *ACT1* samples.

3.4.3 Individual sample MA plots

MA plots compare the log2 fold change for the gene (M) with the average expression level of the gene (A) across the arrays in the comparison. Following the assumption

that the majority of genes in any comparison will not be differentially expressed, most of the normalised data points should lie along an M value of 0. This approach was used here to compare individual samples.

Normalised data from individual *act1-157* samples is compared to other samples from the same strain in Figure 12. These graphs indicate a possible problem with sample 13B124_D, as when this array was compared with either of the other two there was a noticeable region of data points for which the M value increases above 0, while a small number of data points have a large negative value for a similar A value. The MA plot comparing samples B and C is mostly symmetrical along M=0 indicating similar distribution of the data with less spread in the log2 fold change values.

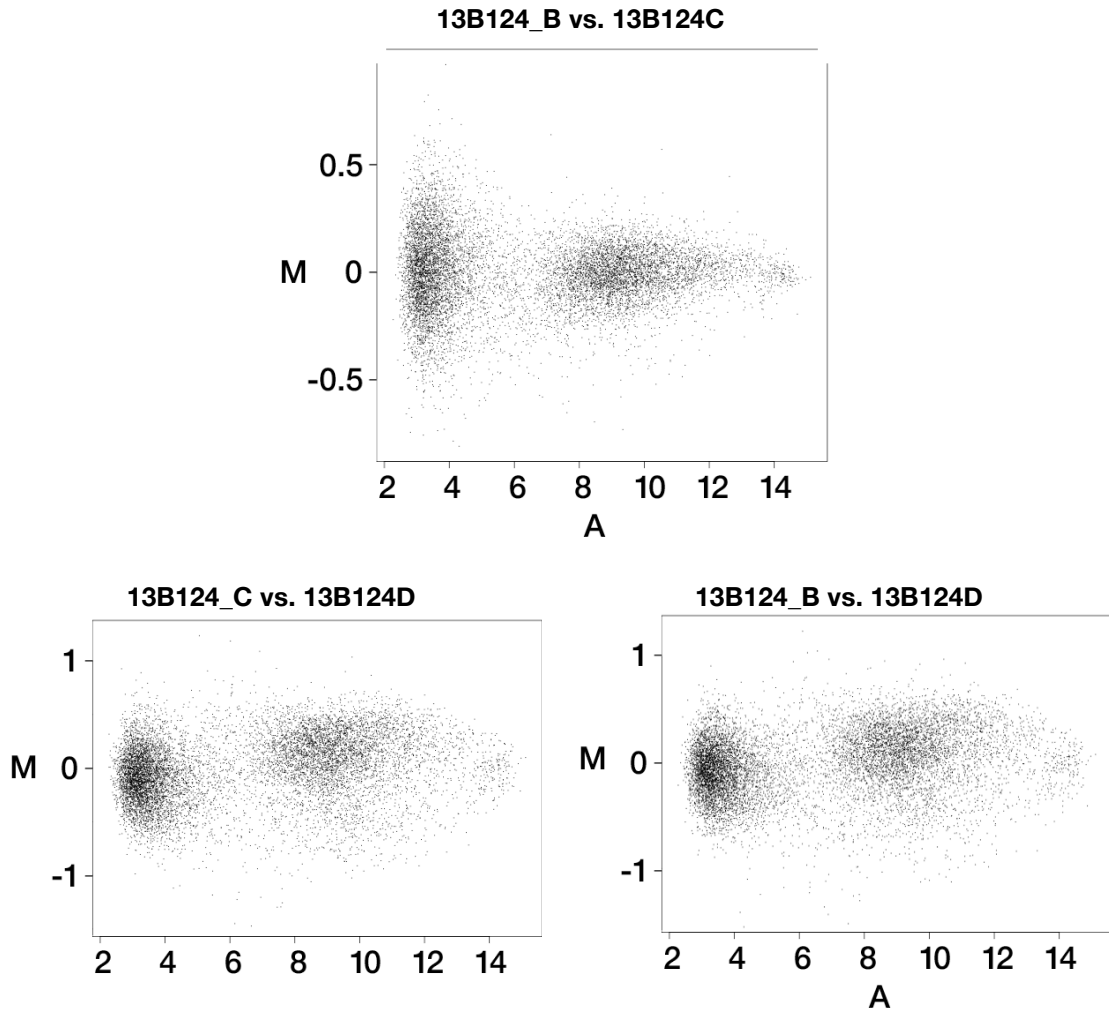

Figure 12. MA plots comparing each individual *act1-157* sample to one another.

3.4.4 Principal component analysis

Principal component analysis is a useful method for visualising large data sets to assess if replicates of a sample are more similar to each other than to samples from other conditions. This analysis was performed using Affymetrix Expression Console. This approach reduces the dimensionality of the data by identifying directions along which the most variation occurs (Ringnér 2008). The first principal component, PCA1, is the direction along which the most variation occurs. PCA2 then covers as much as possible of the remaining variation, and PCA3 covers as much variation as possible not covered in PCA2.

Graphs for this analysis are shown in Figure 13. Samples are displayed in 3D space based on the three principal components. Clustering indicates similar distributions and generally correlates with sample type. In both cases sample types cluster well along PCA1. Again I observed an issue with the *act1-157* sample 13B124_D as it does not cluster with the other two samples of this strain along any of the PCA axes.

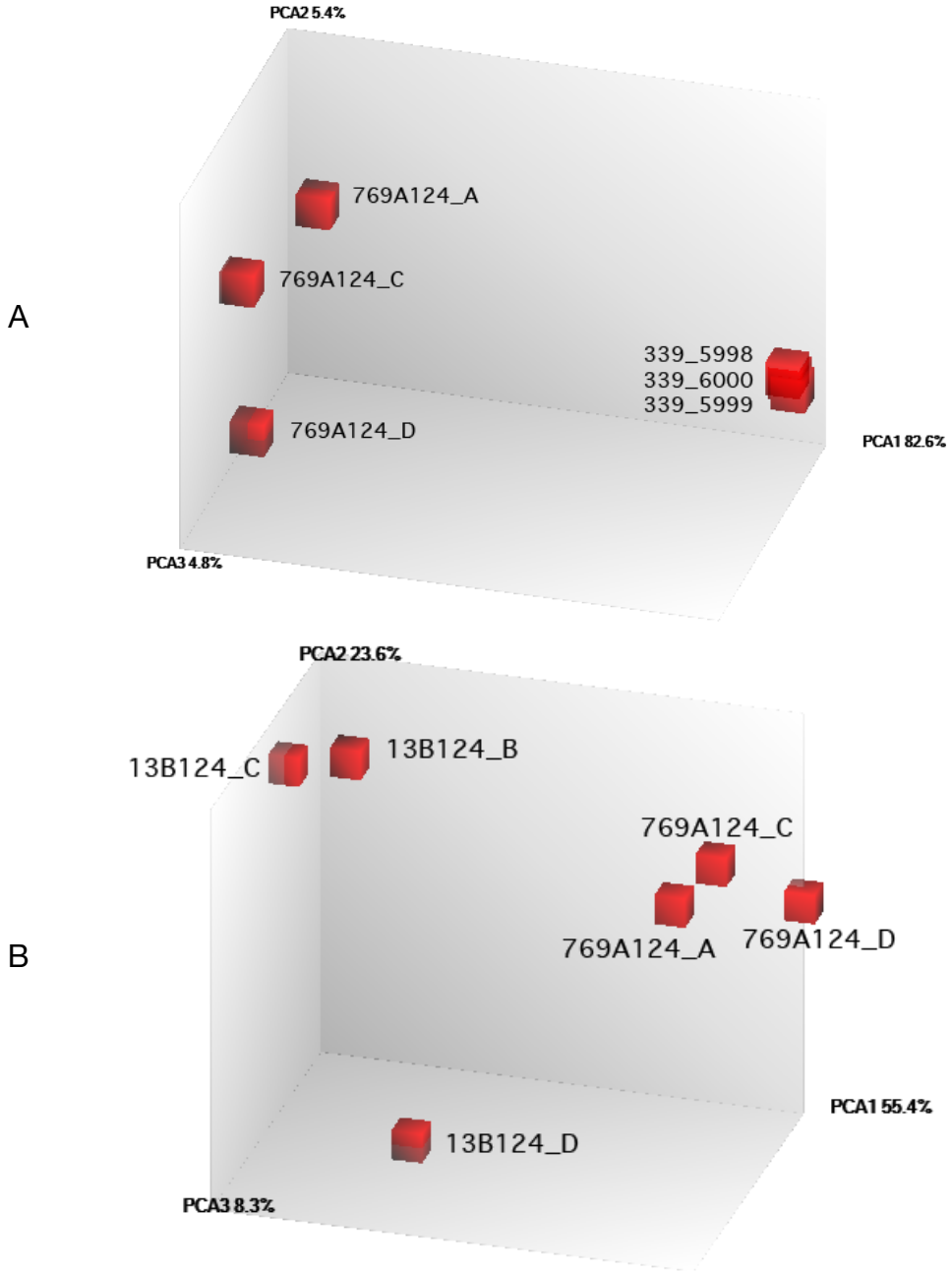

Figure 13. Principal component analysis of *ACT1* and *act1-159* samples (A) and *ACT1* and *act1-157* samples (B)

Both the MA plot and principal component analyses showed that *act1-157* sample 13B124_D did not correlate well with either of the other replicate samples. The reasons for this are not clear but I chose to exclude this sample from the differential expression analysis.

3.5 Analysis of differential expression results

Having assessed the data quality and excluded outlying data sets, the normalised data was used to calculate the differential expression results using affylmGUI. This process compared the expression values from replicate samples for each of the two mutants with those of the wild-type. A number of statistics for each gene were calculated indicating the extent of the difference in expression levels and measures of confidence based on the variation. At this stage the data set still included all of the 5841 *S. cerevisiae* gene probes on the chip, although the majority of these did not indicate differential expression. To analyse the data, I applied a threshold to exclude genes which were not shown to be significantly differentially expressed. The metric I chose to use for this was the B statistic. This is the log odds that a gene is differentially expressed, and is adjusted for multiple testing by assuming that 1% of the genes are differentially expressed. A significance threshold value for of 95% odds of differential expression was chosen, which corresponds to a B statistic of 2.94 and above. Additionally, the lists were filtered to remove any genes not from *S. cerevisiae* (such as those corresponding to the *S. pombe* probes on the yeast2 chip, or any of the spike controls used).

3.5.1 Volcano plots

The volcano plots in Figure 14 shows the log odds of differential expression (B statistic) of each gene against the fold change for the comparisons of *act1-159* and *act1-157* samples against the wild-type. The data forms the characteristic volcano shape with data points with a higher fold change being more statistically likely to be differential expressed. Conversely, the odds of differential expression are low for genes with fold changes approaching zero. It can be seen that there is a trend towards increased expression rather than decreased expression in both mutants, as there are more data points above the threshold line with positive fold change values. These plots show that there were many more differentially expressed genes above the threshold in *act1-159* cells than *act1-157* cells. This was to be expected as the mutation which reduces actin dynamics has more pronounced phenotypes.

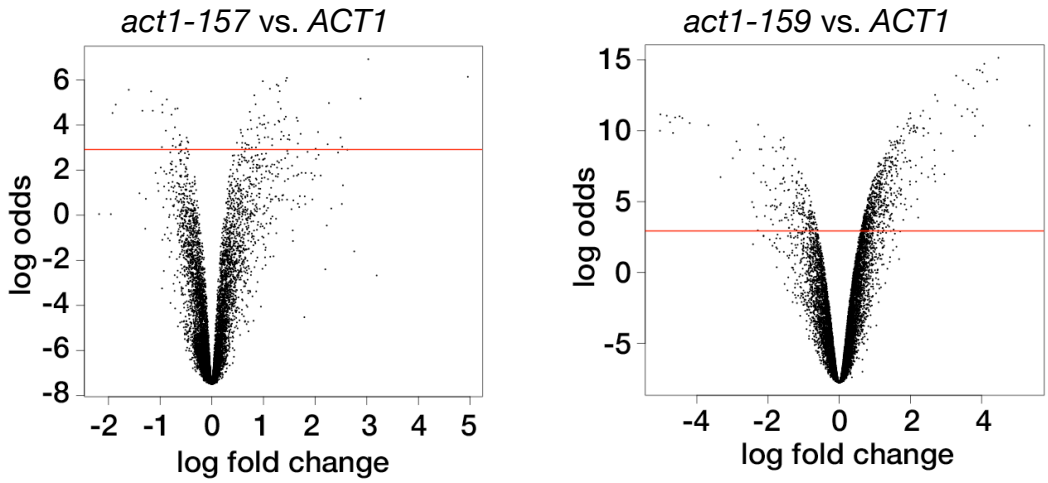

Figure 14. Volcano plot comparing global transcription of *act1-159* and *act1-157* to wild-type. The red line indicates the threshold value, and data points above the line represent genes which had at least 95% odds of differential expression

3.5.2 Identifying processes affected by actin dynamics

Gene ontology uses curated databases of gene information which are queried with a set of genes and returns information about their biological roles (Ashburner et al. 2000). This can be used to identify cellular processes which may be affected in a sample by sorting differentially expressed genes into categories and ranking them by the quantity involved in the process.

To carry out gene ontology analysis, I used the lists of genes which were differentially expressed above the B statistic threshold. In the case of a probe being annotated as hybridizing with multiple transcripts, only the first of these was used in the list to prevent a single probe set being interpreted as multiple genes. Gene lists were submitted to SGD GO Slim Mapper (http://www.yeastgenome.org/cgi-bin/GO/goSlimMapper.pl). In total 748 gene transcripts fell within this threshold for the analysis of *act1-159* cells, with 607 of these being up-regulated and 141 being down-regulated. In *act1-157* cells there were 148 transcripts which were up-regulated and only 18 were down regulated.

3.5.2.1 *act1-159* gene ontology

The top ten GO process terms for genes up-regulated in the *act1-159* mutant are shown in Table 12. This table omits the category of ORFs with unknown biological process roles, of which there were 130. Following this, the largest GO term was 'response to chemical', which includes genes for multi-drug resistance proteins such as *PDR3* and *QDR1*, as well as genes of specific chemical response pathways.

A number of signaling genes, some of which are also involved in response to chemical, are up-regulated. Of note is the increased transcript levels of both the membrane pheromone receptor *STE2* and the MAPK *FUS3*, which is normally activated via *STE2* activation by the presence of extracellular pheromone from cells of the opposite mating type. The transcript for *CLN2*, a cyclin involved in the cell cycle arrest response to mating factor, is also increased. Additionally, the gene with the highest fold change was the pheromone-regulated gene *PRM8*, with a fold change of over 39.

The microarray data also indicates changes in transcriptional regulation of other MAPK pathways. From the *HOG1* pathway, which responds to osmotic shock, the transcript levels of membrane osmosensor *SLN1* are increased in *act1-159* cells. Further down this pathway, levels of transcripts for the kinase *SSK22* and the phosphatase *PTP2* are also increased. A MAPK involved in signaling in response to cell wall stresses, *SLT2* (also called *MPK1*), is up-regulated. The increased transcript level of numerous genes involved in cell wall biogenesis suggests there may be cell wall damage in this mutant. Furthermore several regulators of cAMP signaling have increased transcript levels. These include the cAMP phosphodiesterase *PDE1*, and the cAMP dependent kinase *TPK1*.

24 genes involved in cytoskeletal organization have increased transcript levels, including the Arp2/3 complex activator *ABP1*. Several genes involved in actin cortical patch organization including *VRP1, ENT2* and *BBC1* are up-regulated, as well as the capping protein genes *CAP1* and *CAP2*, which regulate polymerisation of filaments. Viewed together these transcript level changes do not seem to suggest a

well-coordinated transcriptional response to the loss of actin dynamics as a result of the *act1-159* mutation.

Some genes under the response to DNA damage term are up-regulated. These include a 2.4 fold increase in *RAD55*, a member of the RAD52 epistasis group which repairs DNA double-strand breaks (DSBs). *RIF1* which also contributes to DSB repair is also increased. Two components of the NuA4 histone acetyltransferase complex, *EAF1* and *EPL1* are up-regulated. Actin and actin-related proteins are found within this complex (Sunada et al. 2005) and this raises the possibility that cytoskeletal dynamics is linked to histone modification and chromatin remodeling. Significant disruption to transcription patterns could occur as a result of loss of mobility of chromatin remodeling complexes.

A smaller proportion of the differentially expressed genes in *act1-159* cells were found to be down-regulated in this study. The ten GO process terms with the highest frequency are shown in Table 13. As previously, the 32 genes with unknown process were omitted from this table.

The most frequent term was lipid metabolism. This includes genes of a number of diverse roles and cellular locations. A few of the genes under this term are involved in phospholipid metabolism, and have roles at various cellular membranes including the endoplasmic reticulum, nuclear, mitochondrial and outer membranes.

There is down-regulation of genes in the terms for meiotic and mitotic cell cycle control, organelle fission and chromosome segregation. As these processes all relate

GO term	Frequency	Genome Frequency	Gene(s)
response to chemical	54 out of 601 genes, 9%	388 of 6335 genes, 6.1%	*PDR3, FUS3, EDE1, FIG1, ZTA1, FRM2, FUS1, MXR2, GRX1, KAR4, HSP30, FIG2, YDL124W, SNF3, HBT1, SNQ2, NRG1, AFR1, UPC2, MHR1, PDR15, TSA2, FRD1, HPA3, SPI1, HSP12, STE2, PTR3, AGA2, SUT1, ASK10, VMR1, SLT2, GRE3, DOT5, QDR1, YAP5, SIP4, CBF1, IXR1, HAP1, FET3, ROT1, GAD1, MLF3, MET4, AGA1, YNR064C, DDR2, SVS1, USV1, CLN2, OPY2, ASR1*
transcription from RNA polymerase II promoter	51 out of 601 genes, 8.5%	470 of 6335 genes, 7.4%	*DEP1, PDR3, LDB7, CYC8, SMP1, KAR4, REG1, NRG1, UPC2, YAP6, HDA2, SUM1, SPP41, ACA1, DOT6, BUR6, RPH1, EPL1, AFT1, SUT1, ASK10, CAF130, PTI1, STP2, TRA1, YAP5, SIP4, CBF1, IXR1, RGT1, MLP1, BAS1, PPR1, IFH1, HAP1, SEN1, LEU3, YOX1, TAF8, ARG80, RGM1, FCP1, MET4, GCR2, SIN3, GAL11, MED7, YOR338W, MOT1, RLM1, USV1*
mitochondrion organization	46 out of 601 genes, 7.7%	348 of 6335 genes, 5.5%	*SSA1, MRPS9, MIC12, IMG1, SLM3, MRPL11, RSM10, SED1, YDR115W, MRPL1, NUM1, MRPL7, MHR1, MRP1, SDH6, MRP20, SOM1, MDJ1, RPO41, MRF1, MTO1, MRPS35, MRP4, DIA4, MAS2, ARC15, RSM25, MRPL8, NCA3, RSM7, HOT13, PUF3, COX19, MEF1, COA4, ACO1, NAM2, MRPL4, YML6, MRPL3, MRPL19, ATP11, RSM19, MIP1, MSY1, HSP82*
cellular amino acid metabolic process	36 out of 601 genes, 6%	238 of 6335 genes, 3.8%	*DEP1, GDH3, ADH5, ILV6, CIT2, HOM2, TRP4, HPA3, GCG1, UGA1, GTF1, DIA4, ARG4, THR1, LYS12, GTT1, BNA2, CPA2, STR2, ECM4, MET17, NAM2, CAR2, LEU3, ADI1, ARG80, GAD1, GTO3, HER2, IDH1, MET4, MET2, CIT1, IDH2, MSY1, SAM4*
cell wall organization or biogenesis	35 out of 601 genes, 5.8%	199 of 6335 genes, 3.1%	*FLC2, LDB7, RCR1, TIP1, SPS22, SED1, DIT1, HKR1, ZRG8, GSC2, CRH1, SLT2, KIC1, QDR1, YPS6, MHP1, CWP1, PIR3, KTR2, YPS3, YLR194C, CCW14, MYO5, ROT1, DFG5, SLA2, RIM21, KRE1, PKH2, HPF1, MPC54, PTP2, MKK1, SRL1, FLC1*
carbohydrate metabolic process	33 out of 601 genes, 5.5%	267 of 6335 genes, 4.2%	*DEP1, ADH5, MAL33, MAL32, GLK1, CIT2, NTH1, REG1, HKR1, GLC3, GPP2, SAK1, IGD1, HXK1, PYC1, AMS1, GSC2, CRH1, SOL4, ENO1, AAP1, GRE3, TDH1, SIP4, CBF1, RGT1, KTR2, XYL2, GSY2, TSL1, ROT1, GCR2, GDB1*
ion transport	30 out of 601 genes, 5%	230 of 6335 genes, 3.6%	*DRS2, FLC2, BAP2, FTH1, PCA1, ENA5, DNF2, CCC2, PIC2, AVT6, FTR1, AUA1, AFT1, VHT1, TPO2, CCH1, MTM1, YKE4, MRS3, COX19, FRE6, UPS1, FET3, ALP1, ATO2, PHO91, FRE7, MCH5, COT1, FLC1*
signaling	27 out of 601 genes, 4.5%	228 of 6335 genes, 3.6%	*FUS3, EDE1, SSK22, SNF3, SOK1, AFR1, HKR1, STE2, GPG1, MDS3, SIP2, PDE1, MSB2, SLT2, KOG1, SLN1, TPK1, SSK1, ROT1, CMK2, PKH2, BAG7, PTP2, MKK1, RLM1, CLN2, OPY2*
protein complex biogenesis	25 out of 601 genes, 4.2%	310 of 6335 genes, 4.9%	*CYC3, ABP1, EAF1, SDH6, PPM1, SOM1, STE2, SIP2, LSB1, TRS65, CAP2, CAP1, CYT2, CBT1, COX19, POM34, COA4, CTF13, SPO1, BNI1, ATP11, ATG34, MOT1, HSP82, PIN3*
cytoskeleton organization	24 out of 601 genes, 4%	235 of 6335 genes, 3.7%	*ABP1, NUM1, HSP42, LSB1, CAP2, ARC15, PRK1, PAN1, BBC1, MHP1, CAP1, SSK1, POM34, ENT2, VRP1, CTF13, ROT1, SPO1, SLA2, BNI1, PCL1, SCD5, HRR25, PIN3*

Table 12. The 10 GO Slim Mapper process terms with the highest frequencies for transcripts up-regulated in *act1-159* mutant

to cell division, this may represent an attempt to arrest the cell cycle in response to actin damage.

The cytoskeleton organization term contains has 7 down-regulated genes, but unlike the genes appearing under this term from the up-regulated gene list, these are mostly genes involved in chromosome segregation and spindle regulation, and hence may be down-regulated as part of a cell cycle arrest.

GO term	Frequency	Genome Frequency	Gene(s)
lipid metabolic process	17 out of 139 genes, 12.2%	272 of 6335 genes, 4.3%	*HST4, CHO1, ERG28, ATF2, NEM1, EPT1, FAA3, APQ12, MCD4, ERG13, ERG5, GPI15, PSD1, ARE2, ALG8, ALE1, EEB1*
regulation of organelle organization	9 out of 139 genes, 6.5%	235 of 6335 genes, 3.7%	*GEM1, SPC19, DAD4, PET122, DAD2, YPT7, PSD1, ASE1, CLB2*
organelle fission	9 out of 139 genes, 6.5%	288 of 6335 genes, 4.5%	*SWI5, ALK1, SOH1, IME4, DBF2, RFA3, MCK1, SPO19, MCM16*
protein complex biogenesis	8 out of 139 genes, 5.8%	310 of 6335 genes, 4.9%	*SPC19, DAD4, PET122, MPS2, VMA21, VOA1, DAD2, ASE1*
meiotic cell cycle	8 out of 139 genes, 5.8%	274 of 6335 genes, 4.3%	*SOH1, IME4, RFA3, SUR7, RIM9, MCK1, SPS4, SPO19*
transcription from RNA polymerase II promoter	8 out of 139 genes, 5.8%	470 of 6335 genes, 7.4%	*SWI5, NPL3, SOH1, RPI1, PHD1, GAT2, IZH2, RPB10*
mitotic cell cycle	8 out of 139 genes, 5.8%	323 of 6335 genes, 5.1%	*SWI5, ALK1, CDC6, HOF1, MCK1, ASE1, MCM16, CLB2*
nucleobase-containing small molecule metabolic process	8 out of 139 genes, 5.8%	223 of 6335 genes, 3.5%	*CAB5, QCR9, IMD2, ADE13, URA4, ADE17, NRK1, ADE2*
cytoskeleton organization	7 out of 139 genes, 5.0%	235 of 6335 genes, 3.7%	*SPC19, DAD4, MPS2, DAD2, SPC24, ASE1, CLB2*
chromosome segregation	7 out of 139 genes, 5.0%	146 of 6335 genes, 2.3%	*SPC19, DAD4, SOH1, DAD2, SPC24, MCK1, MCM16*

Table 13. The 10 GO Slim Mapper process terms with the highest frequencies for transcripts down-regulated in *act1-159* mutant

3.5.2.2 act1-157 gene ontology

The top GO process terms for genes up-regulated in *act1-157* samples are shown in Table 14, and down-regulated genes are in Table 15. As with *act1-159* samples, the gene with the greatest difference in expression levels is *PRM8*, with a fold change of almost 31. Several genes seen here were also differentially expressed in the *act1-159* samples, which is discussed in the section 3.7.

GO term	Frequency	Genome Frequency	Gene(s)
cell wall organization or biogenesis	11 out of 65 genes, 16.9%	199 of 6335 genes, 3.1%	*SED1, CWH41, GSC2, SLT2, CWP1, KTR2, YPS3, MYO5, DFG5, PTP2, FLC1*
carbohydrate metabolic process	10 out of 65 genes, 15.4%	267 of 6335 genes, 4.2%	*GLK1, CIT2, GAL3, GPP2, HXK1, CWH41, AMS1, GSC2, TDH1, KTR2*
response to chemical	5 out of 65 genes, 7.7%	388 of 6335 genes, 6.1%	*FIG1, GAL3, SPI1, SLT2, SVS1*
Cytokinesis	4 out of 65 genes, 6.2%	97 of 6335 genes, 1.5%	*SDS24, SLT2, VRP1, MYO5*
Sporulation	4 out of 65 genes, 6.2%	133 of 6335 genes, 2.1%	*PRB1, GSC2, CWP1, PTP2*
monocarboxylic acid metabolic process	4 out of 65 genes, 6.2%	125 of 6335 genes, 2%	*GLK1, CIT2, HXK1, TDH1*
ion transport	4 out of 65 genes, 6.2%	230 of 6335 genes, 3.6%	*ENA5, YPK1, FLC1, SAM3*
protein phosphorylation	4 out of 65 genes, 6.2%	181 of 6335 genes, 2.9%	*SLT2, YPK1, CMK2, PTP2*
Endocytosis	4 out of 65 genes, 6.2%	95 of 6335 genes, 1.5%	*SDS24, OSH6, VRP1, MYO5*
response to starvation	4 out of 65 genes, 6.2%	96 of 6335 genes, 1.5%	*PRB1, CLG1, SIP5, PEP4*

Table 14. The 10 GO Slim Mapper process terms with the highest frequencies for transcripts up-regulated in *act1-157* mutant

Only 27 genes were found to be down-regulated in *act1-157* above the threshold odds of differential expression, and little can be concluded from the GO results .

3.6 Identifying transcription factors regulating differential expression

The levels of RNA transcripts can be affected by changes in the activity of the transcription factors (TFs) regulating their expression. The documented regulatory

GO term	Frequency	Genome Frequency	Gene(s)
cellular amino acid metabolic process	4 out of 27 genes, 14.8%	238 of 6335 genes, 3.8%	*HIS4, ARG5, ARG3, ARG8*
nucleobase-containing small molecule metabolic process	4 out of 27 genes, 14.8%	223 of 6335 genes, 3.5%	*URA1, URA4, ADE17, ADE2*
cellular ion homeostasis	3 out of 27 genes, 11.1%	127 of 6335 genes, 2.0%	*IZH1, VPH2, IZH4*
mRNA processing	2 out of 27 genes, 7.4%	196 of 6335 genes, 3.1%	*POP4, RMP1*
rRNA processing	2 out of 27 genes, 7.4%	303 of 6335 genes, 4.8%	*POP4, RMP1*
cytoskeleton organization	1 out of 27 genes, 3.7%	235 of 6335 genes, 3.7%	*SFK1*
lipid metabolic process	1 out of 27 genes, 3.7%	272 of 6335 genes, 4.3%	*ERG28*
vacuole organization	1 out of 27 genes, 3.7%	75 of 6335 genes, 1.2%	*SFK1*
protein folding	1 out of 27 genes, 3.7%	90 of 6335 genes, 1.4%	*EMC5*
protein complex biogenesis	1 out of 27 genes, 3.7%	311 of 6335 genes, 4.9%	*VPH2*

Table 15. The 10 GO Slim Mapper process terms with the highest frequencies for transcripts down-regulated in *act1-157* mutant

associations between target genes and TFs are curated in the Yeastract database (Teixeira et al. 2014). By searching this database with the differentially expressed genes, a list was generated ranking the transcription factors which have been shown to have regulatory control over these transcripts. Target ORF lists were ranked by TF using the TF Rank algorithm with a heat diffusion coefficient of 0.25. The ranking takes into account documented DNA binding and expression evidence. The first ten TFs are listed for both the up- and down-regulated gene lists for both actin mutants in Table 16 and Table 17. The weight value is the score given by the TF Rank algorithm.

There is a large overlap between the lists of genes under the regulatory control of Tec1p, Ste12p and Ace2p, all of which appear high in all four tables. Bas1p, Gcn4p,

Msn2p, Sfp1p all rank highly. Sok2p and Yap1p are within the top 20 for both up and down regulated genes in both strains.

act1-157 up-regulated genes				*act1-157* down-regulated genes			
Rank	TF	Regulations in Yeastract	Weight	Rank	TF	Regulations in Yeastract	Weight
1	Gal3p	88	0.784	1	Bas1p	2755	0.137
2	Sfp1p	4335	0.325	2	Yap1p	2959	0.137
3	Ace2p	4775	0.310	3	Ash1p	3188	0.134
4	Ste12p	3852	0.300	4	Ace2p	4775	0.122
5	Tec1p	3818	0.266	5	Ste12p	3852	0.121
6	Bas1p	2755	0.260	6	Sfp1p	4335	0.116
7	Ash1p	3188	0.238	7	Gcr2p	1308	0.096
8	Msn2p	3411	0.237	8	Gcn4p	2994	0.094
9	Gcn4p	2994	0.225	9	Cbf1p	1523	0.090
10	Sok2p	2255	0.216	10	Tec1p	3818	0.082

Table 16. Top ten TFs regulating differentially expressed genes in *act1-157* microarray ranked using TF Rank in Yeastract

act1-159 up-regulated genes				*act1-159* down-regulated genes			
Rank	TF	Regulations in Yeastract	Weight	Rank	TF	Regulations in Yeastract	Weight
1	Ace2p	4775	3.673	1	Swi5p	1944	1.083
2	Bas1p	2755	3.392	2	Phd1p	763	0.975
3	Tec1p	3818	3.187	3	Ste12p	3852	0.859
4	Ste12p	3852	3.099	4	Hst4p	134	0.809
5	Sfp1p	4335	2.986	5	Rpi1p	173	0.793
6	Sok2p	2255	2.815	6	Ace2p	4775	0.792
7	Msn2p	3411	2.574	7	Ime4p	29	0.778
8	Ash1p	3188	2.555	8	Gcn4p	2994	0.762
9	Gcn4p	2994	2.539	9	Sfp1p	4335	0.730
10	Rap1p	2997	2.371	10	Msn2p	3411	0.726

Table 17. Top ten TFs regulating differentially expressed genes in *act1-159* microarray ranked using TF Rank in Yeastract

Many of the TFs highlighted here correspond with differentially expressed genes noted in the gene ontology analysis. Ste12p and Tec1p are associated with mating and nutrient stress MAPK signals. Msn2p mediated transcription is associated with the HOG1 pathway signaling. These pathways are further studied in Chapter 5.

3.7 Comparison between profiles of reduced and increased actin dynamics

The number of genes differentially expressed using the 95% odds threshold was much greater for the *act1-159* samples, with around ten times more up-regulated genes and five times more down-regulated genes within this threshold compared to the *act1-157* samples. This is in line with the observations that the *act1-159* mutant phenotype is more greatly differentiated from that of the wild-type.

There is a considerable overlap between the up-regulated transcript lists, with 80% of the 65 up-regulated *act1-157* genes appearing in the *act1-159* list. There is also overlap in the down-regulated gene lists, as 43% of the *act1-157* down-regulated gene list appears within the *act1-159* gene list. This indicates that some of the effects of increased and decreased actin dynamics may be the same.

Systematic name	Gene Name
YBL029W	-
YBR257W	*POP4*
YDR492W	*IZH1*
YER044C	*ERG28*
YIL027C	*EMC5*
YLR154W-E	-
YLR420W	*URA4*
YMR120C	*ADE17*
YOL101C	*IZH4*
YOL140W	*ARG8*
YOL143C	*RIB4*
YOR128C	*ADE2*

Table 18. Genes down regulated in both *act1-157* and *act1-159* samples

The list of 12 genes down-regulated in both mutants is shown in Table 18. No major patterns were found in this list. The presence of two ADE genes in the list may be due to non-isogenic disruptions of the adenine synthesis pathway in the compared strains.

Of the 52 genes up-regulated in both conditions, the top GO-slim mapper process terms associated with them are shown in Table 19. These results show disruption of actin dynamics affects cytoskeleton organization, and a number of processes which require a dynamic cytoskeleton, such as cytokinesis and endocytosis. It is interesting that cytoskeleton organization genes (*ABP1*, *BBC1* and *VRP1*) were up-regulated in both actin mutants, as they have opposite effects on filament turnover. Further work on links between endocytosis and actin dynamics is included in Chapter 5.

Three proteins associated with protein folding are up-regulated in both. Additionally *HSP12*, which is has increased transcript levels in *act1-159* samples, also has an increased level of over 3 fold in *act1-157* samples, although below the B statistic threshold that was used to produce the gene lists. Also present in this list is *CIT2*, the citrate synthase which functions as a mitochondrial retrograde signal. This signal is activated during mitochondrial stress, and is further investigated in Chapter 4.

GO-Slim term	Cluster frequency	Genome frequency	Gene(s)
cell wall organization or biogenesis	19.20%	3.10%	*CWP1, DFG5, FLC1, GSC2, KTR2, MYO5, PTP2, SED1, SLT2,YPS3*
carbohydrate metabolic process	15.40%	4.20%	*AMS1, CIT2, GLK1, GPP2, GSC2, HXK1, KTR2, TDH1*
biological process unknown	13.50%	17.70%	*PRM8, PST2, TOS6, YBR056W-A, YJR149W, YLR031W,YNL208W*
cytokinesis	7.70%	1.50%	*MYO5, SDS24, SLT2, VRP1*
response to chemical	7.70%	6.10%	*FIG1, SLT2, SPI1, SVS1*
sporulation	7.70%	2.10%	*CWP1, GSC2, PRB1, PTP2*
monocarboxylic acid metabolic process	7.70%	2%	*CIT2, GLK1, HXK1, TDH1*
endocytosis	7.70%	1.50%	*MYO5, OSH6, SDS24, VRP1*
cytoskeleton organization	5.80%	3.70%	*ABP1, BBC1, VRP1*
protein folding	5.80%	1.40%	*FLC1, HSP26, SSA4*

Table 19. Top 10 GO Slim mapper process terms associated with the list of genes up-regulated in both actin mutant conditions

3.8 Chapter summary

In this chapter I have analysed the transcriptome of yeast strains with actin mutations which alter filament depolymerisation rates. Data was obtained regarding the levels of RNA transcript of almost every gene in the *S. cerevisiae* genome by measuring hybridisation to a microarray chip. The data was processed and analysed to give a list of genes which were significantly differentially expressed between these mutant strains and the wild-type.

The analysis showed that the levels of transcripts for around one eighth of the approximately 6000 protein coding genes were altered when the *act1-159* mutation is present, the majority of which were expressed at increased levels. This indicates the extent of the stress placed on cells with reduced actin dynamics and the numerous cellular processes which are modulated in response. Much fewer genes (under 3%) were differentially expressed in cells with the *act1-157* mutation, which shows that increased actin dynamics has a less dramatic effect on cellular function. I observed that the transcript levels of a number of genes was increased in both actin mutants,

suggesting that despite the different effects on actin dynamics, there may be some phenotypes shared by these strains.

Results from gene ontology and transcription factor analyses raise the possibility that altered actin dynamics can lead to expression of genes involved in multiple signaling pathways. Many genes which are under the control of the TFs Ste12p and Tec1p were differentially expressed, and a number of genes involved in regulation of cell wall regulation, as well as HOG and Ras/cAMP/PKA signaling components. I also observed some DNA repair mechanisms may be activated with reduced actin dynamics. These data allow the generation of numerous hypotheses which are investigated further in chapters 4 and 5.

4 Roles for actin in the regulation of cellular homeostasis

4.1 Chapter introduction

The importance of actin dynamics to the transcription patterns of cells was shown in the previous chapter. The microarray data analysis has provided an insight into the extent of the cellular changes imposed by alterations to the dynamic status of actin filaments, and the gene expression programs which are activated in response. The observations generated by the analysis included changes to the transcription patterns of genes involved in response to DNA damage, cell wall structure, mitochondrial dysfunction and signaling pathways which respond to environmental change. Together this indicates that actin dynamics contributes to processes which regulate homeostasis. In this chapter experiments are described which were used to probe and validate some of these observations using more directed assays. Investigation of environmental sensing pathways developed into a larger study, and is discussed in Chapter 5.

4.2 Roles for actin in the response to DNA damage

Following on from several observations made in the previous chapter concerning transcript level changes in DNA repair and chromatin remodeling processes in strains with altered cytoskeletal dynamics, I aimed to characterise the ability of these strains to tolerate DNA damage. Actin monomers participate in several complexes associated with chromatin remodeling and histone deacetylation, and there is a requirement for chromatin structure to be modified for DNA double strand break (DSB) repair pathways to function (Jazayeri 2004). It has been shown that DSB repair factors

associate with actin polymers *in vitro* (Andrin et al. 2012). Previous work has shown that levels of ROS, which can cause DNA damage, are elevated in *act1-159* mutants (Gourlay et al. 2004). Therefore I was interested in finding whether the documented effects of the *act1-159* mutation on filament turnover might have an impact on nuclear actin interactions, specifically those involved in DNA integrity and repair.

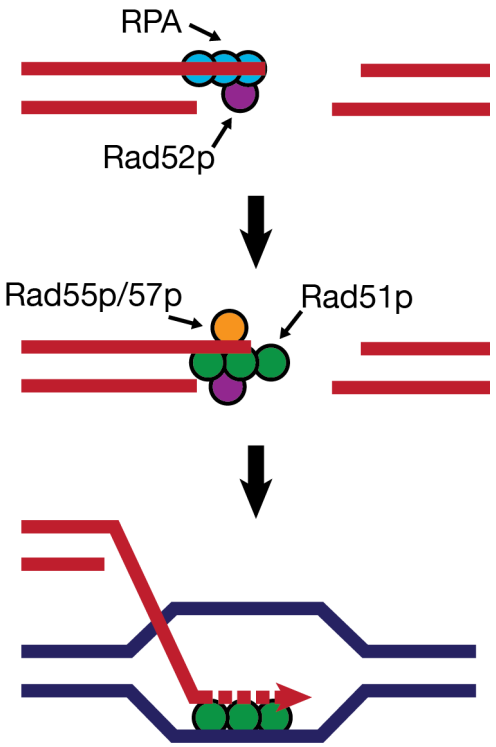

Figure 15. A model for DNA double strand break repair by Rad51p, modified from Symington 2002 and Featherstone & Jackson 1999. Replication protein A (RPA) and Rad52p bind at DSB sites. Rad51p is recruited, displacing RPA and forms filaments along the strand. The interaction between Rad51p and DNA is stabilised by Rad55p and Rad57p. The broken strand invades homologous DNA for use as a replication template.

The *RAD52* epistasis group is strongly linked to DSB repair as well as other lesions by the homologous recombination (HR) pathway (outlined in Figure 15), and mutants of these genes are sensitive to both chemical and physical agents of DNA damage including MMS and UV light (McKinney et al. 2013). Mutation of *RAD55*, which is up regulated in the *act1-159* strain microarray compared to wild-type, results in MMS sensitivity (Prakash & Prakash 1977). Rad55p phosphorylation occurs following activation of the DNA damage checkpoint which can be induced by both UV and MMS (Bashkirov et al. 2000). *RAD51* transcript up-regulation was observed in *act1-*

157 mutants, suggesting an alternate activity in the *RAD52* group with this mutation, but this strain was not available at the time of these experiments.

4.2.1 Effect of DNA damage on agar colony growth of *act1-159* mutant

To investigate the effects of DNA damage on growth, I grew colonies either on agar impregnated with chemical agents, or subjected cells to radiation after applying to agar. Two chemicals were used, methyl methanesulfonate (MMS) which is an alkylating agent, and hydroxyurea (HU) which stalls replication forks. Ultraviolet light (UV) was also used in the UVB range which causes pyrimidine dimerisation (Pfeifer et al. 2005).

In these agar spot assays, stationary cultures were diluted to an OD_{600} of 0.1 and then serial diluted 1 in 10 across adjacent columns and transferred to agar plates. Here I compare the growth with increasing perturbation of *act1-159* mutants and wild-type as well as a *Δrad52* strain (which is known to be sensitive to DNA damage) and the *RAD52* wild-type.

4.2.1.1 UVB exposure

Ultraviolet light in the UVB range (280-320nm) induces DNA damage primarily in the form of pyrimidine dimers, which block progression of replication forks (Pfeifer et al. 2005). Work in higher eukaryotes has suggested that pyrimidine dimers are removed by nucleotide excision and this may produce DSBs which are then subsequently processed by HR (Garinis et al. 2005; Stergiou et al. 2011).

Cultures were transferred to YPD agar as described above and UV radiation at 302nm was applied from a lamp at a distance of 10cm. Figure 16 shows the colony growth following UV exposure. With this treatment wild-type strains were only mildly affected after 20s exposure but showed a reduction in surviving cells after 40s exposure. Both *act1-159* and *Δrad52* strains were affected after 20s and only showed very minimal survival after 40s.

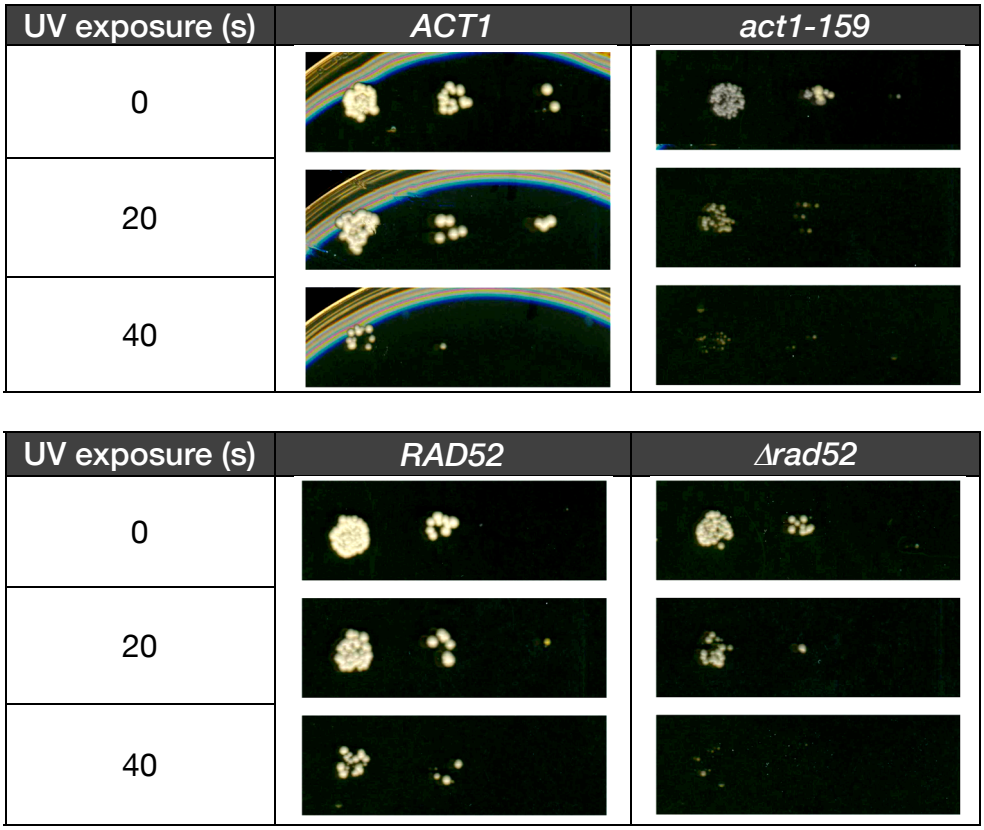

Figure 16. *ACT1*, *act1-159*, *RAD52* and *Δrad52* cultures plated in a dilution series (left to right) on YPD agar and exposed to 302nm UV for the increasing lengths of time.

4.2.1.2 Hydroxyurea

Hydroxyurea retards cell cycle progression by depleting the nucleotide pool, leading to activation of the DNA damage checkpoint, and at higher concentrations also causes DSBs (Jazayeri 2004; Merrill & Holm 1999; Desany et al. 1998).

Colony growth on YPD containing 20 and 200mM HU is shown in Figure 17. Wild-type strains showed reduced colony number at 20mM and reduced colony number and smaller colonies at 200mM. Colonies of *act1-159* strain were smaller even without treatment due to their slower growth, and colony number was reduced at 20mM, with none surviving at 200mM. However this strain was not as sensitive to the treatment as the *Δrad52* strain.

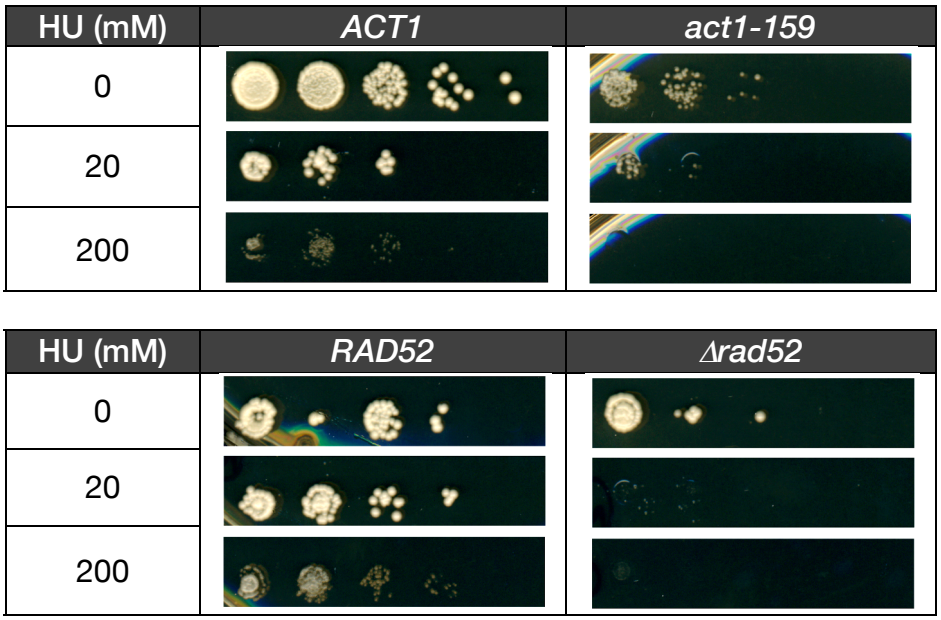

Figure 17. *ACT1*, *act1-159*, *RAD52* and *Δrad52* cultures plated in a dilution series (left to right) on YPD agar containing HU at increasing concentrations.

4.2.1.3 MMS

MMS has been used extensively as an agent of DNA damage. MMS is an alkylating agent which causes DNA damage by methyating at N^7-deoxyguanine and N^3-deoxyadenine residues (Pegg 1984; cited in Chang et al. 2002) which can result in various DNA lesions including DSBs. For agar assays I added MMS to the media at concentrations around 0.02% based on previous studies (Bandyopadhyay et al. 2010) and found that lower concentrations than this were sufficient to produce an effect.

The results are shown in Figure 18. Wild-type strains are able to tolerate 0.005% MMS well and colony number was reduced at 0.01%. A similar effect was seen with *act1-159* cultures, which produced smaller colonies without any treatment, and had a similar reduction in number with increasing MMS. Deletion of *RAD52* prevented growth at all concentrations of MMS.

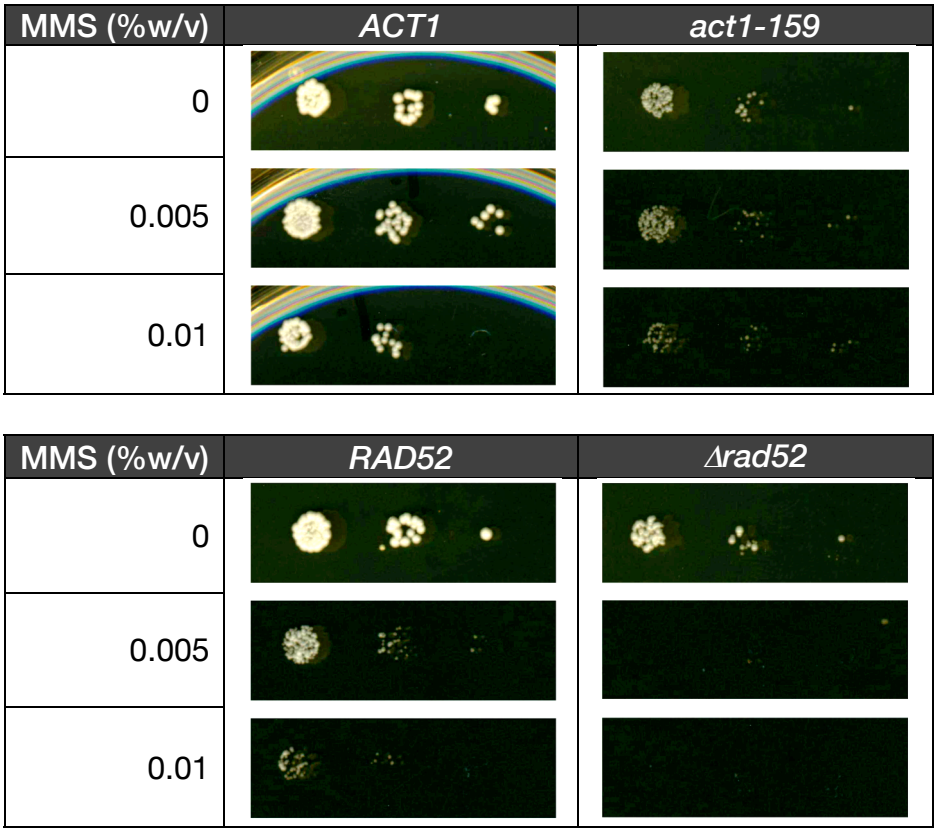

Figure 18. Spot assay of *ACT1*, *act1-159, RAD52* and *Δrad52* cultures plated in a dilution series (left to right) on YPD agar containing MMS at increasing concentrations.

While all three methods show that a reduction in actin dynamics lead to reduced tolerance of DNA damage, it was also clear that survival was already reduced even in the absence of extrinsic damage. The *Δrad52* strain was more sensitive than *act1-159* to both chemical treatments. It is therefore not clear from this assay whether the ability to repair DNA damage is significantly affected by actin stabilisation.

4.2.1.4 Effect of MMS on log phase growth of *act1-159* mutant

To further assess the effect of DNA damage on the growth of strains with reduced actin dynamics, liquid cultures were grown in a plate reader instrument in the presence of MMS concentrations up to 0.02% w/v. The growth curves are shown in Figure 19. At the two lower concentrations (0.005% and 0.01%), both strains displayed a decrease in growth rate and delay of the diauxic shift. Noticeably, at the highest concentration, *act1-159* mutants did not grow, while *ACT1* cells grew very slowly for over 20 hours before a period of rapid growth occurred. The very late recovery of this culture may occur when MMS in the media has been depleted and unaffected cells or those in which any DNA lesions have been successfully repaired are able to grow without impediment.

To clarify the observations from growth curves, some alternative metrics were used to interrogate the data, shown in Figure 20. This analysis shows that MMS had a greater relative effect on wild-type cultures on the maximum rate of growth, the cell density at which diauxic shift occurred, and the length of time to reach diauxic shift. As noted in reference to Figure 19, the rapid growth rate of *ACT1* at 0.02% MMS occurred after 20 hours of slow growth. The maximum growth rates of *act1-159* cultures treated with 0.005% and 0.01% MMS were 91% and 80% of the untreated culture. However at 0.02% very little growth occurred within the time period of the experiment. By comparison, all treated *Δrad52* cultures showed a maximum growth rate below 15% of untreated cultures, demonstrating that Rad52p dependent DNA repair is crucial for MMS resistance.

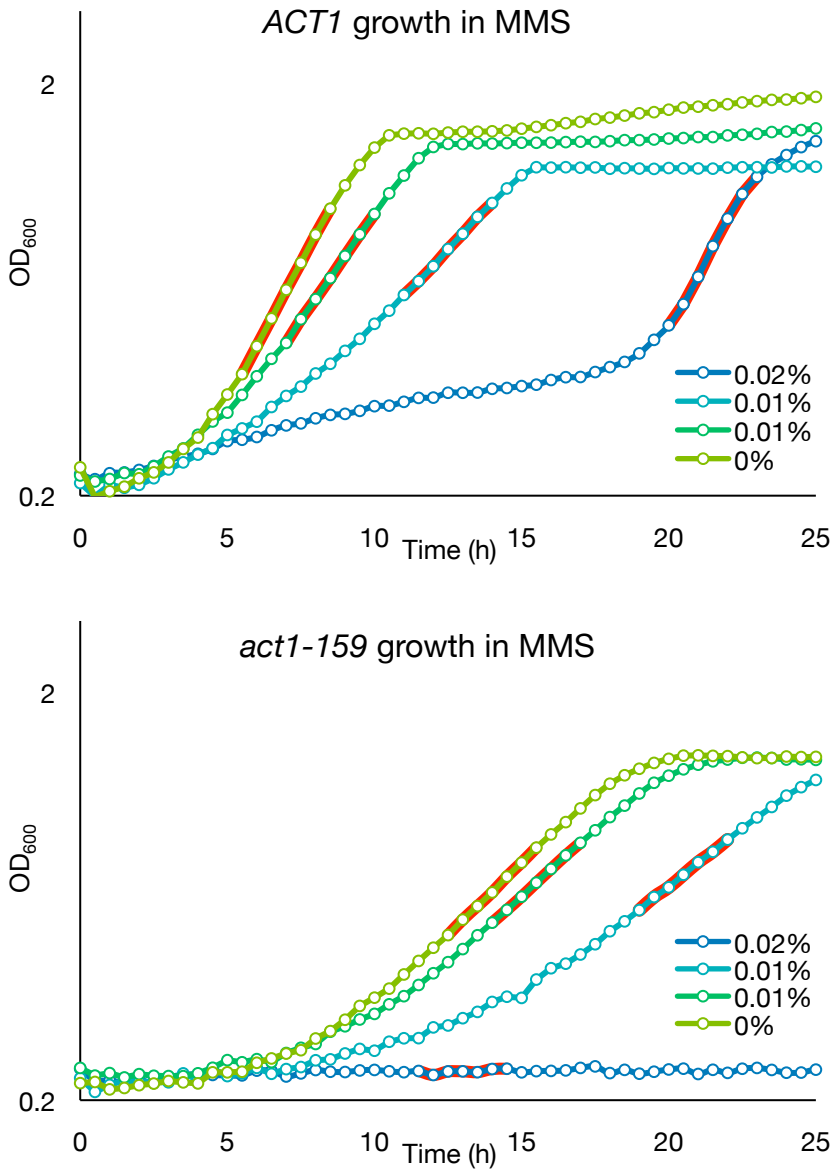

Figure 19. Log phase growth curves for *ACT1* and *act1-159* cultures in YPD with increasing MMS concentrations. Segments highlighted in red indicate the maximum growth rate period used for Figure 20A.

The data suggests that whilst actin stabilisation reduces growth rate in untreated cultures, damage to DNA has a less pronounced effect on growth than on cells with dynamic actin. It is possible that due to the reported increased ROS levels in *act1-159* cells, DNA damage occurs without treatment and repair mechanisms are already active in response to this. Alternatively, the reduced lag phase length when treated with MMS may represent a failure to undergo cell cycle arrest when DNA is

damaged, with growth being prevented at 0.02% MMS when damage is so severe that division cannot occur.

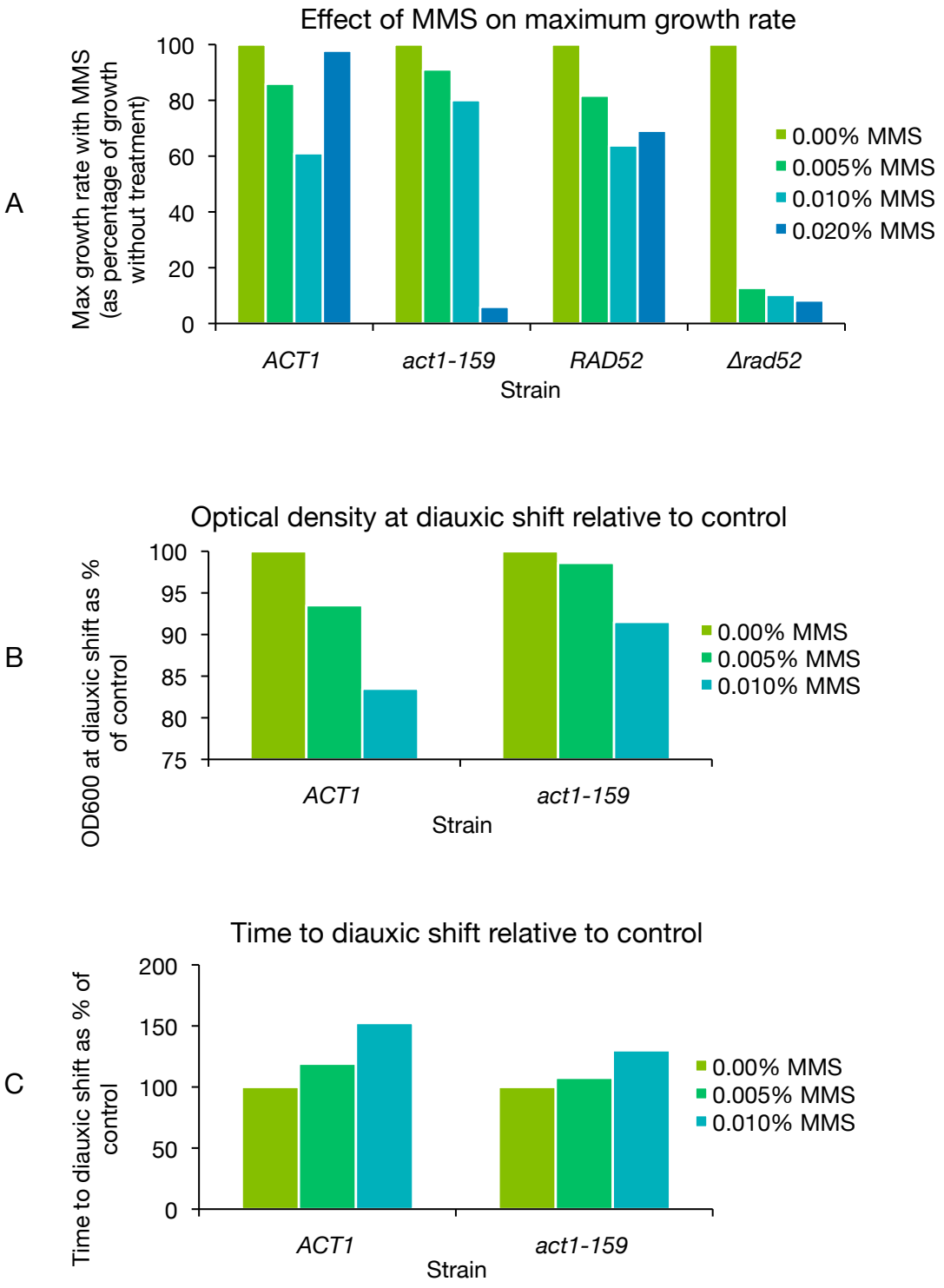

Figure 20. Growth data for ACT1 and *act1-159* strains grown in YPD with increasing MMS concentrations, displayed relative to the value of the untreated control culture. (A) shows the effect of MMS concentration on the maximum log phase growth rate achieved by the culture. (B) shows the optical density of the culture when diauxic shift was reached and (C) shows the time at which diauxic shift occurred

4.2.2 Actin phalloidin staining with MMS treatment

I sought to establish if there is a direct effect of MMS treatment on actin structures. Actin was visualised with a fluorescent phalloidin label to confirm that MMS does not reduce viability by inducing actin aggregation, and thereby support that any observed effects of MMS treatment were a result of perturbation of DNA rather than cytoskeletal assemblies.

To visualise the actin, cultures in log growth phase were incubated with MMS at 0.04% for 4 hours before being stained with phalloidin and viewed under a fluorescence microscope. The effects of acute MMS treatment on wild-type and *act1-159* cells is shown in fluorescence micrographs in Figure 21 and Figure 22.

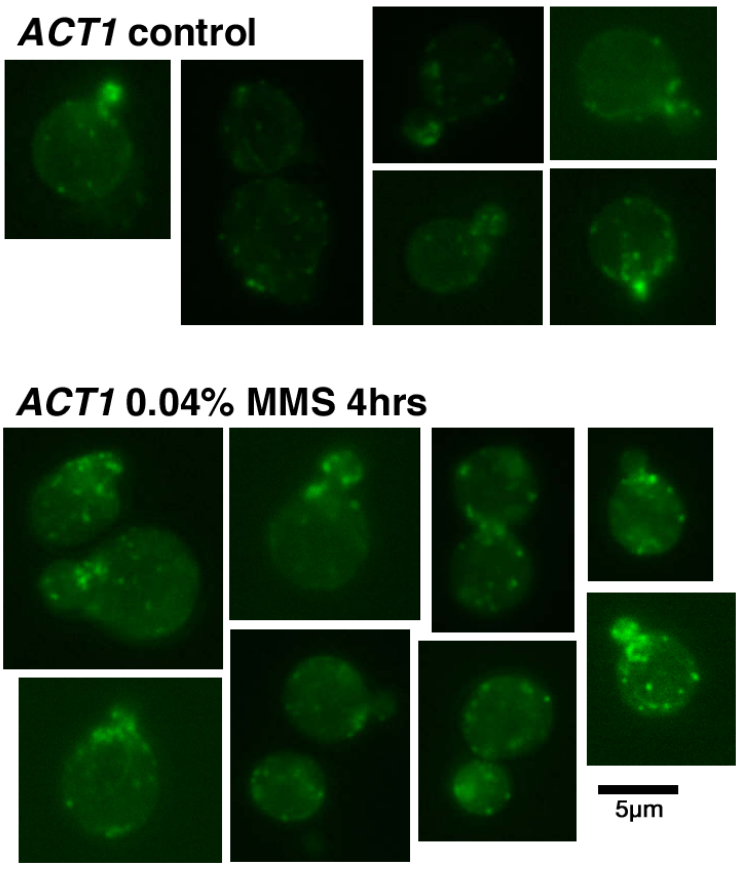

Figure 21. *ACT1* cells incubated with and without MMS at 0.04% for 4 hours and stained with actin-phalloidin. 100x magnification

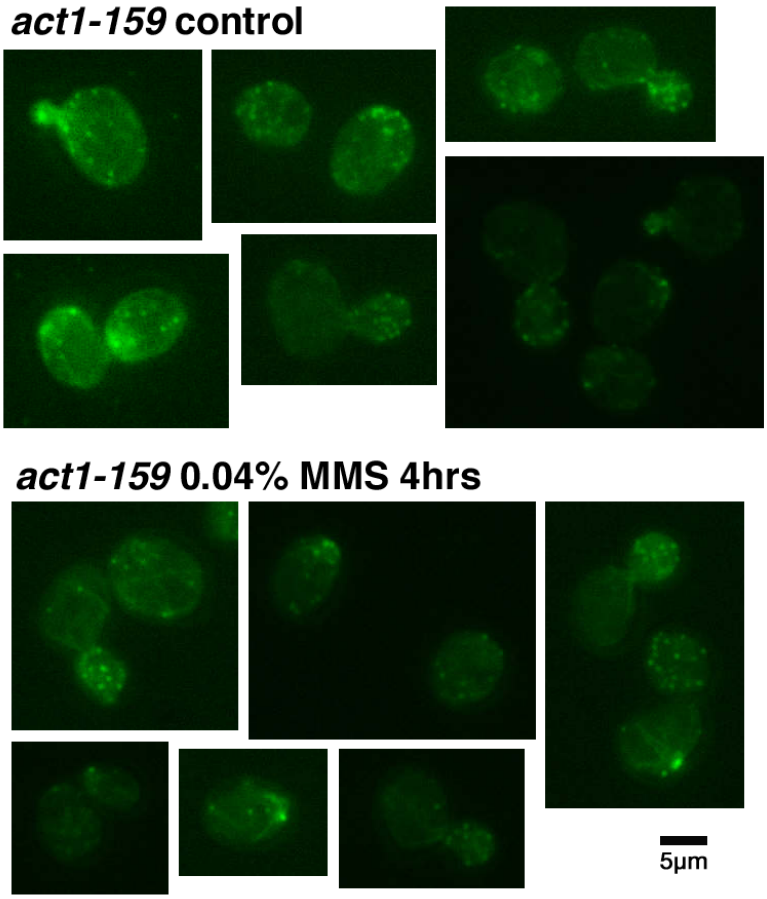

Figure 22. *act1-159* cells incubated with and without MMS at 0.04% for 4 hours and stained with actin-phalloidin. 60x magnification

The cytoskeleton of *act1-159* cells was more disordered than that of wild-type cells with some visible aggregated actin structures and filaments. Cortical patches were often larger, reflecting the slow depolymerisation rate. In *ACT1* cells actin was seen to cluster at emerging buds while in *act1-159* mutants it was often clustered where there is no visible bud, and conversely buds may often contain very little actin. There is no apparent effect of MMS treatment on the organisation of actin structures in either strain.

4.2.3 Spot assay screen of actin-related knockouts

To investigate if actin interactions were involved in coordinating a response to DNA damage, MMS was applied to a library of yeast strains in which a single actin-interacting gene had been deleted. Colonies grown on YPD agar containing up to 0.02% MMS are shown in Figure 23.

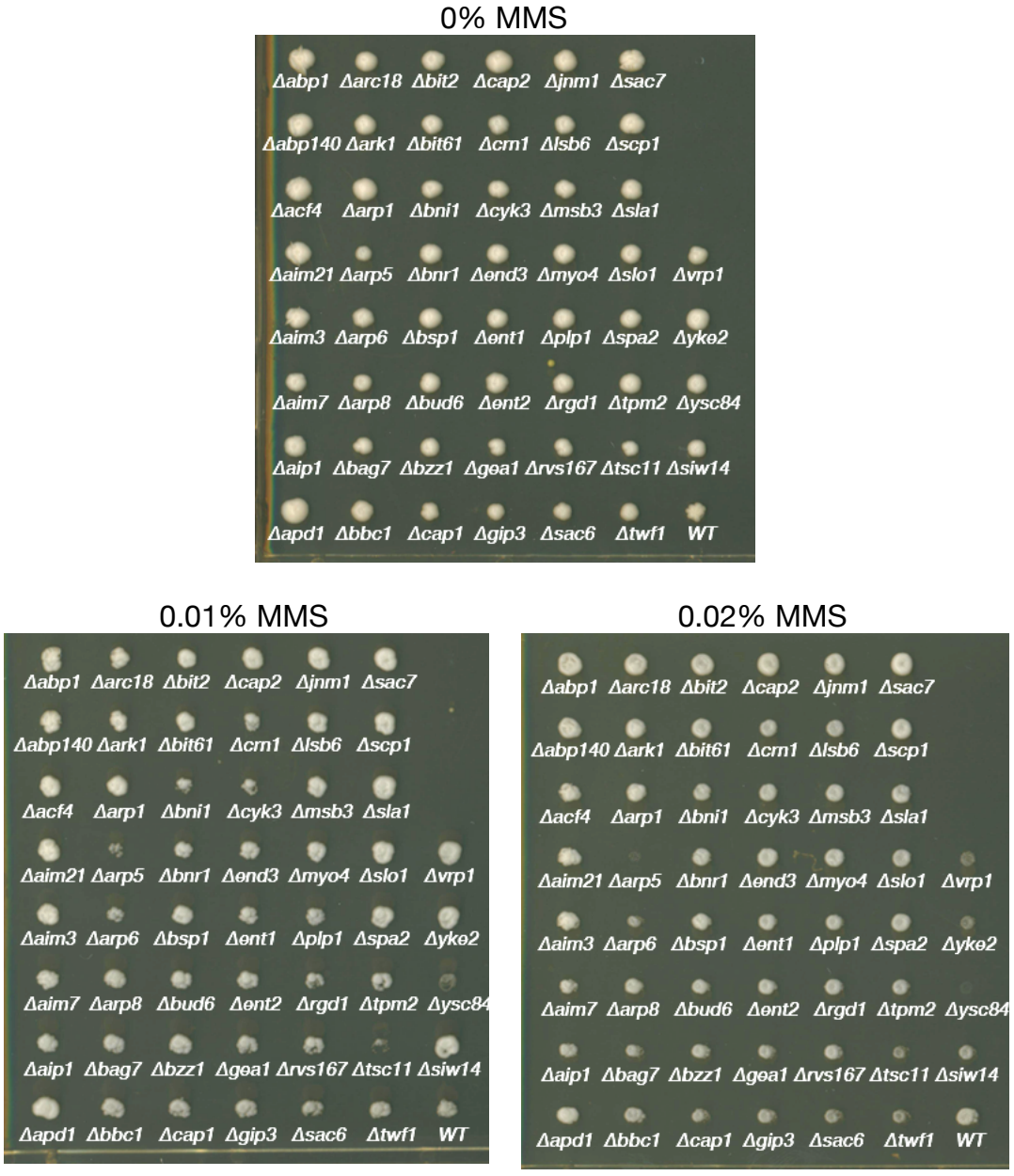

Figure 23. Colonies of strains with a single actin-interacting gene deleted grown on YPD agar containing increasing MMS concentrations

The growth of deletion strains on agar containing MMS was used to assess their ability to withstand DNA damage. The majority of the colonies grew well at 0.02% MMS in this assay, as did the wild-type, but several deletion strains showed sensitivity to DNA damage. In particular *Δarp5* and *Δarp6* are sensitive to MMS, reflecting the roles of Arp5p and Arp6p in the INO80 and Swr1 chromatin remodeling complexes, which are recruited to sites of DNA damage (Papamichos-Chronakis et al. 2006). Deletion of *YSC84* or *VRP1*, genes associated with actin organisation at cortical patches, also resulted in sensitivity to MMS, while deletion of many other important cortical patch genes, such as *SLA1 or ABP1* had no effect. The strain with deleted *TSC11*, a component of a TOR signaling complex which regulates actin dynamics, showed reduced growth from 0.01% MMS.

4.3 Actin dynamics and cell wall integrity

The yeast cell wall is a complex structure consisting of glucan polymers, chitin and glycoproteins which maintains cell shape and size and influences cell cycle progression (Klis et al. 2006). Cell wall remodeling is regulated during growth and in response to environmental inputs through the cell wall integrity (CWI) MAPK pathway (Levin 2011).

Data analysed in the previous chapter indicated an enrichment of transcripts in the GO category for processes related to cell wall integrity. Of the genes up-regulated in both the *act1-157* and *act1-159* mutants, this was the GO term with the largest complement of genes. Several transcripts up-regulated in *act1-159* cells are involved in the CWI pathway, including MAP kinases *MKK1*, *SLT2 (MPK1)* and the transcription factor *RLM1*. Further microscopy observations support a disturbance in cell wall

maintenance when actin dynamics are altered, including the wider variations in cell size and apparent failed budding events when actin dynamics were reduced.

To further investigate the cell wall in these strains I employed calcofluor white (CFW), a cell wall antagonist which binds to chitin and upon binding exhibits fluorescence (Garcia-Rodriguez et al. 2000; Elorza et al. 1983). This allows it to be used both to test the ability of cells to resist CFW-induced cell wall damage and to visualise cell wall structures by fluorescent microscopy.

4.3.1 Calcofluor white toxicity

CFW interacts specifically with chitin in the fungal cell wall resulting in an increase in the rate of chitin synthesis, although the chitin produced is abnormal and weakens the cell wall (Garcia-Rodriguez et al. 2000). Mutants with reduced chitin synthesis are resistant to CFW (Roncero et al. 1988) and disrupted cell wall structure can lead to sensitivity to the compound (Lussier et al. 1997).

To assess the integrity of the cell wall in our actin mutants, I plated a dilution series of triplicate cultures onto agar containing increasing concentrations of CFW (Figure 24). In these experiments it can be seen that both actin mutants were more sensitive to the toxic effect of CFW than the *ACT1* wild-type. This suggests that the cell wall is disrupted in the mutants, making cells more susceptible to the action of CFW. It may indicate some change in chitin biosynthesis although I observed no changes in chitin synthesis genes at the transcript level. Actin dynamics may contribute to the cell wall disruption which in turn activate a CWI signal and cell wall synthetic processes which enhances the effect of CFW.

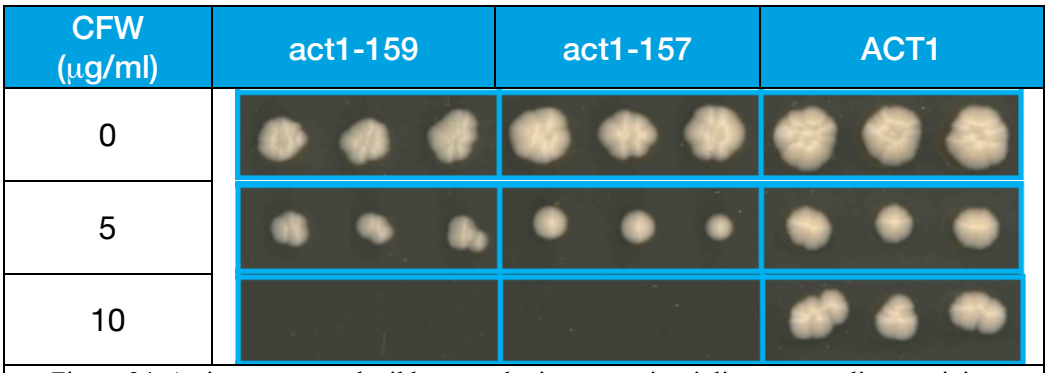

Figure 24. Actin mutants and wild-type colonies grown in triplicate on media containing increasing concentrations of calcofluor white (CFW).

4.3.2 Calcofluor white staining microscopy

CFW staining was used to visualise the cell wall of actin mutant and wild-type strains to gain insight into how actin dynamics affects this cellular structure. Cultures grown to log phase in YPD were incubated for 5 minutes in 25μM CFW at room temperature and viewed using a fluorescence microscope. Micrographs are shown in Figure 25.

Wild-type *ACT1* cells showed fairly uniform staining with CFW present around the outer surfaces of cells and some cells with what are likely to be bud scars. Minor differences were visible between the *act1-157* cells and the wild-type cells, such as some abnormally shaped cells and abnormal cell wall structures. The *act1-159* cells were more drastically affected and in general were more strongly stained than wild-type cells. This is not apparent in these micrographs as the intensity of incident light was reduced to obtain clear images. The common phenotype of increased cell size can be seen particularly in these micrographs and there are several unusual aspects of the cell wall appearance. Some cells appear to have numerous lumps and others display areas of thicker cell wall deposition.

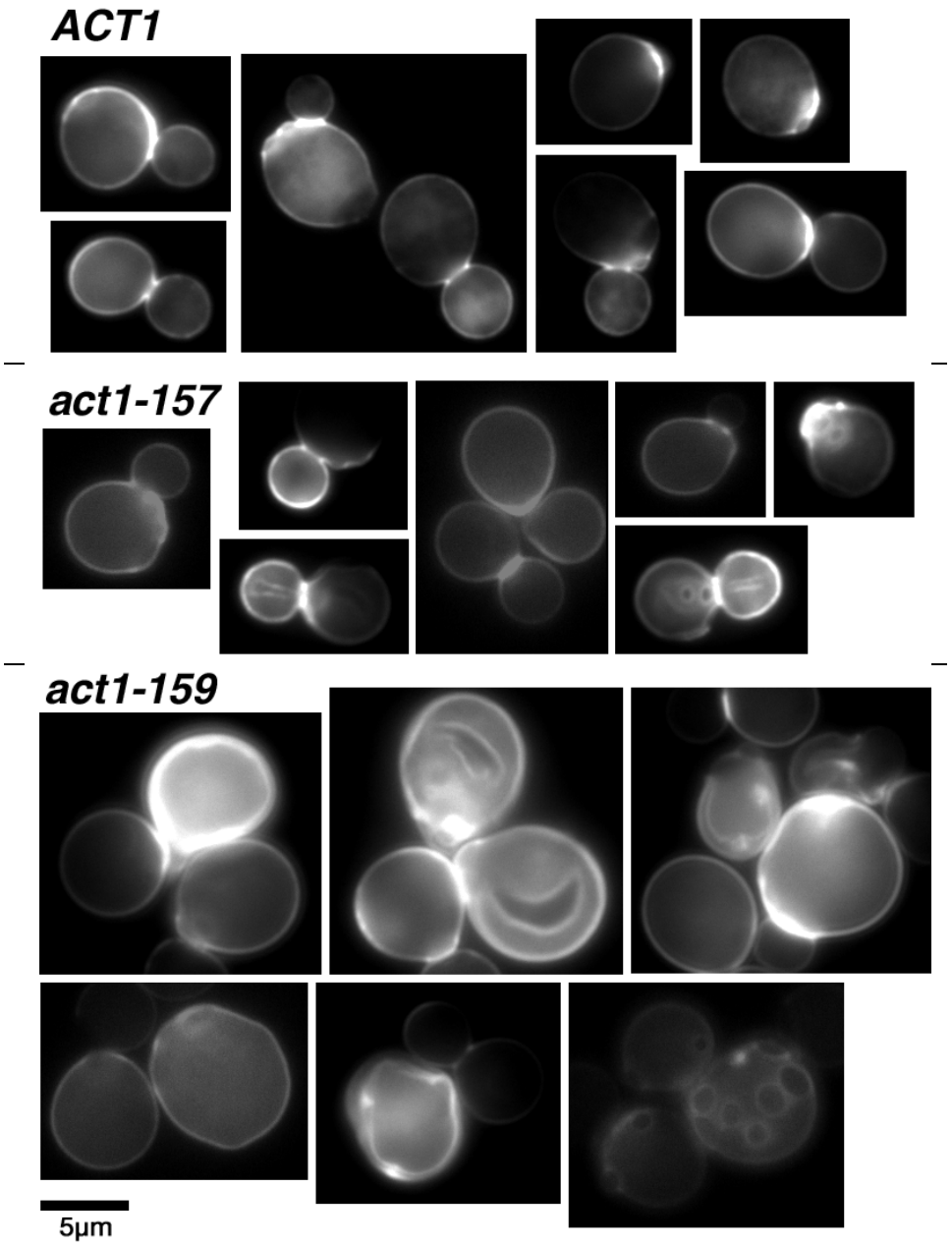

Figure 25. Fluorescence micrographs of *ACT1*, *act1-157* and *act1-159* cells follwing staining of the cell wall with calcofluor white

It is also worth noting that both actin mutants were similarly sensitive to CFW toxicity, while the disruption to the cell wall is much more pronounced in *act1-159* cells viewed under the microscope. It remains unclear how both decreased and increased actin filament turnover elicits the same sensitivity to CFW.

4.4 Heat shock proteins and heat tolerance

It has been reported that increased temperatures cause actin structures to be redistributed, with a loss of visible cables and random distribution of cortical structures (Desrivieres 1998). Heat stress is known to activate CWI signaling and CWI components redistribute to the cell periphery, possibly as part of an effort to repair cell wall damage (Kamada et al. 1995; Levin 2011). HOG signaling is also activated by heat stress, and HOG components are required for survival at elevated temperatures (Winkler et al. 2002). As I have shown transcripts of components of both of these pathways are differentially expressed with altered actin dynamics, I investigated whether these changes caused cells to be primed against heat stress and thereby more able to tolerate high temperatures. Further to this, I chose to investigate the protein levels of two heat shock proteins, Hsp12p and Hsp104p, of which there was an indication from the microarray analysis that the levels were altered. In *act1-157* samples I observed an increase in transcript levels of over 2.3 fold for *HSP104*, and 3.1 fold for *HSP12* although it fell outside of the significance criteria used in the gene ontology analyses (46% and 62% probabilities of differential expression respectively). In *act1-159* samples *HSP104* was up-regulated over 1.7 fold and with a 90% probability of differential expression. *HSP12* was up-regulated nearly 5 fold and with a 99.9 % probability of differential expression. Additionally, genes involved in the synthesis of trehalose were up-regulated in both mutants. Synthesis of trehalose occurs during heat stress and levels are regulated by in part by Hsp104p (Iwahashi et al. 1998).

Following from the observations discussed above, I attempted to test the ability of these strains to withstand a high temperature for increasing time periods. Cultures

were grown to log phase, pipetted into a dilution series and incubated at 52°C. At multiple time intervals up to one hour, samples were pipetted to YPD agar and colonies allowed to grow at 30°C. While there was some indication that *act1-159* cells had an increased ability to resist heat stress, the observation was not reproducible and I could not validate a significant difference between mutant and wild-type.

4.4.1 Heat shock protein expression

4.4.1.1 Hsp12p

Hsp12p expression is induced in response to diverse stresses and is regulated by both HOG and Ras/cAMP/PKA signaling. Growth in low glucose media has been reported to induce expression of *HSP12* (Herbert et al. 2012), and this was used in our investigation. Protein extracts were obtained from cultures which had grown for 4 hours in 2% glucose (control) or 0.05% glucose YPD. Western blots were then carried out with antibody for Hsp12p, and these are shown in Figure 26.

This data shows that when glucose was present at high levels Hsp12p was not detectable in wild-type or mutants, while all three strains were able to induce expression in low glucose media. The observed increase in *HSP12* transcripts did not result in increased protein without induction.

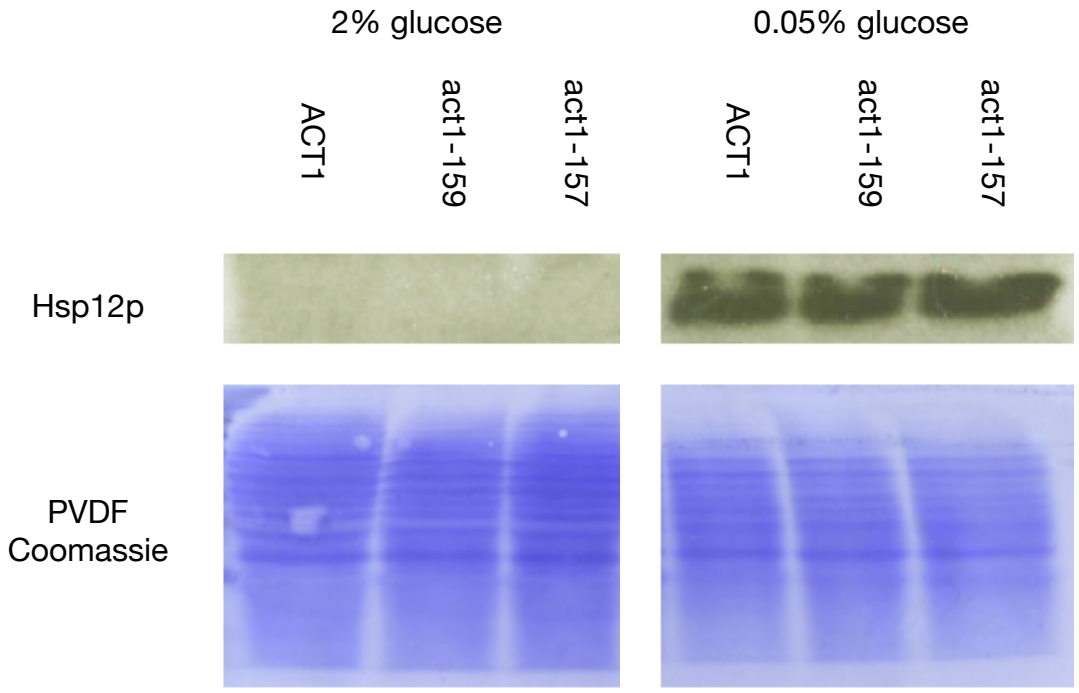

Figure 26. Western blots showing levels of Hsp12p in actin mutants and WT following 4 hours of growth in 0.05% or 2% glucose YPD

4.4.1.2 Hsp104p

Expression of Hsp104p was induced by heating log cultures to 52°C for 10 minutes and then returning them to 30°C for 4 hours to allow expression of genes induced by the heat stress. Western blot results are shown in Figure 27. All strains increased levels of Hsp104p following heat stress, and the increase is uniform between WT and both mutant strains.

The change in levels of Hsp104p was tested under the low glucose conditions used to induce Hsp12p expression. Expression of Hsp104p is not associated with glucose starvation. The western blot in Figure 28 reveals that under these conditions all three strains had a similar levels of Hsp104p when in high glucose medium. In low glucose medium only the *act1-159* mutant had detectable Hsp104p levels.

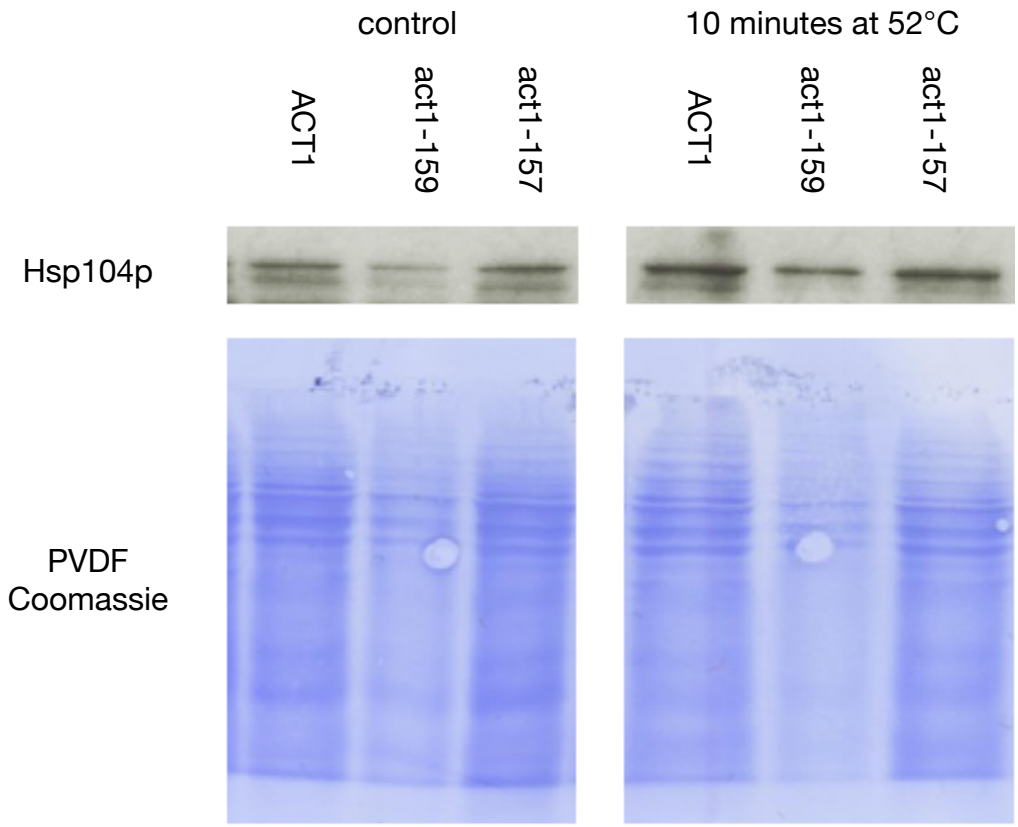

Figure 27. Western blots showing levels of Hsp104p with and without heat stress (10 minutes at 52°C) in actin mutants and WT.

This result suggests that with reduced actin dynamics, there was an altered response to glucose starvation resulting in cells maintaining Hsp104p when wild-type cells cease expression of this protein. Together with the inconsistent results concerning thermal tolerance, the heat shock protein expression data presented here indicates that actin stabilisation may result in cells which mount an uncoordinated response to heat shock and glucose starvation.

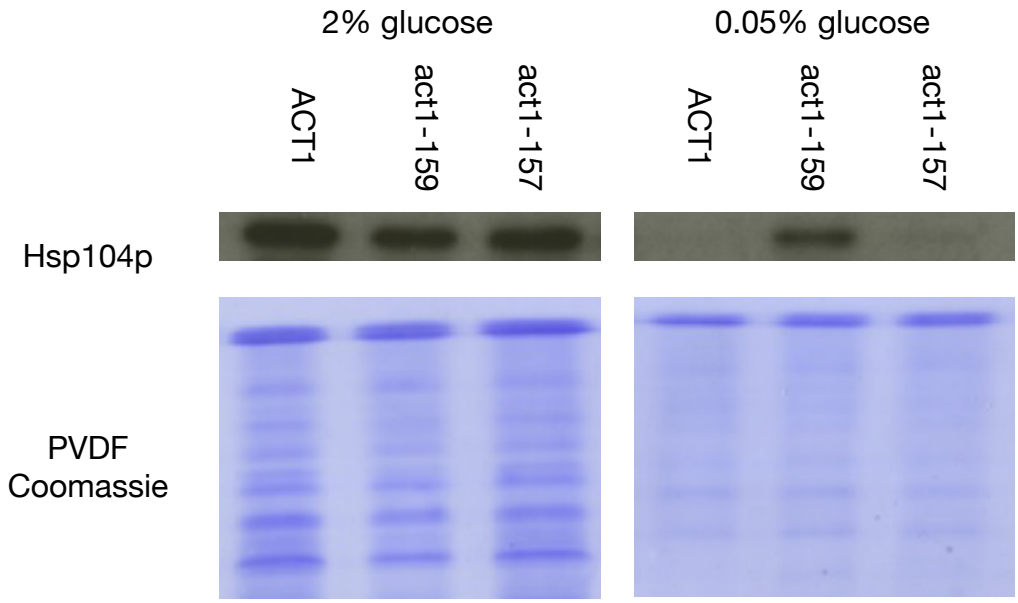

Figure 28. Western blots showing levels of Hsp104p following 4 hours of growth in 0.05% or 2% glucose YPD

4.5 Actin dynamics in regulation of mitochondria and endoplasmic reticulum

Mitochondrial function, morphology and motility are dependent on actin dynamics, and interactions between the cytoskeleton and mitochondria can affect cell lifespan and influence entry into apoptosis (Boldogh et al. 2001; Boldogh & Pon 2006; Higuchi et al. 2013; Leadsham & Gourlay 2008). Reduced actin dynamics in *act1-159* mutants leads to increased ROS levels, which can be a result of mitochondrial damage, and conversely ROS are decreased in *act1-157* mutants (Gourlay et al. 2004). Previous work from our group has shown that proteins regulating actin dynamics can interact with mitochondria under stress conditions, which is covered further in Chapter 5. Additionally, the endoplasmic reticulum and the mitochondria are closely associated (Kornmann et al. 2011). The actin interactions which regulate

mitochondrial morphology and motility have been reported to depend on its association with the ER (Frederick et al. 2004).

Our microarray data showed up-regulation of *CIT2* transcripts in both actin mutants. *CIT2* encodes a citrate synthase protein which is the prototypical marker for the mitochondrial retrograde response by which mitochondrial dysfunction is signaled to the nucleus. This signal results in an adjustment of metabolic processes to maintain supplies of glutamate (Butow & Avadhani 2004).

4.5.1 Respiratory capacity with altered actin dynamics

Respiratory capacity of actin mutants was measured using an Oroboros Oxygraph-2k. The steady state respiration rate (Routine) was measured as oxygen consumption at 30°C. LEAK respiration was measured with addition of triethyltin (TET) which inhibits ATP synthase (Complex V), the complex responsible for pumping protons into the mitochondrial matrix. Oxygen flux under these conditions represents respiration occurring when protons only enter the matrix by free diffusion across the membrane. The ETS (electron transport system) value represents a maximal capacity of the electron transport chain. This is induced with carbonylcyanide p-trifluoromethoxyphenylhydrazone (FCCP), which transports protons freely across the membrane. As a result of this, a proton gradient cannot build up and electrons are able to rapidly move through the transport chain. Finally the nmt (non-mitochondrial) respiration is measured when cytochrome c reductase (complex III) is inhibited by antimycin A (AntA), effectively blocking the electron transport chain.

Oxygen consumption of cells with the addition of these drugs is shown in Figure 29. These data indicate that steady state and maximum respiratory capacity was increased in *act1-157* cells compared to wild-type. Wild-type and *act1-157* cells showed reduced respiration when ATP synthase is inhibited, indicating that ATP synthesis is coupled to oxygen consumption. No respiratory function was detected in *act1-159* cells.

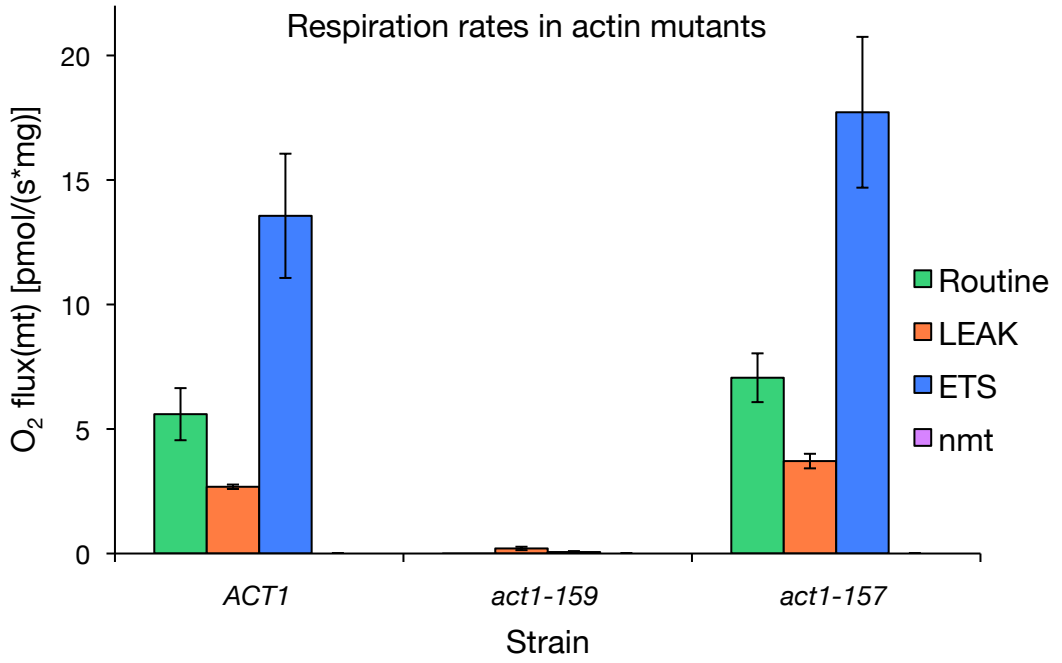

Figure 29. Mean respiration rates of duplicate actin mutant and wild-type strains in log phase in YPD at 30°C. Respiration was measured as oxygen flux per cell using an Oroboros Oxygraph-2k.

4.5.2 Mitochondrial retrograde signaling activity in *act1-159* mutant

At the transcript level *CIT2*, which encodes a peroxisomal citrate synthase, is up-regulated in *act1-159* mutants. To test if there was an increase in Cit2p in line with the increase in transcript level and the decreased mitochondrial function, I transformed *ACT1* and *act1-159* strains with a *CIT2-lacZ* reporter plasmid, and the carried out a β-galactosidase assay. The results, shown in Figure 30, indicate that there was an increase Cit2p in *act1-159* cells. This confirms the results of the

microarray study and previous work which has indicated mitochondrial dysfunction with reduced actin dynamics, and also illustrates that actin dynamics is linked to cellular signaling pathways regulating homeostasis.

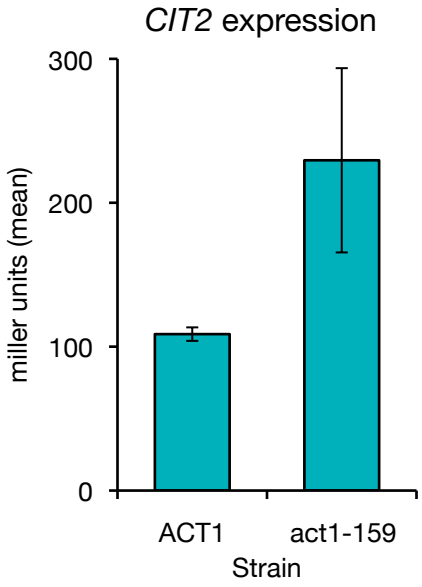

Figure 30. Expression levels of *CIT2* measured by β-galactosidase assay in *ACT1* and *act1-159* strains.

4.5.3 Mitochondrial morphology

To characterise the effect of actin dynamics on mitochondrial localization and morphology, I used a mitochondrial GFP marker construct (described in Westermann & Neupert 2000) to visualise mitochondria by fluorescence microscopy. Mitochondria in *S. cerevisiae* form tubular structures which are aligned along the cell axis and accumulate at the daughter and mother cell tips during budding (Boldogh & Pon 2006).

Micrographs with GFP labeled mitochondria are shown in Figure 31. Filamentous and punctate mitochondrial structures were present in *ACT1* cells and could be seen in a variety of positions, in the periphery and across the centre of the cell, and in some

cells appeared to localise to opposite ends of dividing cells. In some *act1-159* cells the mitochondria were clustered together, although usually still in a filamentous form. Mitochondria in *act1-157* cells appeared to have more mitochondrial filaments in each cell, some of which were longer and more convoluted than those in *ACT1* cells. This correlates with the increased respiration in *act1-157* cells and suggests this may be a result of increased mitochondrial biogenesis. It was not clear from my observations whether reduced or increased actin filament turnover disrupted the ability of cells to distribute mitochondria between mother and daughter cells.

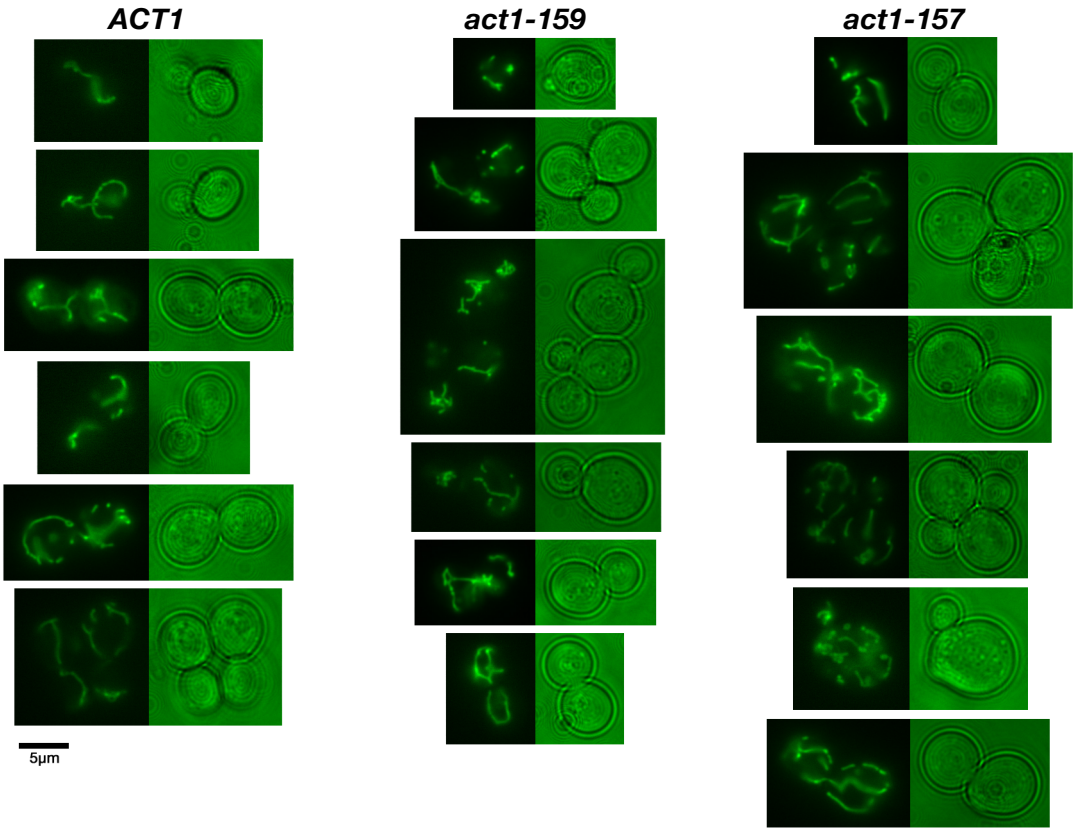

Figure 31. Cells expressing GFP fused to a mitochondrial targeting sequence to visualise mitochondria by fluorescence microscopy. Fluorescence images are showed with adjacent light images.

4.5.4 ER morphology in *act1-159* mutant

The endoplasmic reticulum extends throughout the cell as a network of tubules and membranes, and in *S. cerevisiae* exists mainly at the cortex and surrounding the

nucleus, with some interconnecting membrane. The ER requires a functional cytoskeleton to remain dynamic. There is evidence of close interaction between the ER network and mitochondria, and peripheral ER tubules often align with mitochondrial tubules (Prinz et al. 2000; Kornmann et al. 2011). Sec63p is a component of the super elongation complex (SEC) found in the ER membrane. Both cortical and nuclear ER structures are well visualised by expression of Sec63p-GFP from a plasmid construct (Fehrenbacher et al. 2002).

Micrographs in Figure 32 show the Sec63-GFP marker localised to both the nuclear and cortical ER and that both of these structures were present in wild-type and mutant cells. There appeared to be more fluorescence from the cortical ER in *act1-159* mutants. The structure of the nuclear ER was convoluted in both strains and the morphology is difficult to assess as it extends outside the plane of the viewing field. Additionally there were more small unconnected fluorescent structures visible in *act1-159* cells.

These data show that actin dynamics is important in regulating mitochondrial and endoplasmic reticulum morphologies, and at least in the case of mitochondria actin can have dramatic effects on ability to function normally.

4.6 Chapter summary

A number of phenotypes of strains with altered actin dynamics were analysed revealing the wide reach of the cytoskeleton within eukaryotic cells and the considerable ability to influence crucial processes.

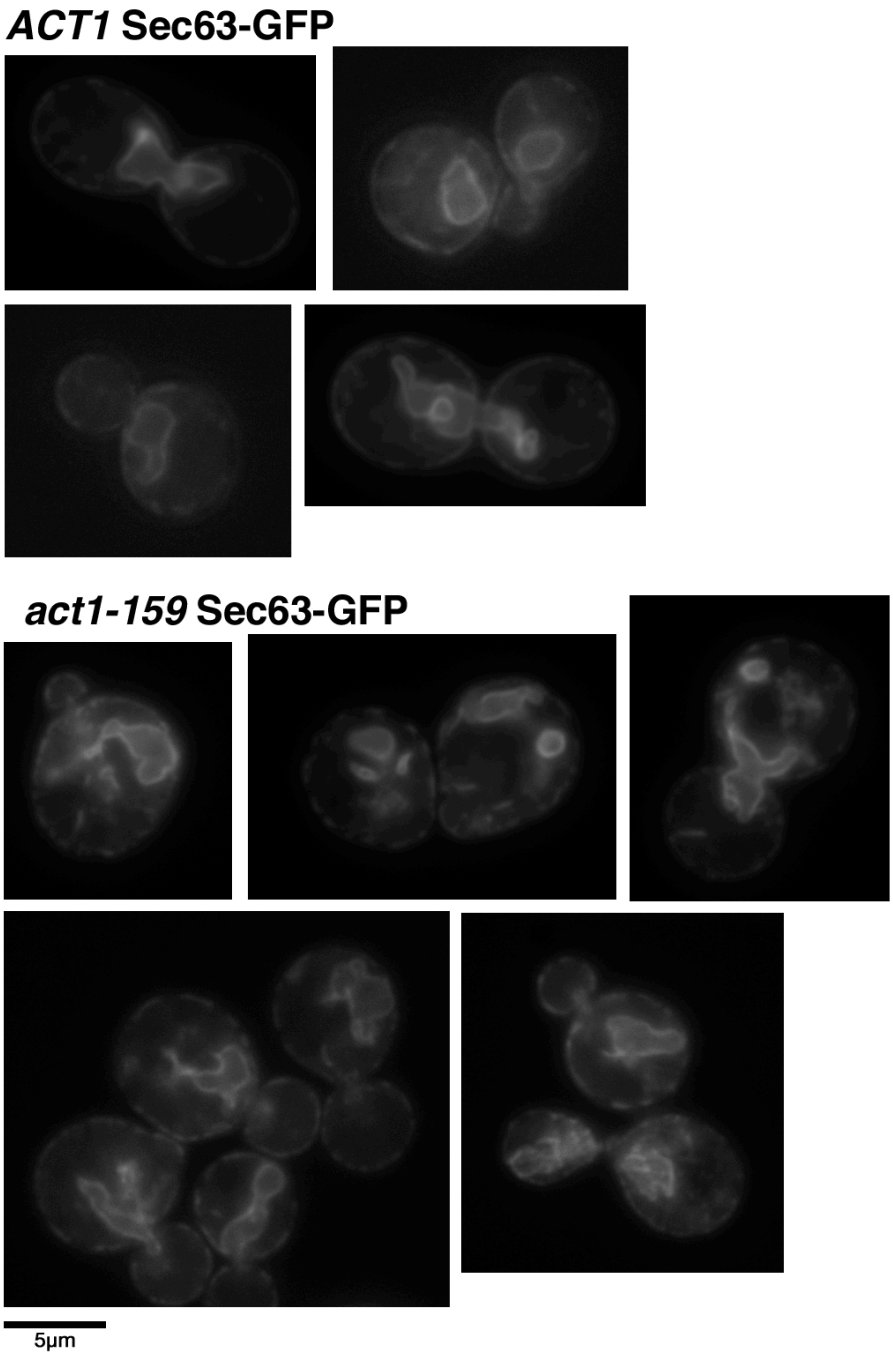

Figure 32. ACT1 and *act1-159* cells transformed with Sec63-GFP vector were viewed under a fluorescence microscope to visualise endoplasmic reticulum membranes. 150x magnification

The investigation into roles for actin in protecting DNA damage have shown that the *act1-159* mutant is not any more able to survive DNA perturbation when compared to wild-type. However the growth of cultures in the presence of a DNA damaging agent was not as severely affected as that of wild-type cells. It is not clear whether these

observations indicate altered ability to repair DNA damage in *act1-159* cells, or whether growth in the presence of MMS represent a failure of cells to detect DNA damage or enter cell cycle arrest. Several actin-regulating genes may have roles in regulating DNA damage responses, including some with documented nuclear activities, and others which are associated with other functions such as cortical patch organisation.

One of the more interesting findings were those regarding the mitochondria. While mitochondrial dysfunction was previously reported following loss of actin dynamics, respiratory function of mitochondria in *act1-159* mutants was shown to be completely lost. This illustrates the need for a dynamic cytoskeleton for function of this organelle. The activation of retrograde signaling was also shown and this indicates that cellular stresses occurring due to differences in actin dynamics illicit signaling responses to promote homeostasis. The morphologies of the ER, mitochondria and the cell wall were all seen to affected by actin dynamics. The altered cell wall in both actin mutants supports our gene ontology data which highlighted cell wall biogenesis as an altered process, and raises the question of how signaling pathways activate this in response to actin filament stabilisation.

Responses to heat stress and the roles of heat shock proteins in the actin mutant phenotypes remain unclear. I did not see an increased background level of either of the HSP proteins I investigated, nor was the induction any greater, but the data indicated some disruption to the stress responses in which these proteins are involved.

5 Cytoskeletal dynamics in the regulation of environmental sensing signals

5.1 Chapter introduction

The actin cytoskeleton is modulated in response to environmental changes and is both the target of numerous signaling pathways, and an important regulator of signal transduction. As outlined earlier, one of the most studied yeast signaling pathways is the mating response pathway, and the closely linked filamentous/invasive growth pathway. The microarray data presented in Chapter 3 indicated that altered actin dynamics may be influencing signaling events at the level of mRNA transcript expression, and data in Chapter 4 has confirmed that these correspond to protein expression changes. Additionally, the up-regulation of mitochondrial retrograde signaling markers shows that the loss of actin dynamics produces cellular stresses and that the cell activates mechanisms to maintain homeostasis in response. In this chapter I employ experimental techniques to investigate the connections between the dynamic status of actin and the Ras/cAMP/PKA, mating response, filamentous/invasive growth response and HOG signaling pathways.

5.2 Ste12p and Ste12p-Tec1p complex activity and actin dynamics

The filamentous/invasive growth pathway and the pheromone response pathway have an overlapping subset of components including Ste20p, Cdc42p and Ste12p, but produce distinct responses (Posas et al. 1998). The transcriptional program directed by each pathway is defined by the activation of Ste12p, which binds PRE-containing promoters, or Ste12p in complex with Tec1p, which binds promoters containing both

a PRE and a TCS element, which together form an FRE. *STE12* was first identified in *S. cerevisiae* in screens for mutants which were sterile and unresponsive to mating factor, along with several other genes which are now known to be upstream of it in the mating pathway. Sterile mutants also have reduced basal expression of mating genes, indicating that there can be activity of the pathway outside of inducing conditions (Adler & Errede 1988). Ste12p-like proteins have been found across fungi and are associated with activating a range of adaptive responses to environmental change (Wong Sak Hoi & Dumas 2010). I aimed to establish a connection between the dynamics of the actin cytoskeleton and induction of the mating pathway target Ste12p and the filamentous/invasive growth pathway Ste12p-Tec1p.

A reporter construct was used in our studies to measure the activity of Ste12p-Tec1p complexes under several conditions. The plasmid pCG394 was constructed with a promoter fused to the *lacZ* gene (which encodes β-galactosidase), downstream of the FRE sequence from the retrotransposon Ty1. This plasmid is described in (Madhani & Fink 1997), and a version of this with an alternative selection marker pCG525 was also used and is described in L. Bardwell et al. (1998).

5.2.1 β-galactosidase assays for Ste12p-Tec1p activity in actin mutants

To determine whether Ste12p-Tec1p is activated by reduced actin dynamics, I transformed *act1-159* mutant and *ACT1* wild-type strains with a *lacZ* reporter plasmid, and assayed the expression of Ste12-Tec1p regulated genes by measuring the β-galactosidase activity. Figure 33 shows the results of an assay using the standard assay substrate ONPG, which produces the yellow ortho-nitrophenol product upon hydrolysation by β-galactosidase. Wild-type cells in this genetic background

displayed almost no detectable β-galactosidase activity suggesting low levels of Ste12p-Tec1p activity. In contrast to this, Ste12p-Tec1p activity was elevated in *act1-159* mutants.

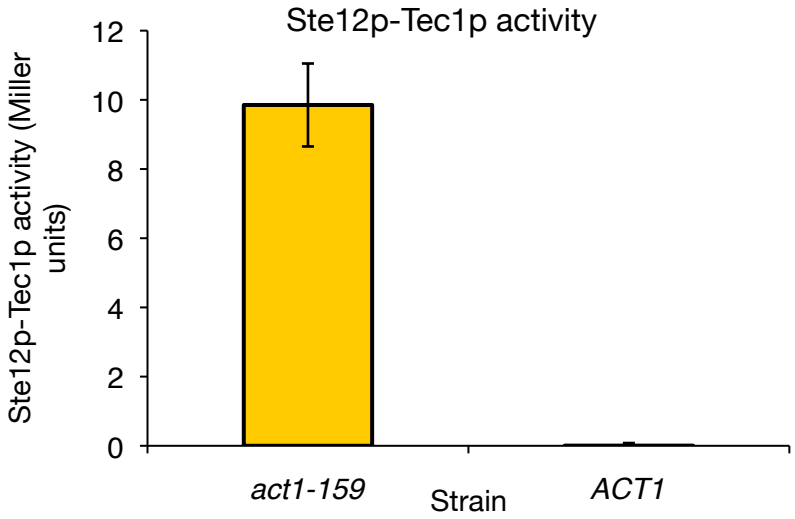

Figure 33. Ste12p-Tec1p activity in log phase cultures of *act1-159* mutant and *ACT1* wild-type transformed with *FRE(Ty1)*::*lacZ* plasmid and measured by β-galactosidase assay

Using the same reporter constructs but with the alternative X-gal substrate which allows the assay to be performed with colonies grown on agar, the same phenotype was observed in *act1-159* mutants and was also seen in *act1-157* mutants (Figure 34).

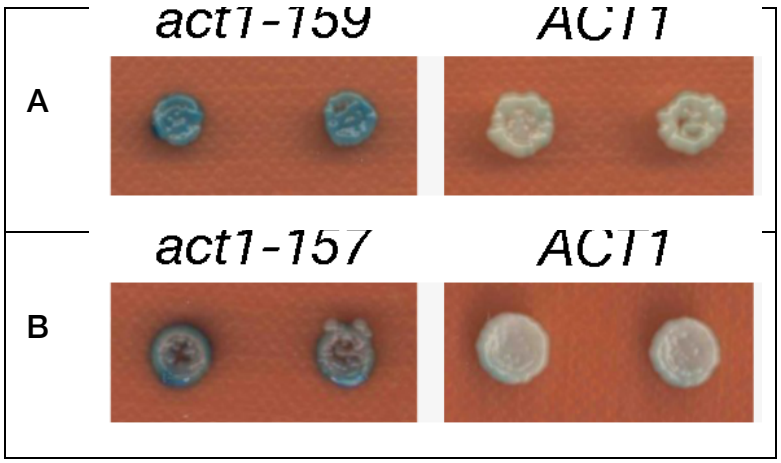

Figure 34. Ste12p-Tec1p activity of colonies of *act1-159* (A) and *act1-157* (B) mutants and wild-type transformed with *FRE(Ty1)*::*lacZ* plasmid detected using X-gal assay, in which substrate is converted to a blue compound when *lacZ* gene is expressed.

The activity of Ste12p-Tec1p in both actin mutant strains is also shown using *FRE(Ty1)*::*lacZ* plasmid as the controls for further assays (see section 5.9.2)

5.2.2 Actin stabilisation with jasplakinolide and Ste12p-Tec1p activity

I sought to find if the presence of mutant alleles of the actin gene was causing the increased expression of Ste12p-Tec1p targets as a result of altered cytoskeletal dynamics, rather than any other changes which might have occurred. To achieve this I employed the drug jasplakinolide, a cyclic peptide isolated from the marine sponge *Jaspis johnstoni*, which binds to and stabilises actin filaments, resulting in rapid formation of large filament aggregates (Gourlay et al. 2004).

A strain in which the multidrug resistance genes *PRD5* and *SNQ2* were deleted (CGY997) was used for these assays, and is described in (Ayscough 2000). These mutations increase sensitivity to many chemicals, including jasplakinolide, whilst maintaining normal cytoskeletal morphology. Growth effects were reported from 10μM concentrations within 30 minutes, and I observed growth inhibition from lower concentrations when incubated for periods of several hours, as shown in Figure 35. The growth curves (A) show a decrease in gradient as concentrations of the drug increased. The maximum gradient for each culture was calculated using R and are shown in Figure 35 B.

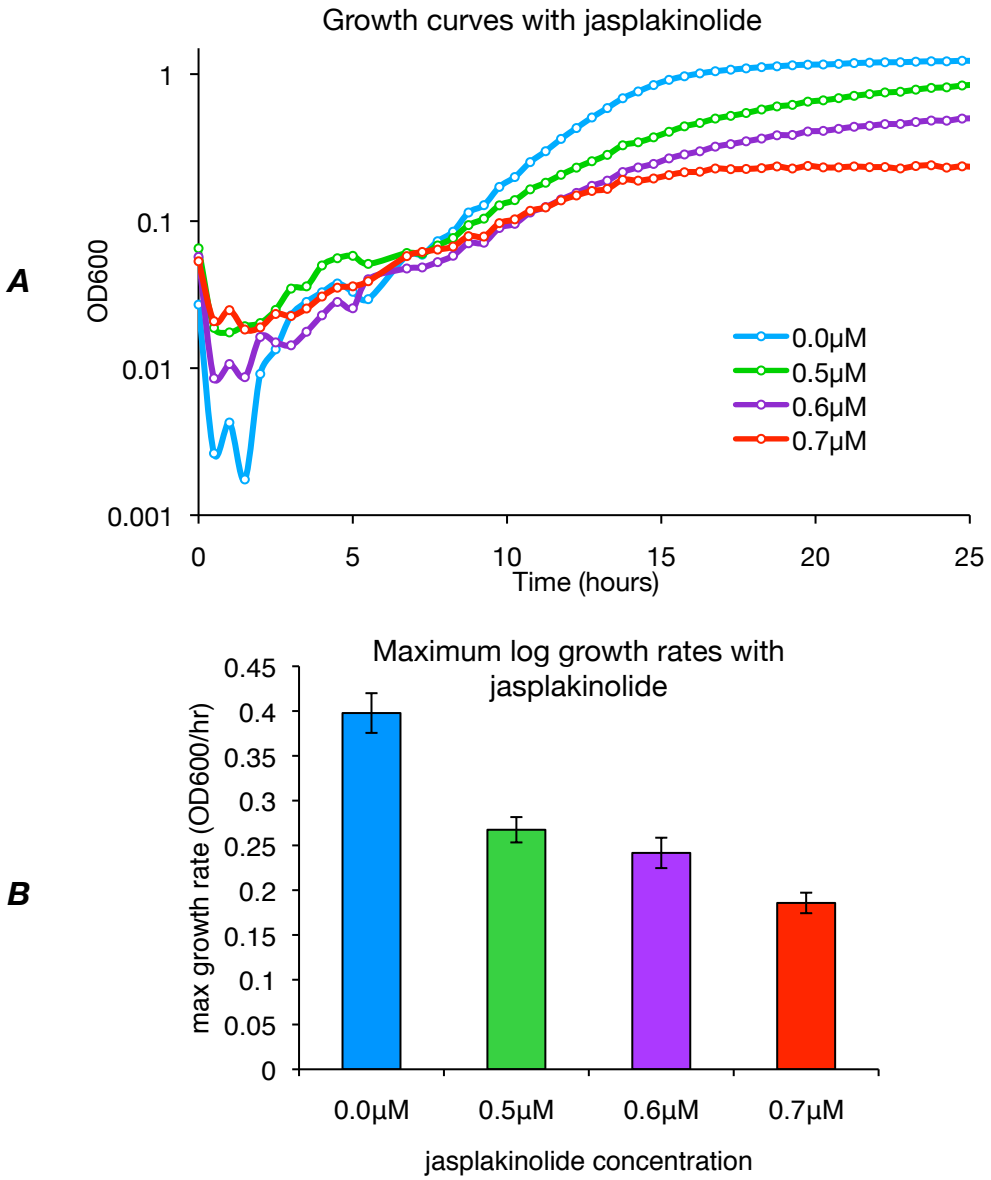

Figure 35. Growth curves (A) and maximum growth rates (B) of cultures grown in increasing concentrations of jasplakinolide. Cultures were transformed with *FRE(Ty1)*::*lacZ* plasmid and grown in SD –URA. Mean data from triplicate repeats was used and error bars represent SEM.

Having confirmed that jasplakinolide is effective against this strain, I investigated the activity of Ste12p-Tec1p when actin filaments are stabilised by the treatment. Cultures transformed with *FRE(Ty1)*::*lacZ* plasmid were grown to an OD600 of 1 in SD –URA before jasplakinolide was added, and then incubated for 6 hours before a β-galactosidase assay was performed. The density of cultures was measured at two hour intervals and under this treatment protocol the density of all cultures had increased

equally after 2 and 4 hours. Only after 6 hours was there a reduction in growth rate and this was only seen at the 1μM concentrations. Figure 36 shows the Ste12p-Tec1p activity was elevated with 1μM jasplakinolide but was not detectable at the lower concentration or with no treatment.

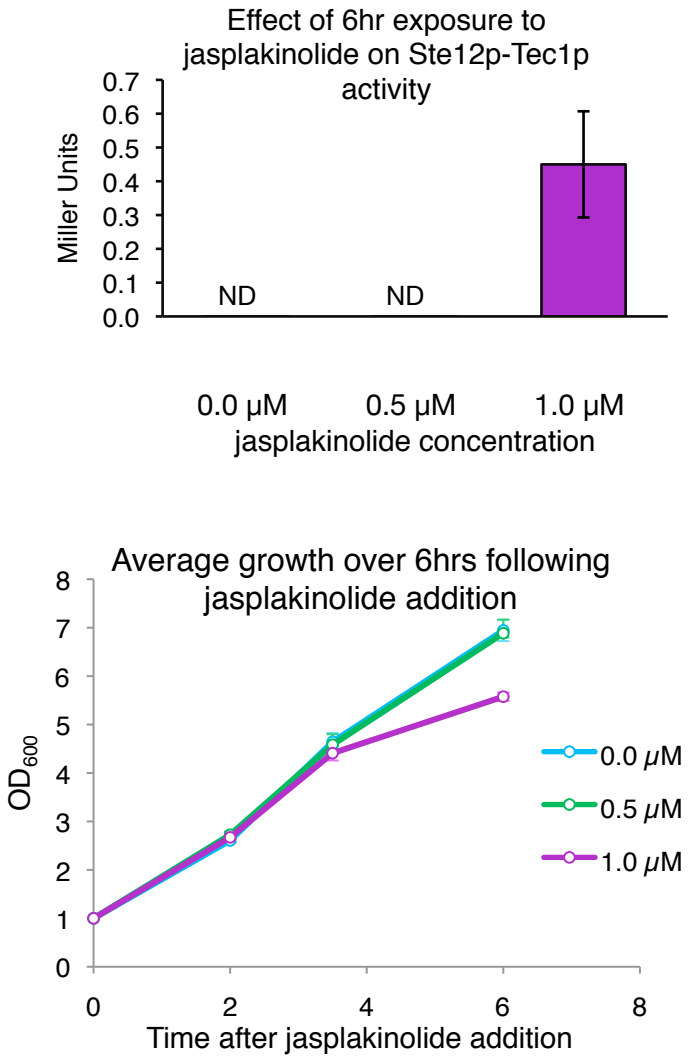

Figure 36. Top: Ste12p-Tec1p activity of cultures grown in YPD exposed to jasplakinolide at increasing concentrations for 6 hours. ND = not detectable. Bottom: Growth of cultures in YPD after jasplakinolide added.

These results show that reduced actin dynamics correlates with reduced log growth rates. The use of different strain backgrounds and both chemical and genetic methods of stabilising the cytoskeleton has resulted in both slow growth and increased

expression of Ste12p-Tec1p targets. This confirms that these phenotypes occur as a result of altered actin dynamics.

5.2.3 Expression of mating pathway targets measured by Fus1p levels

A marker of expression in response to pheromone was used to assess if a transcription program associated with this response is activated when the cytoskeleton is stabilised. Fus1p is a protein which is involved in cell fusion during mating. Transcription of the *FUS1* gene increases in the presence of pheromone, as a result of pheromone pathway signaling. Ste12p induces expression independently of Tec1p via multiple PREs positioned upstream of *FUS1,* allowing its use as a marker of the mating pathway (Staleva et al. 2004; Hagen et al. 1991). I used a plasmid construct (pCG515) in which the *FUS1* promoter was fused to a luciferase protein allowing the levels of Fus1p expression to be quantified. In line with our transcriptome observations there is an increase in expression of Fus1p, indicating Ste12p activity is increased with reduced actin dynamics.

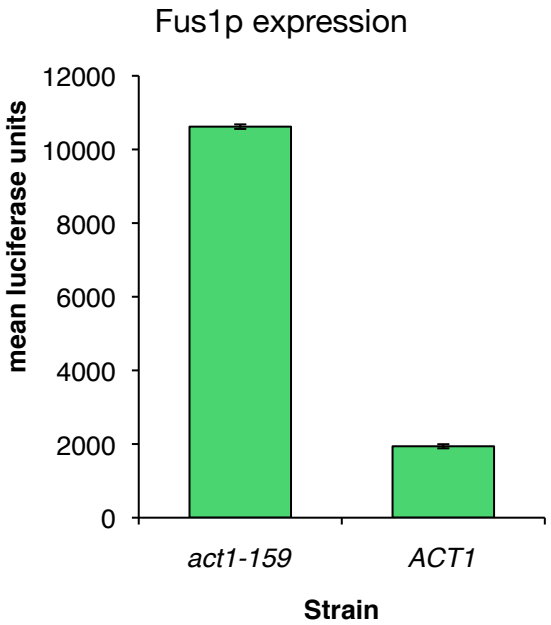

Figure 37. Fus1p expression in *act1-159* mutant strain quantified by luciferase levels in cells expressing luciferase from a FUS1 promoter.

5.3 Identifying actin residues which influence Ste12p-Tec1p activation

I wished to investigate whether changes to other amino acids in the actin molecule led to Ste12p-Tec1p activation. To do this I made use of a library of isogenic strains in which surface exposed amino acids have been mutated to alanine (Whitacre et al. 2001). This library has been previously used to show that several common phenotypes of cytoskeletal mutants corresponded with mutations in a small region of the folded actin structure. Unfortunately only a subset of the collection was available to us and of these, several failed to grow under our assay conditions. However I aimed to assess if Ste12p-Tec1p targets were being expressed in any of the strains and if so, if it correlated with an actin domain.

Actin mutant strains were grown on agar containing X-gal as shown in Figure 38. When compared to *ACT1* wild-type, three mutants produced colonies of noticeably darker colour (indicated by **), three had a slightly darker colour (indicated by *) and three showed no change (indicated by -), revealing that Ste12p-Tec1p activity is increased as a result of 6 out of the 9 actin mutations in this assay.

The mutated residues in the 6 mutants with increased Ste12p-Tec1p activity were mapped to the crystal structure of rabbit muscle G-actin (Wang et al. 2010, PDB structure ID:3HBT) to determine if they were clustered to a region of the molecule. Two views of the structure with relevant residues labeled are shown in Figure 39 (A, B).

Actin residue change	X-gal colony	Colour difference
Wild-type	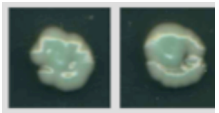	N/A
D222A, E224A, E226A		* *
P32L	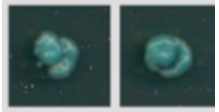	* *
R116A, E117A, K118A		* *
R177A, D179A	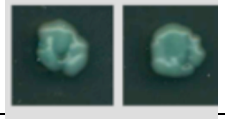	*
D80A, D81A		*
D56A, E57A	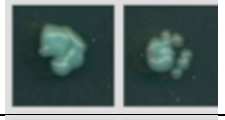	*
E4A		-
K315A, K316A	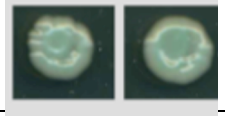	-
R210A, D211A	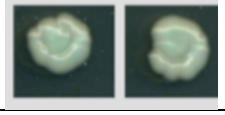	-

Figure 38. Duplicate cultures of actin mutants transformed with *FRE(Ty1)*::*lacZ* plasmid and grown on SD-URA with X-gal to show activity of Ste12p-Tec1p.

Several residues of interest from Figure 38 are found in subdomains 1 and 2. This includes the mutations at residues 32, 56, 57 in subdomain 2 and residues 80, 81, 116, 117 and 118 in subdomain 1. A binding site for the depolymerisation factor cofilin has been reported in subdomain 2, centered around Gln 41 (Benchaar et al. 2007). It is possible that these mutations in subdomain 2 inhibit cofilin-mediated

depolymerisation and these mutants may generate stable actin structures, but analysis of further mutants is required to clarify this.

Figure 39 (C) shows that the side chains of Arg177 and Asp199 are in close proximity with Val159 and so could potentially be involved in nucleotide binding. The increased Ste12p-Tec1p activity observed with this mutation therefore may be due to a similar effect on filament dynamics as occurs with mutations at residues 157 and 159. It has been reported that this mutant form of actin forms stabilised filaments *in vitro* which polymerise more slowly than wild-type (Buzan & Frieden 1996).

The other residues, which increased Ste12p-Tec1p activity when mutated, were 222, 224, and 226. These are in subdomain 4. As this domain is in close contact with other monomers in a filament it is possible that small changes in configuration would affect filament stability. There is also a calcium cation binding site in the region of these residue, and calcium binding is known to affect filament stability (Otterbein et al. 2001).

A

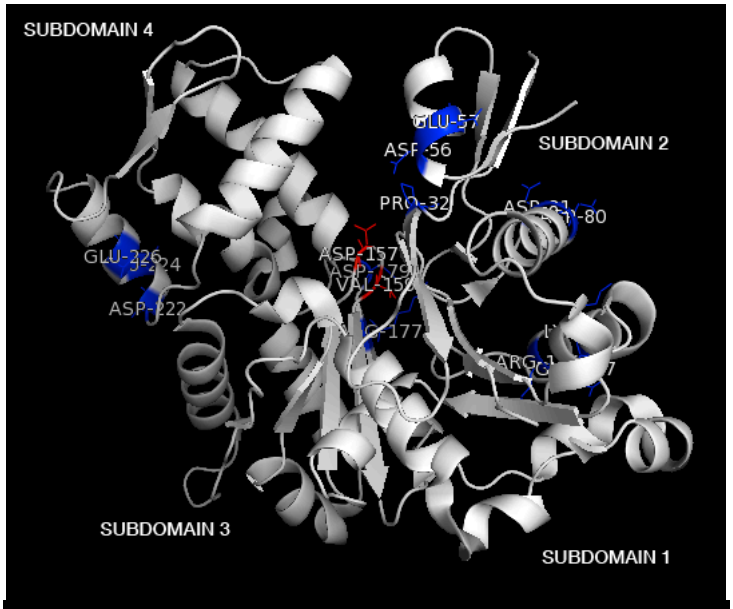

B

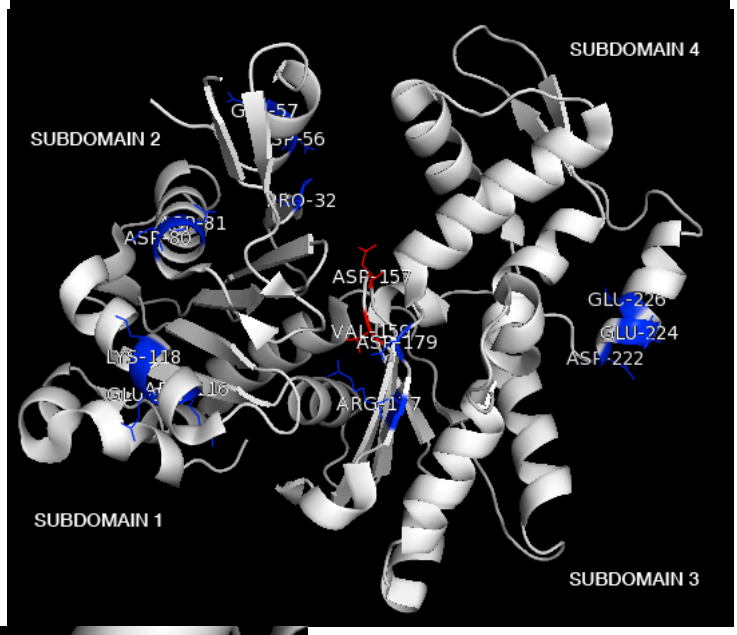

C

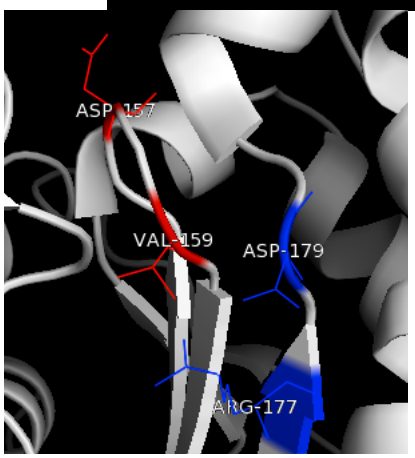

Figure 39. Crystal structure of rabbit muscle actin with mutations labeled. Residues of interest from Figure 38 are shown in blue and residues 157 and 159 are shown in red. (A & B) Two views of ribbon diagram of actin molecule showing positions of residues which when mutated increase Ste12p-Tec1p activity. These residues are more common in subdomains 1 and 2 (right in A, left in B). (C) Close up view of nucleotide binding cleft showing proximity of the side chains of Asp177 and Arg179.

5.4 Ste12p-Tec1p activity in actin-regulating gene deletion library

I aimed to establish whether particular actin related functions may be required to regulate Ste12p-Tec1p activity phenotype. To do this, a knockout collection in which each non-essential ORF has been systematically disrupted was used (Kelly et al. 2001). From this collection I created a sub-library of strains each with a GO-assigned actin-regulating gene deleted. These were transformed with the *FRE(Ty1)*::*lacZ* plasmid reporter and grown in triplicate on selective agar containing X-gal to produce the colonies shown in Figure 40. These have been organised into three groups based on the colour difference between the deletion mutants and the wild-type colonies. Ste12p-Tec1p activity was increased in 10 strains, reduced in 4 strains and showed no perceptible change in 10 strains.

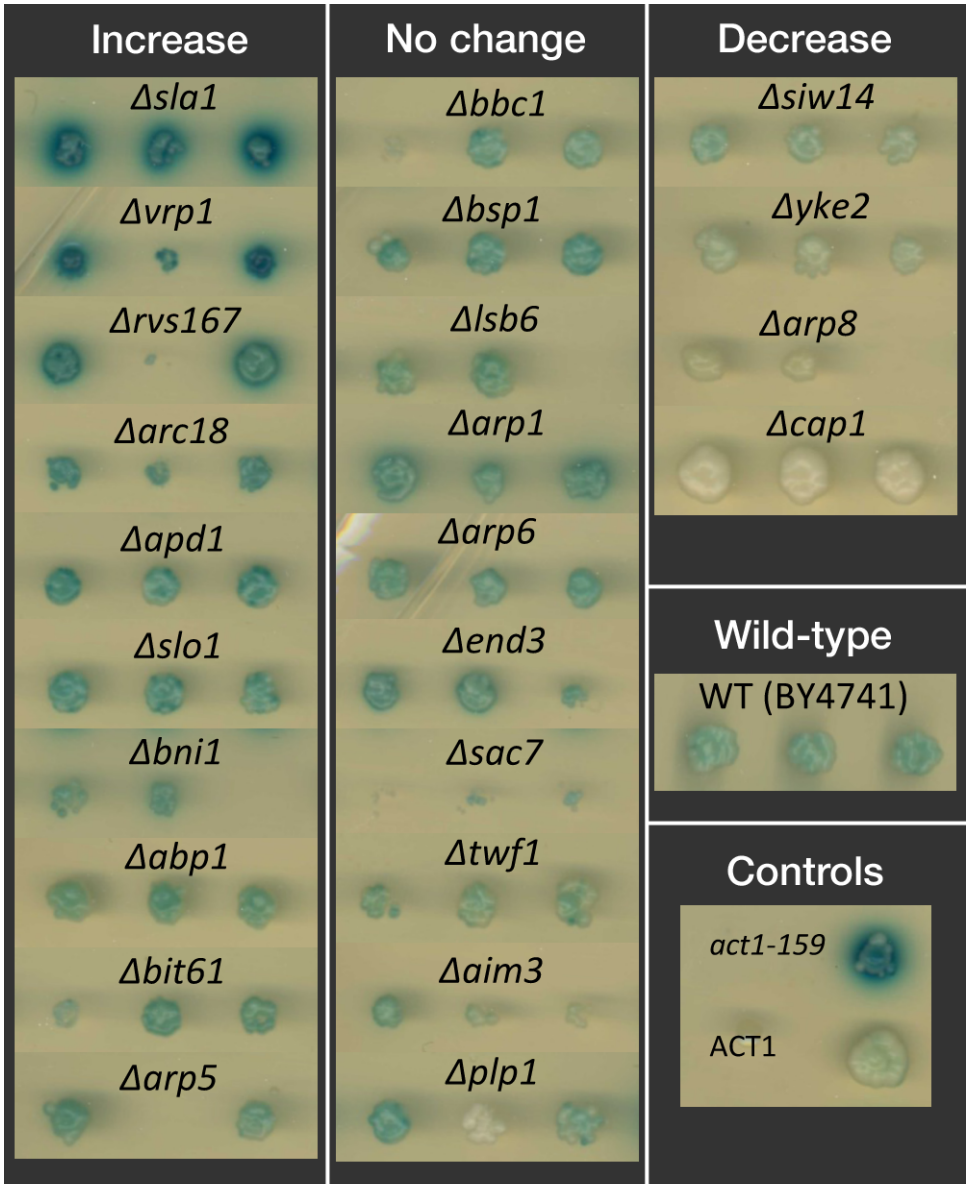

Figure 40. Colonies of strains deleted for actin regulating genes transformed with *FRE(Ty1)*::*lacZ* plasmid and grown on SD –URA agar containing X-gal to show activity of Ste12p-Tec1p.

A noticeable increase in Ste12p-Tec1p activity occurred with deletion of *SLA1*, which encodes a regulator of cortical patch assembly and endocytic actin dynamics. Sla1p interacts with the Arp2/3 complex regulators Pan1p, Las17p and Abp1, and also regulates the targeting of membrane receptors (Warren et al. 2002; Howard et al. 2002). The five genes which when deleted produced the most marked colour change in the assay (*SLA1, VRP1, RVS167, ARC18, APD1*), and also *ABP1* all encode regulators of cortical patches. Both Arc18p and Abp1p have roles in the Arp2/3

complex. Vrp1p affects several diverse processes including endocytosis and budding, and is required for Las17p localisation. Rvs167p is found in cortical patches with roles in endocytic vesicle scission and actin organization (Sivadon et al. 1997).

Other gene deletions which increased Ste12p-Tec1p activity have a variety of actin interactions. The formin Bni1p is associated with actin cable assembly, although it is partially redundant with Bnr1p, and it has been reported that cell viability is not affected by deletion of either one (Moseley et al. 2006). However Bni1p has a role in localising Ste5p in the mating pathway which is not fulfilled by Bnr1p (Qi & Elion 2007). Bit61p is a subunit of the TOR complex 2 which regulates the cytoskeleton (Loewith & Hall 2011). Two actin-related components INO80 chromatin remodeling complexes, Arp5p and Arp8p give different results in this assay. Deletion of *ARP5* resulted in a small increase in expression from the FRE promoter, while deletion of *ARP8* reduced expression.

The *Δcap1* strain produced colonies with no blue pigment visible. Cap1p is found largely at the cortical patches and acts to block actin filament polymerization by binding to the (+) ends. Phenotypes of null mutants include reduction in actin cables, large heterogenous cell sizes, and normal mating efficiency (Amatruda et al. 1992; Amatruda et al. 1990)

The observation of increased Ste12p-Tec1p activity in strains deleted for cortical patch organizing genes implicates membrane processes in the activity of the invasive growth pathway when there is cytoskeletal damage. In particular many of these genes

have specific roles in endocytosis, suggesting this process is important in regulating signaling.

5.4.1 Expression of mutant forms of Sla1p alters Ste12p-Tec1p activity

Previous studies have shown that the phenotypes of *sla1* mutants are functionally separated as shown by deletion of specific domains (Ayscough et al. 1999). Plasmids expressing truncated forms of Sla1p were expressed in *Δsla1* cells to investigate if specific regions regulated the increased Ste12p-Tec1p activity phenotype observed in this null mutant.

Three Src homology (SH3) domains are present toward the N-terminal end of Sla1p, two close together and one separated by a gap (Gap1). SH3 domains are found in many proteins, including components of the cytoskeleton, and are known to mediate protein-protein interactions (Mayer & Eck 1995). In the centre third of the protein (Gap2) is a putative SH3-binding proline helix motif. Within this central third are two domains termed SHD1 and SHD2, which are not homologous with each other or any other known domain. The SHD1 domain has SH3-like topology and is responsible for endocytic signal recognition, while SHD2 is a sterile α-motif (SAM) domain with roles in clathrin-mediated endocytosis (Di Pietro et al. 2010; Mahadev et al. 2007) The C-terminal section consists of multiple LXXQXTG consensus repeats (Ayscough et al. 1999).

The *Δsla1* strain was transformed with six plasmids each expressing *sla1* constructs which were disrupted in a particular region or regions. The regions of native Sla1p are outlined in Figure 41. The mutant constructs included those in which one, two, or all

three SH3 domains were removed, the Gap1 or Gap2 regions were removed or in which there a single residue change (P626S) was introduced to the proline helix sequence. Subsequently a second set of *SLA1* mutants plasmids were used in which the SHD1 and SHD2 domains were removed.

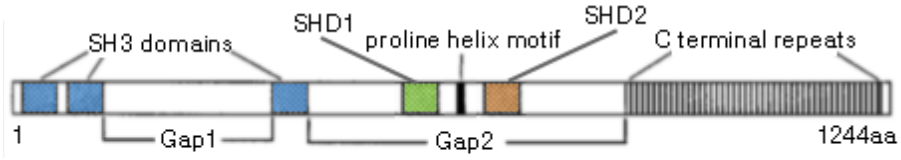

Figure 41. Diagrams Sla1p amino acid sequence, showing SH3, SHD1, SHD2 domains, Gap/Gap2 regions, proline helix motif and C terminal repeats. Adapted from Ayscough et al., 1999.

The *Δsla1* strain was transformed with *FRE(Ty1)*::*lacZ* plasmid to report Ste12p-Tec1p activity, and with plasmid expressing native Sla1p to confirm that the increased activity phenotype could be lost by reintroducing the gene on a plasmid. Colonies grown on selective agar media and then overlaid with X-gal agar are shown in Figure 42. Re-expression of full length Sla1p from the vector was sufficient to inhibit the high levels of Ste12p-Tec1p activity in *Δsla1* containing the control plasmid alone.

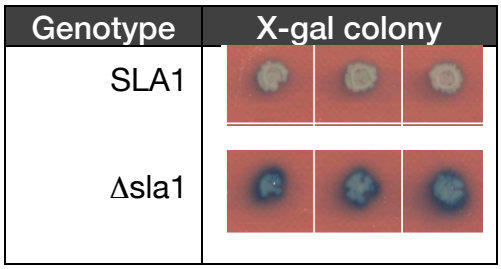

Figure 42. Triplicate *Δsla1* strains grown on SD-LEU–HIS agar and then overlaid with X-gal agar. Strains were transformed with both *FRE(Ty1)*::*lacZ* plasmid and either SLA1 expression plasmid or empty vector.

The null mutant strain was transformed with each of the six Sla1p domain mutant expressing plasmids, shown in Figure 43. Deletion of the Gap1 and the third SH3 domain from the N-terminus resulted in Ste12p-Tec1p activity comparable to that of *Δsla1* , but removal of Gap1 only did not, suggesting a role for the third SH3 domain

in regulating Ste12p-Tec1p activity. Removal of all three SH3 domains increased Ste12p-Tec1p activity, but to a lesser extent. A similar activity level was seen with removal of only the first two SH3 domains. Ste12p-Tec1p was activated when the Gap2 domain was removed. Mutation of the proline helix did not appear to increase Ste12p-Tec1p activity.

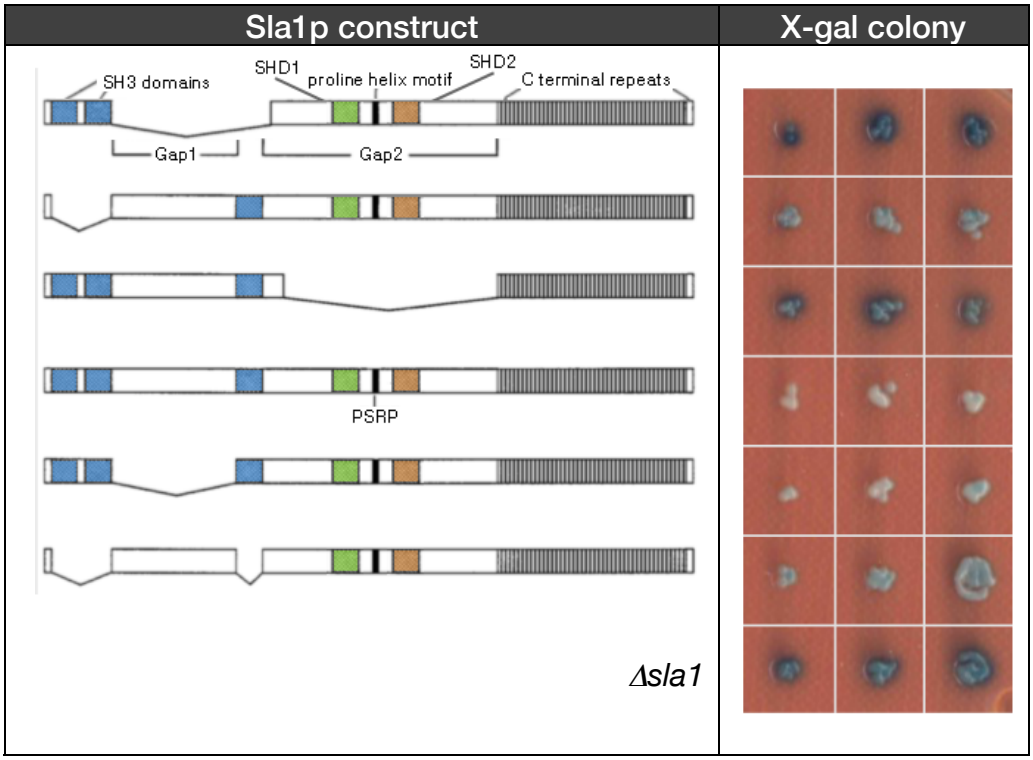

Figure 43. Triplicate *Δsla1* strains grown on SD-LEU–HIS X-gal agar. Strains were transformed with both *FRE(Ty1)*::*lacZ* plasmid and a second plasmid expressing a Sla1p domain mutant or empty vector.

A further set of *sla1* mutants was tested to clarify the role of the Gap2 region and the SHD1 and SHD2 domains (Figure 44). In these colonies the absence of SHD2 in did not affect Ste12p-Tec1p activity, but the loss of both SHD1 and SHD2 resulted in an increase in activity. A similar level of Ste12p-Tec1p activity was seen in colonies transformed with the Sla1p construct missing part of SHD1 only.

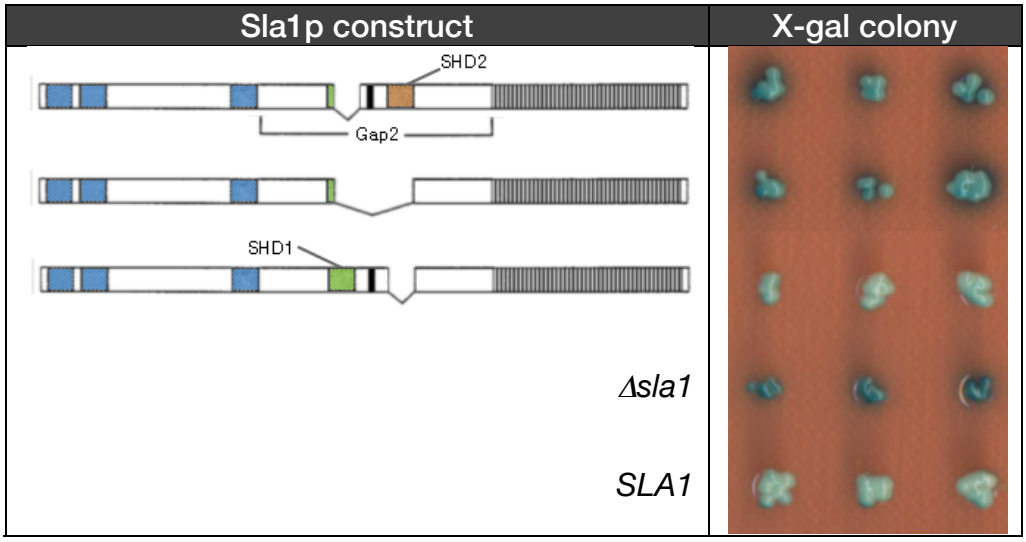

Figure 44. Triplicate *Δsla1* strains grown on SD-LEU–HIS X-gal agar. Strains were transformed with both *FRE(Ty1)*::*lacZ* plasmid and a second plasmid expressing a Sla1p domain mutant or control plasmid.

Overall, this data suggests that there is a role for the third SH3 domain in the Sla1p function that results in wild-type low Ste12p-Tec1p activity, and it has been reported that this domain is important for correct actin organisation (Ayscough et al. 1999). The first and/or second SH3 domain may also influence this role to a lesser extent. Additionally there appears to be some involvement of the SHD1 domain, as its removal also results in increased Ste12p-Tec1p activity.

5.4.2 Effect of Sla1p nuclear localisation on Ste12p-Tec1p activity

Further to its established role in endocytic processes at the cortex, Sla1p also localises to the nucleus in a karyopherin-dependent manner, and this nuclear transport of is required for its endocytic function (Gardiner et al. 2007) In the study a number of nuclear localisation signals (NLSs) and nuclear export signals (NESs) were predicted from analysis of the primary sequence. These included three classic NLSs in the N terminal third of the protein, as well as three bipartite NLSs and two NESs towards

the centre. I aimed to test if nuclear localisation of Sla1p was relevant to the Ste12p-Tec1p activity phenotype.

A plasmid was obtained from the Ayscough lab (pCG537) which expressed a mutant form of Sla1p with the first NLS mutagenised. This was transformed into the *Δsla1* strains and grown on selective agar containing X-gal. Images of the colonies are shown in Figure 45. The *Δsla1* colonies expressing Sla1p with mutagenised NLS were the same colour as those expressing wild-type Sla1p. Therefore this NLS does not appear to play a part in the Ste12p-Tec1p activation phenotype of *Δsla1* cells.

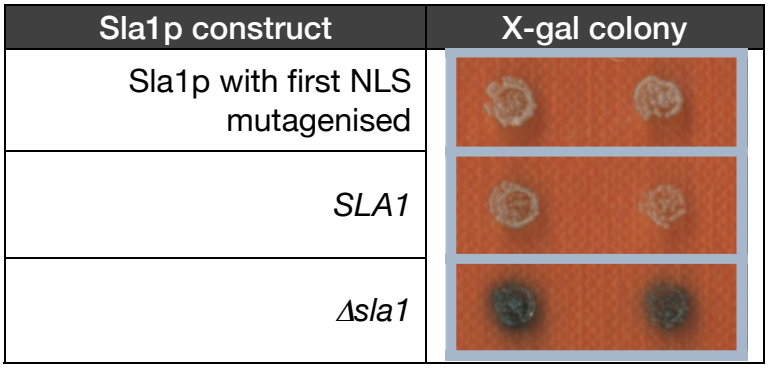

Figure 45. Triplicate *Δsla1* strains grown on SD-LEU–URA X-gal agar. Strains were transformed with both *FRE(Ty1)*::*lacZ* plasmid and a second plasmid expressing a Sla1p NLS mutant or control plasmid.

5.5 Growth of actin dynamics mutants in the presence of pheromone

Our data suggested that a reduction in actin dynamics leads to activation of Ste12p which normally responds to pheromone. Therefore I tested the effect of extracellular pheromone exposure on the growth of cells with stabilised actin when compared to wild-type. Cultures of the mating type a *act1-159* mutant and wild type were grown to an OD_{600} of 1 before being diluted to OD_{600} of 0.1 in YPD containing mating factor α. Growth of these cultures over 25 hours is shown in Figure 46. Initially 12.5 - 50μM

concentrations were used, and then the assay was repeated with concentrations between 3μM and 9μM.

As cultures were in log phase at the start of the assay, untreated samples rapidly increase in cell density from the start. The addition of mating factor produced a phase of slow growth of several hours followed by a return to fast growth, which is noticeable in the graphs from concentrations of 9μM and above.

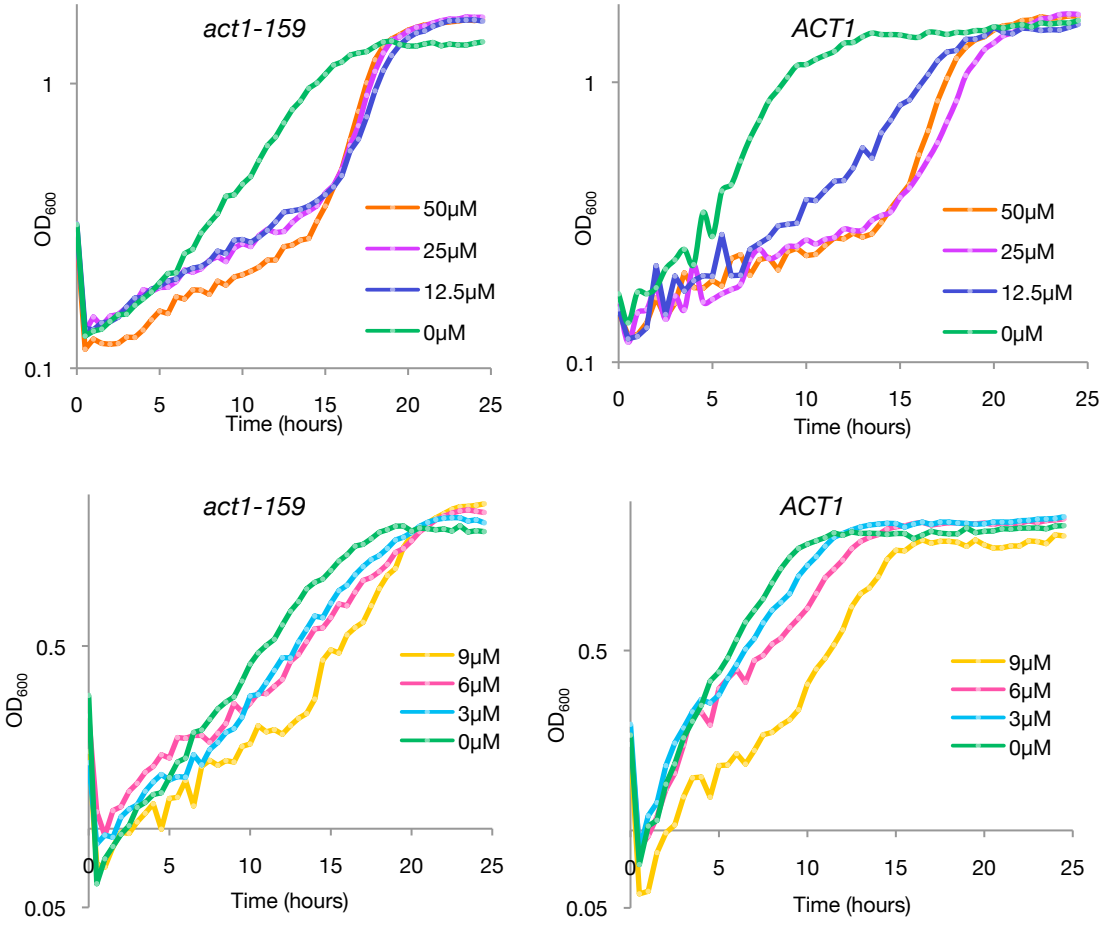

Figure 46. Log phase growth curves for mat a *act1-159* mutants and WT grown in YPD with increasing concentrations of mating factor α. Two sets of concentrations were tested and growth curves for these are shown separately. These measurements were taken from replicate cultures but only data from a single representative culture of each condition is shown here.

The mean maximum growth rates of replicate cultures in increasing mating factor α concentrations are shown in Figure 47. Wild-type cultures had a slower maximum growth rate as mating factor α concentration increased from 3μM to 12.5μM, after which the rate increased and returned to that of untreated cultures by 50μM. However the growth curves show that the rapid growth at 25μM and 50μM occurred after a 15 hour phase where growth is greatly retarded, suggesting this occurred following depletion of the pheromone. Interestingly, the maximum growth rates of *act1-159* cultures with 3μM and 6μM mating factor α was largely unchanged, and from 9μM and above the rate actually increases. At 50μM concentration, the growth rate was over double that of untreated *act1-159* cultures, and also exceeded that of untreated wild-type cultures. This fast growth again only occurred after a 15 hour slow growth phase. In contrast, the fastest growth in all untreated samples was at the start of the assay.

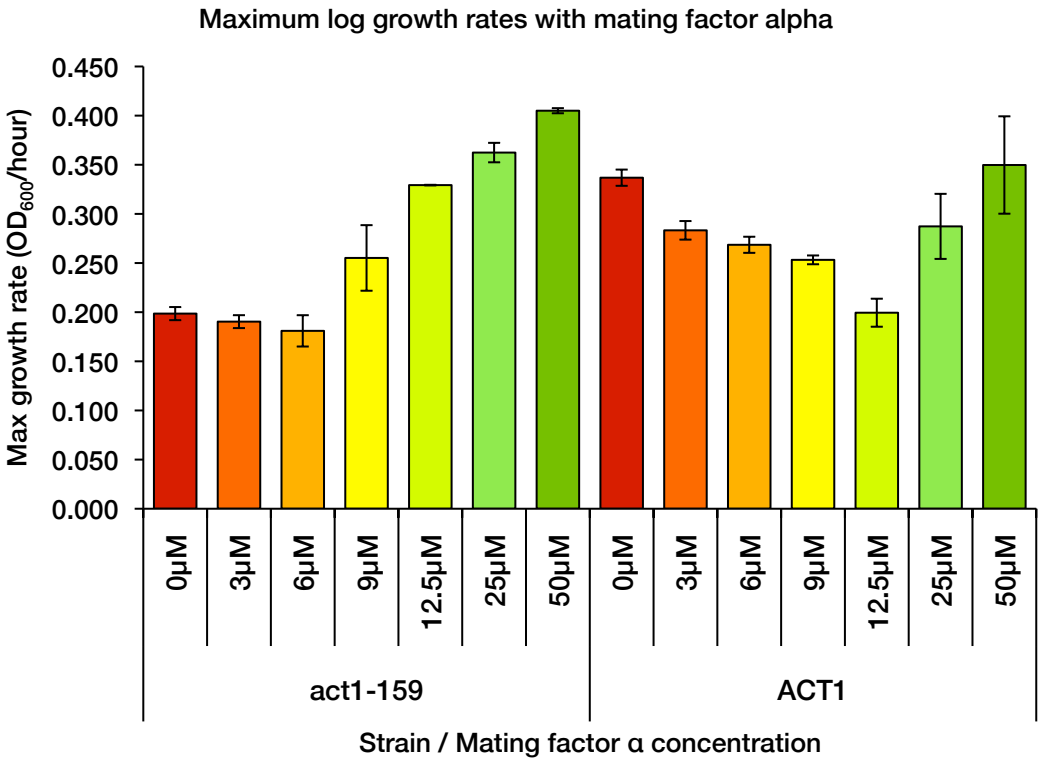

Figure 47. Maximum rates of growth calculated from duplicate growth curves in which cultures of *ACT1* and *act1-159* cells were grown in the presence of increasing concentrations of mating factor

These data show that *act1-159* cells are able to respond to the presence of mating factor and arrest growth in response to pheromone. They also have an enhanced recovery from growth arrest compared to wild-type, and interestingly are able to even increase their growth rate following recovery.

5.6 Interactions between actin dynamics and mitochondrial function

Results presented in Chapter 3 suggested that mitochondrial retrograde signaling is active when actin dynamics is reduced, and respiratory capacity is severely reduced. In this section I investigated how mitochondrial function might be involved in the regulation of Ste12p-Tec1p activity and the growth rates when there is altered cytoskeletal dynamics.

5.6.1 Effect of interactions between cofilin and mitochondrial permeability on Ste12p-Tec1p activity

Previous work from our group has found that ertain mutations in the actin depolymerisation factor cofilin increase both respiratory capacity and Ste12p-Tec1p activity, and that loss of mitochondrial respiration in these mutants abolishes the Ste12p-Tec1p activity (Kotiadis et al. 2012, unpublished work). Research in mammalian models has indicated that cofilin can act to induce apoptosis under oxidative stress by interacting with mitochondrial permeability transition pores (PTPs) and allowing the release of cytochrome c (Zdanov et al. 2010; Klamt et al. 2009).

The yeast gene *POR1* encodes a mitochondrial membrane protein porin which is a component of the yeast PTP. I sought to investigate the role of cofilin and porin in the activation of Ste12p-Tec1p. A Ste12p-Tec1p-activating cofilin mutant (*cof1-7*) and a double mutant in which *POR1* had also been deleted were transformed with Ste12p-Tec1p *lacZ* reporter plasmid and grown on X-gal agar (Figure 48). Deletion of *POR1* did not abolish the Ste12p-Tec1p activity and may actually have increased it a small amount, while activity remained low in the wild-type with or without *POR1*.

Genotype	X-gal colony
cof1-7	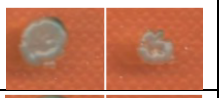
cof1-7 Δpor1	
COF1	
COF1 Δpor1	

Figure 48. Triplicate rho^0 strains grown on SD-LEU X-gal agar. Strains were transformed with *FRE(Ty1)*::*lacZ* plasmid.

5.6.2 Ste12p-Tec1p activity in *act1-159* and Δsla1 mutants in the absence of functional mitochondria

To investigate if mitochondrial function affected Ste12p-Tec1p activity observed in *act1-159* and *Δsla1* mutants, cultures were depleted of mitochondrial DNA by ethidium bromide treatment to produce rho^0 versions. Mitochondrial respiration depends upon a series of complexes in the inner mitochondrial membrane which transfer electrons from NADP to molecular oxygen (O_2). Genes encoding proteins of the respiratory transport chain are split between the mitochondrial and nuclear genomes. Rho^0 cells do not respire due to loss of components of the respiratory chain which are encoded within the mitochondrial genome. As I have already shown, *act1-159* cells have no respiratory capacity, but DNA is present in their mitochondria (unpublished data).

Growth analysis of rho^0 strains is shown in Figure 49. Growth rates of wild-type cultures were noticeably affected by loss of respiratory function while there was very little change in *act1-159* cultures. The maximum growth rate of *ACT1* rho^0 is

comparable to that of *act1-159*, which suggests the growth defects in the strain with reduced actin dynamics might be attributed to loss of functional mitochondria.

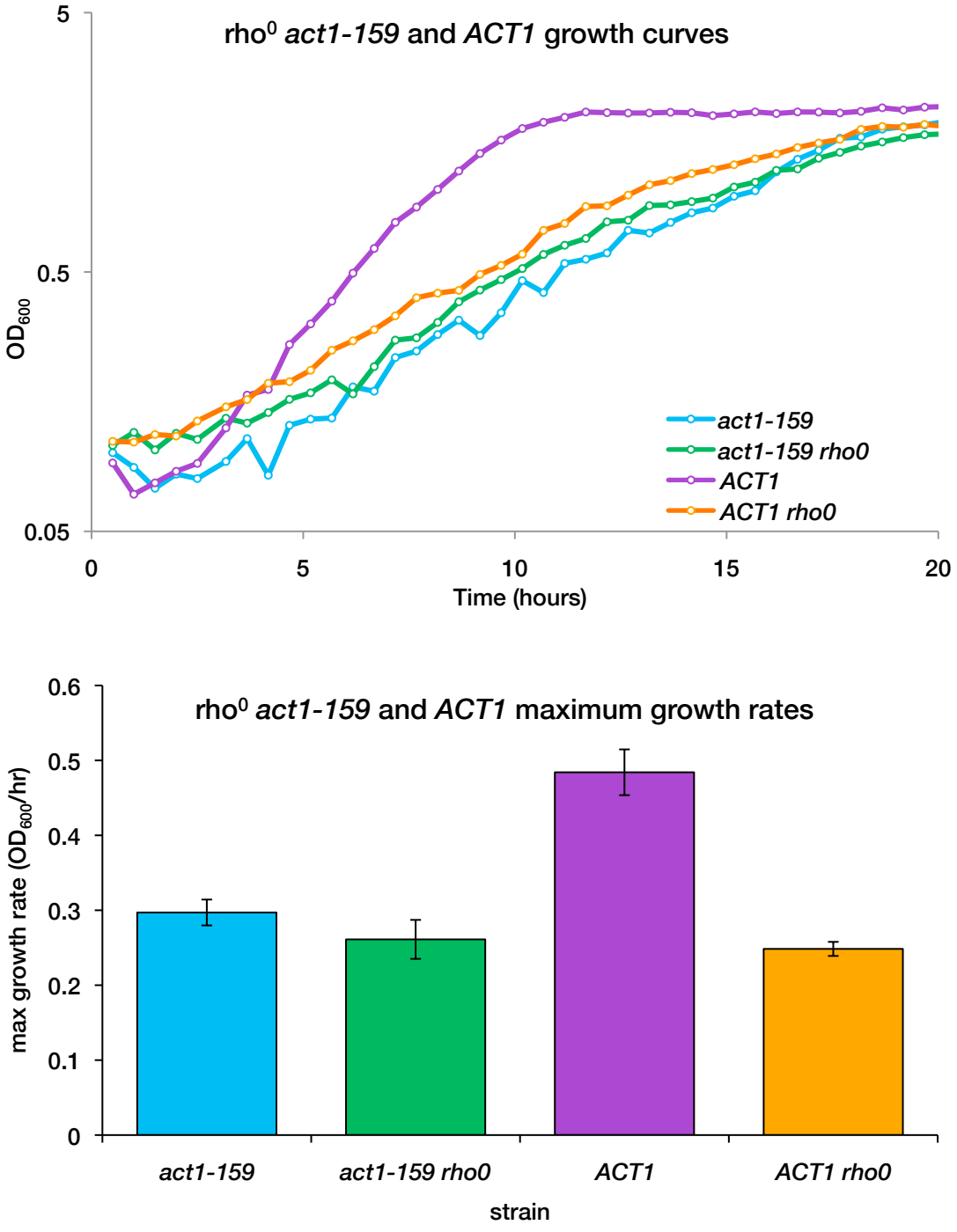

Figure 49. Growth of rho^0 *act1-159* and *ACT1* in YPD over 20 hours shown as growth curves (top) and the average maximum growth rates from three replicate experiments (bottom).

Figure 50 shows colonies of rho^0 *act1-159* and *ACT1* strains transformed with Ste12 *lacZ* reporter and grown on X-gal agar. The phenotype was not changed from the normal versions of these strains.

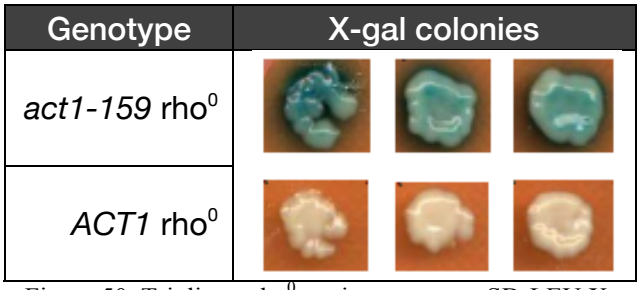

Figure 50. Triplicate rho^0 strains grown on SD-LEU X-gal agar. Strains were transformed with *FRE(Ty1)*::*lacZ* plasmid

I also investigated the effects of altering mitochondrial function in *Δsla1* cells, which were seen to have increased Ste12p-Tec1p activity similar to that of *act1-159* cells. It was observed that unlike *act1-159* cultures, *Δsla1* cultures did not appear to grow more slowly than wild type, so a growth assay was perfomed to clarify this difference (Figure 51). The maximum growth rates of *Δsla1* cultures were similar to that of wild-type with functional mitochondria, but were more markedly reduced by loss of respiratory function in the rho^0 cultures. This is in contrast to the difference between *act1-159* and its rho^0 version and indicates mitochondrial respiration is unlikely to be reduced in the absence of Sla1p.

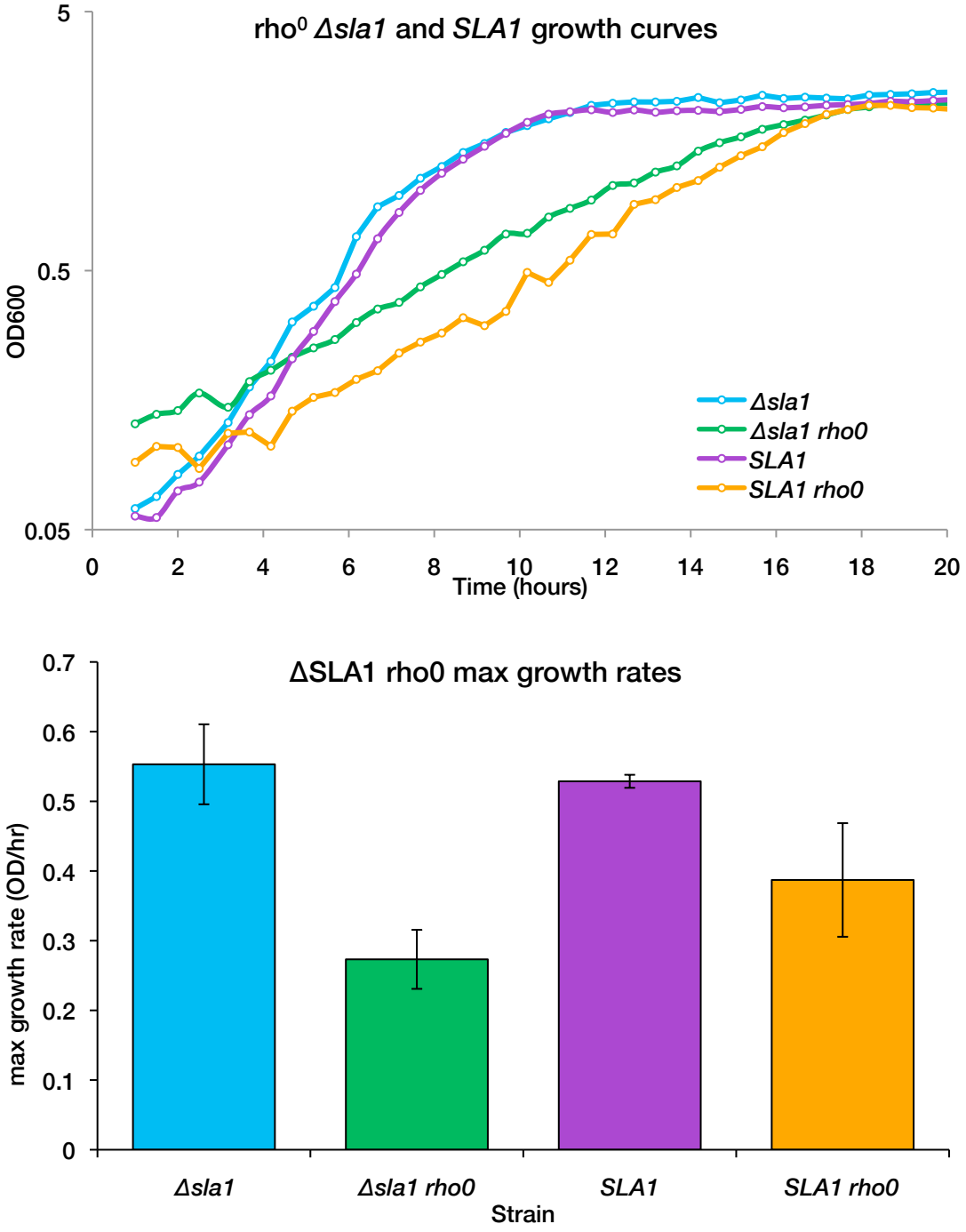

Figure 51. Growth of rho^0 *Δsla1* and *SLA1* in YPD over 20 hours shown as growth curves (top) and the average maximum growth rates from three replicate experiments (bottom).

5.6.3 Ste12p-Tec1p activity in *cox4* mutants

To further investigate if mitochondrial respiration defects could induce Ste12p-Tec1p, I tested the effect of reduced in respiratory capacity on Ste12p-Tec1p activity to

compare with that of actin dynamics mutants. A set of mutants with reductions in function of cytochrome c oxidase (COX) (described in Leadsham et al. 2013) were used. These strains carried forms of the *cox4* gene (*cox4d-1* and *cox4d-2*) which were mutated in the 3'UTR causing destabilization of mRNA transcripts. This results in reduced Cox4p levels and reduced respiratory capacity, with *coxd-1* and *coxd-2* mutants having approximately 55% and 40% of wild-type respiratory function respectively. These strains, as well as a *Δcox4* strain which has no respiratory function, were transformed with a Ste12p-Tec1p *lacZ* reporter and a β galactosidase assay was carried out. The increased activity observed in *act1-159* did not occur in any of the three *cox4* mutants. Levels remained similar to that of wild-type, although there was a reduction of signal in the *cox4d-2* strain.

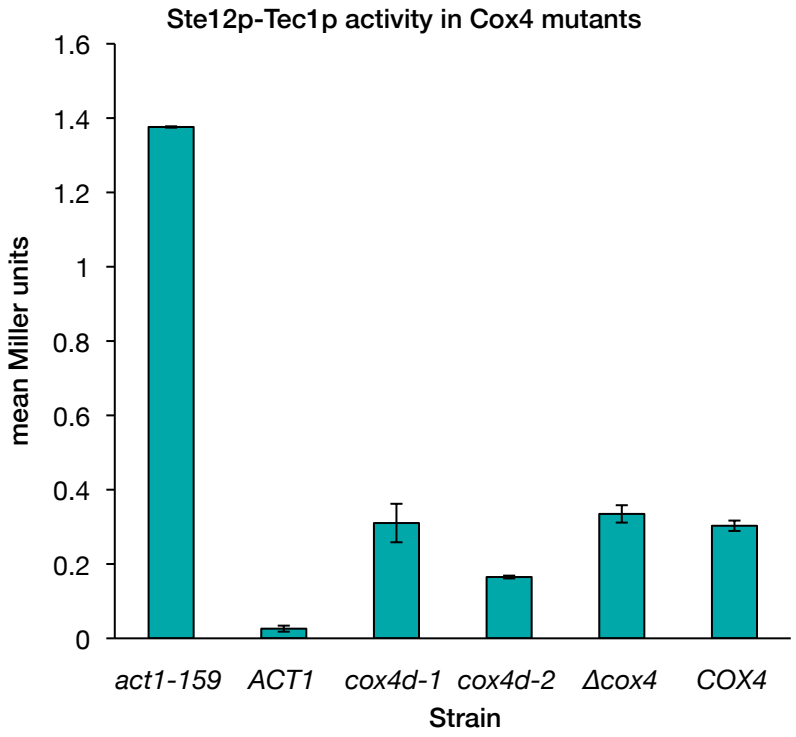

Figure 52. Ste12p-Tec1p activity in cox4 mutants transformed with *FRE(Ty1)*::*lacZ* plasmid grown in SD- URA compared to *act1-159* mutants as measured by β-galactosidase assay

Viewed together, the mitochondria data shows that partial or complete loss of mitochondrial respiration did not affect growth rate or Ste12p-Tec1p activity in *act1-159* cells, and they appear to already have severe mitochondrial dysfunction. The difference in results between *act1-159* and *Δsla*1 shows that Sla1p is not required for mitochondrial function, and that Ste12p-Tec1p can be activated without disrupting mitochondrial respiration. This suggests that the mitochondrial dysfunction in *act1-159* cells is not the source of Ste12p-Tec1 activity.

5.7 Localisation of Hog1p with altered actin dynamics

The microarray analysis of the *act1-159* strain highlighted transcripts of elements of the HOG MAPK pathway which were differentially expressed, including up-regulation of the membrane osmosensor *SLN1* and the kinase *SSK22*, but most significantly the phosphatase *PTP2*, levels of which were increased three-fold. Ptp2p dephosphorylates the transcription factor Hog1p and regulates its localisation. Hog1p is transported to the nucleus when phosphorylated, but it has also been reported that rather than promoting nuclear export, Ptp2p acts as a nuclear anchor causing Hog1p to remain in the nucleus for longer periods of time (Ferrigno et al. 1998; Mattison & Ota 2000). This suggests that Hog1p activity might be increased in *act1-159* mutants if Ptp2p levels are increased. I investigated the localisation of Hog1p in *act1-159* cells to determine if it accumulates in the nucleus.

A Hog1p-GFP plasmid (pCG498) described in Ferrigno et al. 1998 was transformed into *act1-159* and *ACT1* cells and grown to mid-log phase in low-fluorescence SC media. Fluorescence micrographs (Figure 53) show Hog1p was present in the

cytoplasm in both the mutant and wild-type. In many cells a darker staining organelle within the cytoplasm which is likely to be the nucleus.

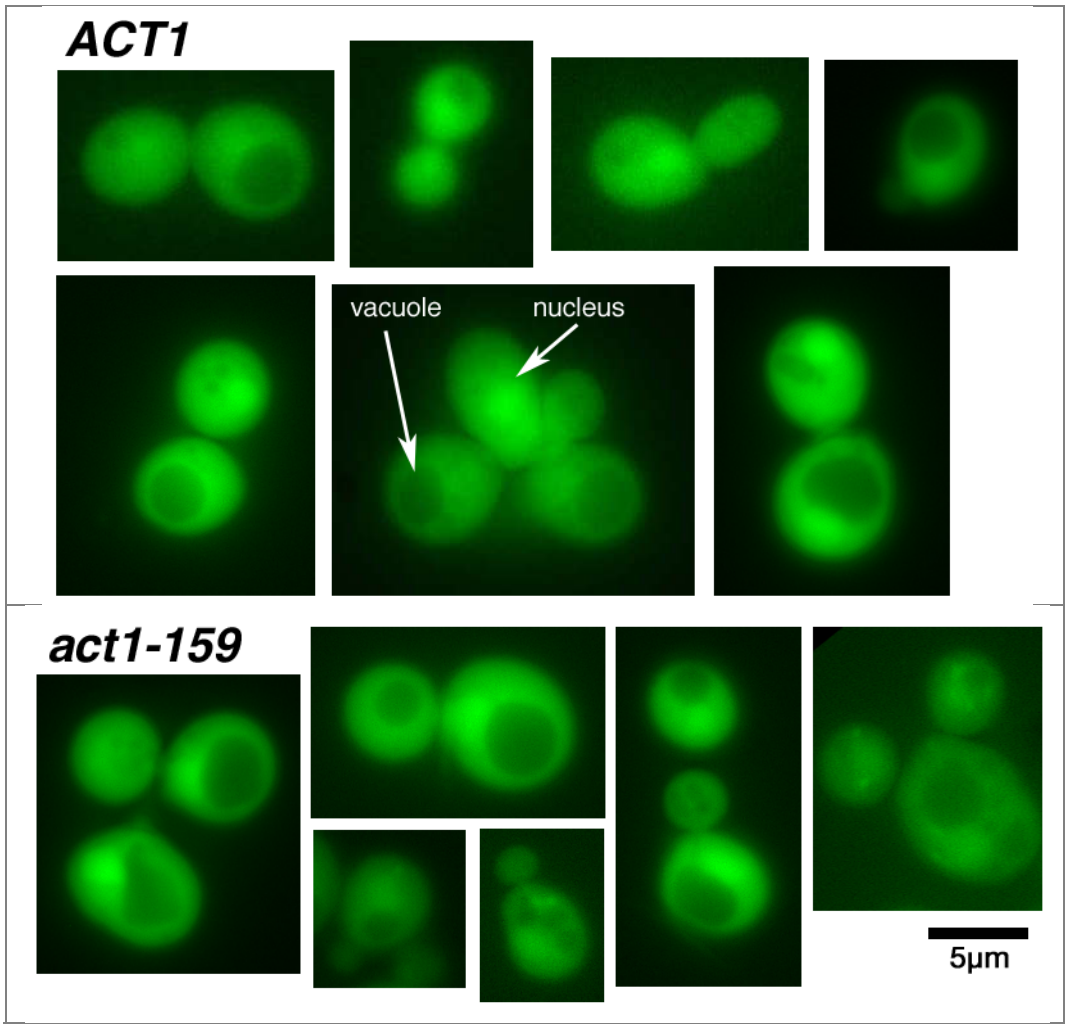

Figure 53. Fluorescence micrographs of *ACT1* and *act1-159* cells expressing Hog1p-GFP.

There did not appear to be an increase in nuclear localisation of Hog1p in *act1-159* cells, which corresponds with the Yeastract data showing few Hog1p-targets were differentially expressed. While Hog1p may not be basally active in the mutant, it would be interesting to test if it was retained in the nucleus for longer following osmotic stress.

5.8 Effects of actin dynamics on pheromone receptor localisation

Ste2p and Ste3p are membrane receptor proteins which are recycled through endosomal and vacuolar compartments and are the starting point for pheromone signaling pathway which culminates in Ste12p induction. Both *STE3* mRNA transcript and protein levels rapidly increase in mat a strains following exposure to mating factor a (Hagen & Sprague 1984), and transcript levels of the receptor were seen to be elevated in our microarray. Following from the findings that cortical actin organization is important for maintaining normal Ste12p activity, I hypothesised that increased Ste12p activity in *act1-159* cells could be a result of an aberrant Ste2p/Ste3p receptor signaling at the plasma membrane.

MATα act1-159 and wild-type cells were transformed with a Ste3p-GFP plasmid and fluorescence micrographs are shown in Figure 54. Previous studies have shown that Ste3p-GFP identify the vacuole and late endosomes in wild-type cells, and that with defective endocytosis it accumulated mainly at the plasma membrane (Gabriely et al. 2007). In wild-type cells Ste3p-GFP was present at the membrane and in the vacuole and often in smaller vacuole-associated compartments which are likely to be endosomes trafficking the receptor to the vacuole. The GFP signal was observed to be stronger at the membrane in *act1-159* cells suggesting accumulation, and the small compartments were rarely seen. Membrane GFP signal in *act1-157* cells appeared normal and Ste3p-GFP is also visible in the vacuole, which is revealed to have an unusual extensively lobed morphology.

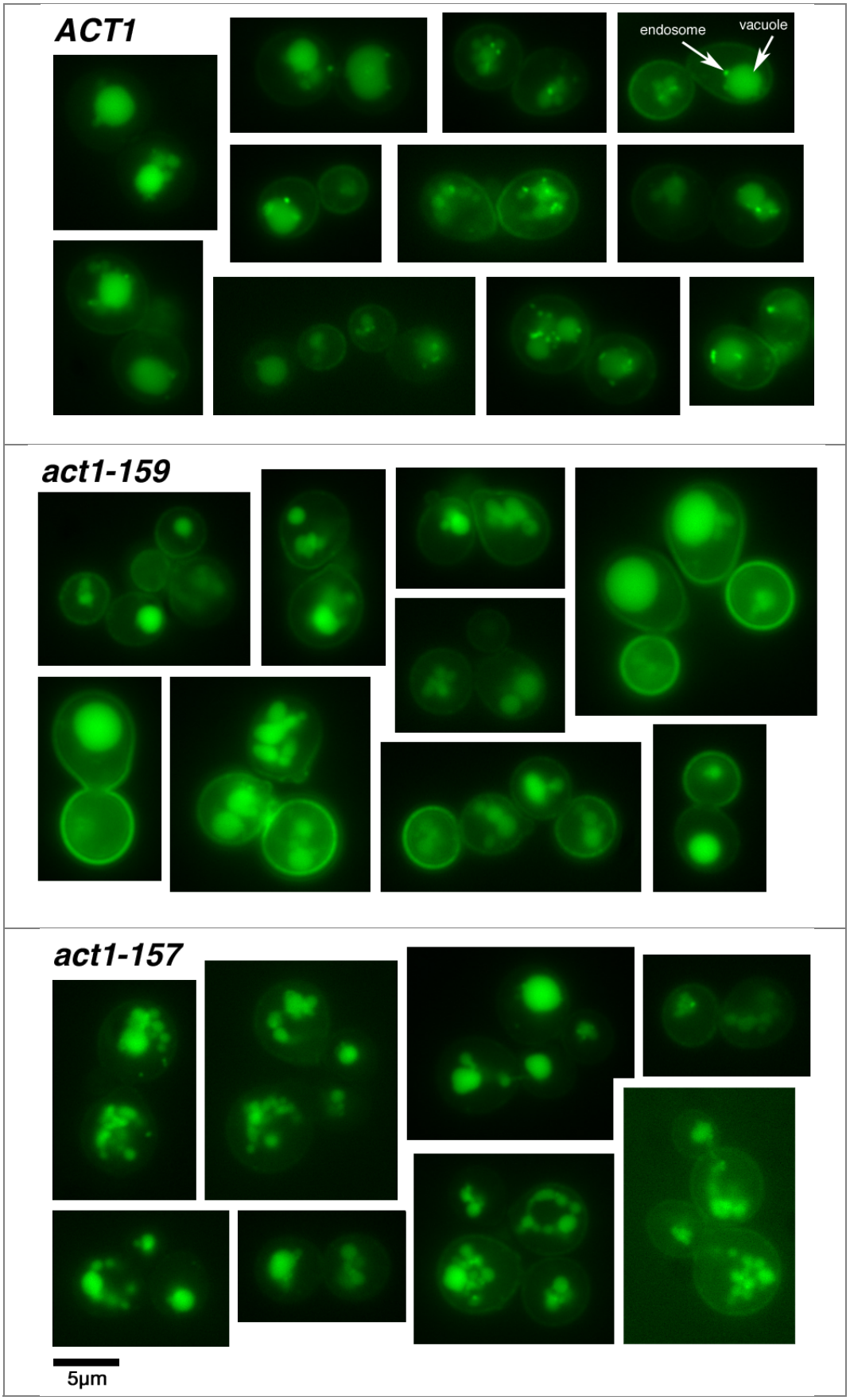

Figure 54. Fluorescence micrographs of *ACT1*, *act1-159* and *act1-157* cells expressing Ste3p-GFP. Exposure and contrast settings are consistent between images.

The observation of increased mating factor receptor at the membrane in *act1-159* cells raises the possibility that this may be involved in the activation of signaling events which lead to increased Ste12p-Tec1p activity. However Ste12p-Tec1p activity is also increased in *act1-157* cells, which I did not observe to have abnormal membrane localisation of Ste3p-GFP.

5.9 Effects of *Δste12* and *Δfus3* deletion in actin mutants

To investigate the origin of increased mating pathway and invasive/filamentous pathway signaling when actin dynamics is altered, I generated strains containing both an actin mutation and deletion of either *STE12* or *FUS3*. Strains were made using loxP deletion cassettes and confirmed by nuclease digestion and gel electrophoresis. Attempts were made to delete *TEC1* but these were unsuccessful in *act1-159* and *act1-157* strains.

The deletion of *STE12* was expected to abolish the up-regulation of targets of both the mating and filamentous/invasive growth pathways. The second gene deleted for these experiments was *FUS3*, which encodes the MAPK that activates Ste12p in the mating pathway and also has an inhibitory effect on Tec1p.

5.9.1 Growth rates of *Δste12* and *Δfus3* actin mutants

The effect of the *Δfus3* and *Δste12* mutations in *act1-157* and *act1-159 b*ackgrounds was investigated by growth analysis. The growth curves and maximum log growth rates of cultures are shown in Figure 55. Growth curves and maximum rates were not affected by either deletions in all three backgrounds.

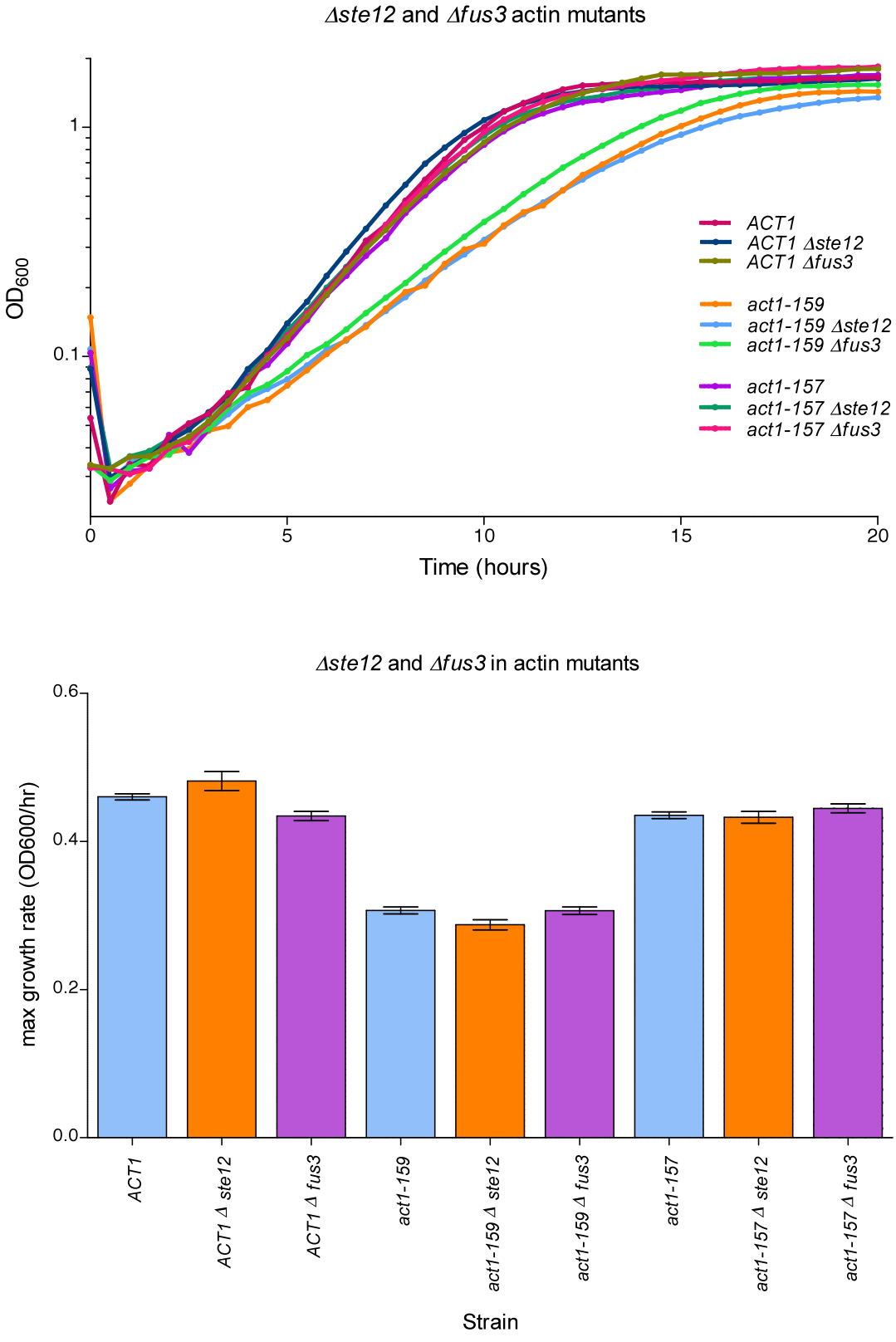

Figure 55. Growth curves and maximum log growth rates of mean data from cultures of actin mutants and WT with *Δste12* or *Δfus3* mutations. Cultures were grown in YPD in triplicate.

5.9.2 Ste12p-Tec1p activity in *Δste12* and *Δfus3* actin mutants

The expression of Ste12p-Tec1p targets was tested in actin mutants with *Δste12* and *Δfus3* mutations by transformation with *FRE(Ty1)*::*lacZ* plasmid and growth on X-gal agar (Figure 56, Figure 57). As anticipated, there was no Ste12p-Tec1p activity detected in *Δste12* strains. The *Δfus3* mutation appears to have induced Ste12p-Tec1p activity in the wild-type and may have further increased activity in the *act1-157* and *act1-159* mutants.

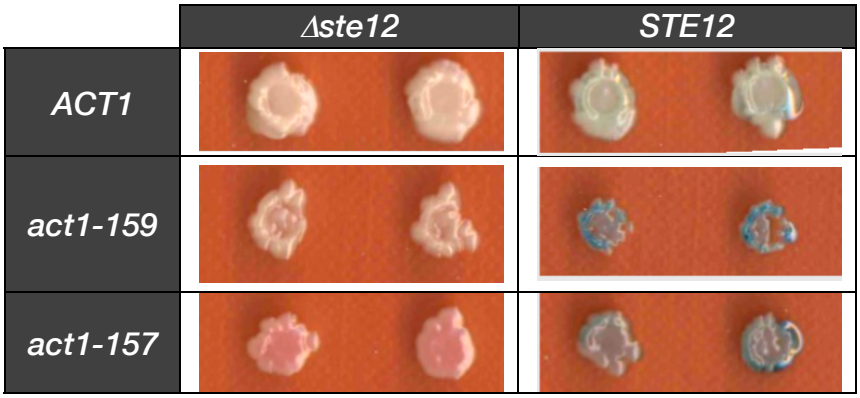

Figure 56. Ste12p-Tec1p activity in actin mutants with *Δste12* mutation. Strains transformed with *FRE(Ty1)*::*lacZ* plasmid and grown on SD-URA X-gal agar

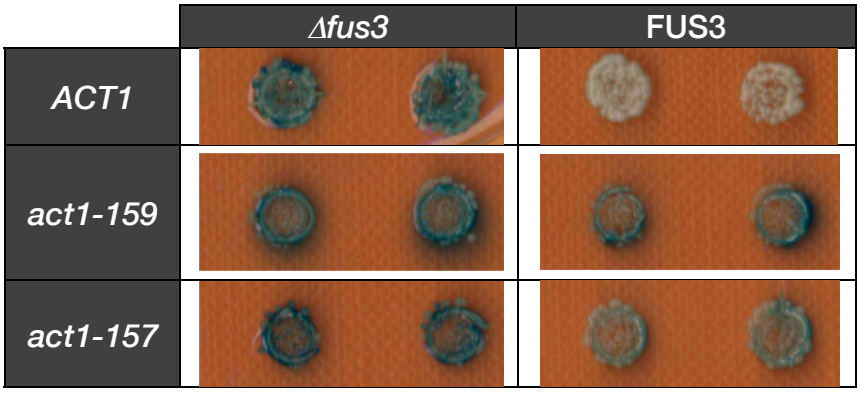

Figure 57. Ste12p-Tec1p activity in actin mutants with *Δfus3* mutation. Strains transformed with *FRE(Ty1)*::*lacZ* plasmid and grown on SD-URA X-gal agar.

The duration of lag phase and the log growth rates did not appear to be changed by deletion of either genes. Under these conditions activity of the mating and

filamentous/invasive growth pathways did not impact growth rate. Ste12p was required for Ste12p-Tec1p activity, while Fus3p was required for repression of this activity in wild-type cells. The observation that loss of *FUS3* activates Ste12p-Tec1p activity suggests that the activity of Fus3p may be reduced in *act1-159* and *act1-157* cells as a result of altered actin dynamics.

5.10 RAS/cAMP/PKA signaling

Actin dynamics are involved in regulation of RAS/cAMP/PKA signaling, and actin aggregation has been shown to result in hyperactivity of this pathway (Moseley & Goode 2006). Ras2p is linked to the filamentous/invasive growth response which signals to Ste12p-Tec1p (Posas et al. 1998). A constitutively active *RAS2-ala18val19* mutation was used in this study, which in previous studies has been shown to induce increased oxidative stress (Heeren et al. 2004).

5.10.1 Constitutive Ras2p and Ste12p-Tec1p activity

I tested the activity of Ste12p-Tec1p in a *Δras2* mutant and a constitutively active *RAS2 ala18val19* mutant in an X-gal assay (Figure 58). Constitutive mutants did not grow in selective liquid media following transformation with the reporter plasmid and so the cells were plated directly to X-gal agar following the transformation procedure. Unfortunately the transformation efficiency of *Δras2* cells is very low so few colonies were present for this mutant. However it can still be seen that constitutive Ras2p signaling resulted in increased Ste12p-Tec1p activity, while in the absence of Ras2 the activity was low. Therefore, I can confirm that Ras2p activity and Ste12p-Tec1p activity are linked.

Genotype	X-gal colonies
RAS2	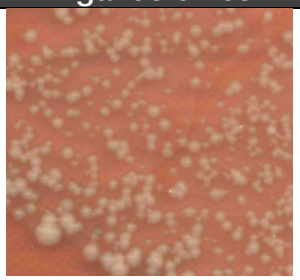
RAS2-ala18val19	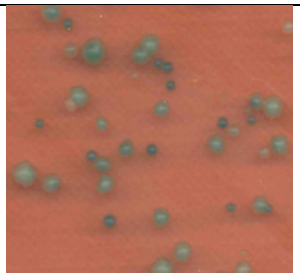
Δras2	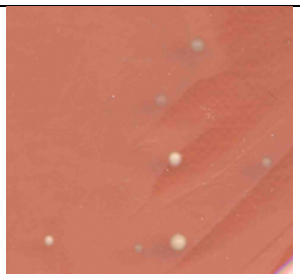

Figure 58. Ste12p-Tec1p activity in *RAS2*, *RAS-ala18val19, Δras2* and strains transformed with *FRE(Ty1)*::*lacZ* plasmid and grown on SD-URA X-gal agar.

5.10.2 Effect of *PDE2* overexpression in actin mutants

Ras2p signaling extends to multiple pathways, one of which is via cAMP. I hypothesised that if Ras2p was active in strains with reduced actin dynamics, the cAMP branch may mediate some of the phenotypes. I overexpressed a cAMP inhibitor, the phosphodiesterase Pde2p, in actin mutants to test if this has an effect on growth rate or Ste12p-Tec1p activity.

5.10.2.1 Growth rate of actin mutants with *PDE2* overexpression

Cultures transformed with either the *PDE2* overexpression plasmid or the equivalent empty vector pCG393 were subjected to growth analysis (Figure 59, Figure 60). All

three strains exhibited a similarly small reduction in maximum growth rate when expressing the cAMP inhibitor. Therefore cAMP signaling had a small positive influence on growth but it was not dependent on actin dynamics.

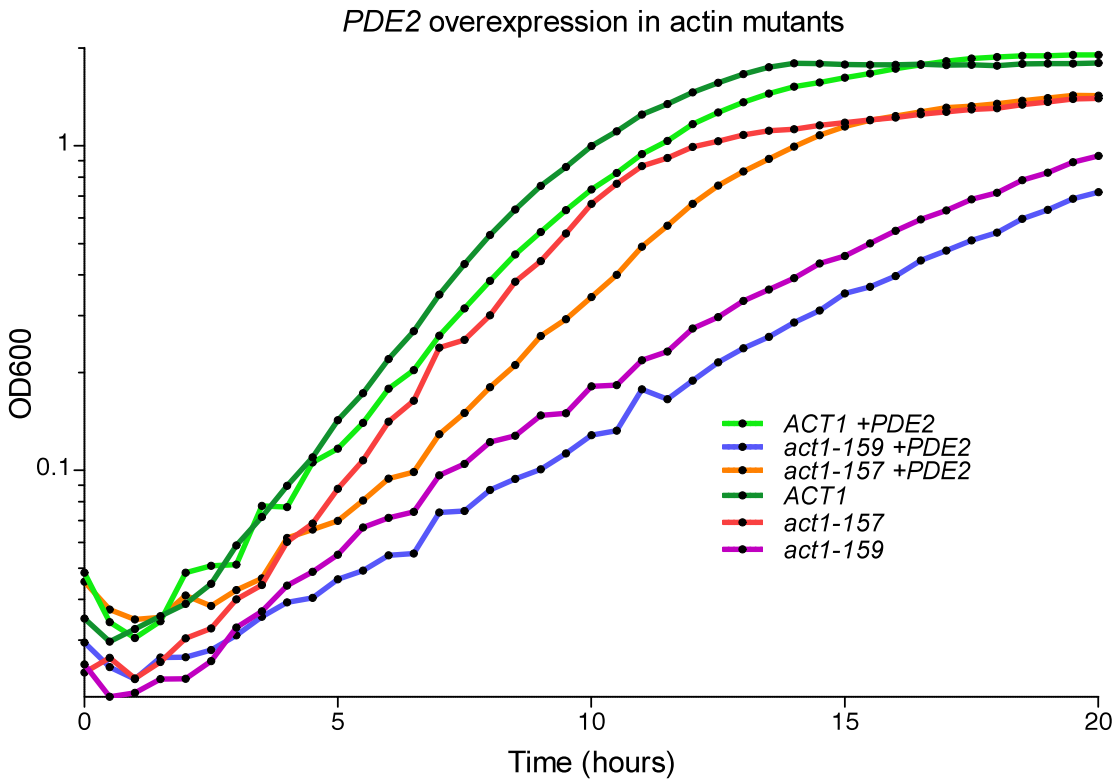

Figure 59. Growth curves from mean data of triplicate cultures of actin mutants and WT transformed with a plasmid expressing *PDE2* or an empty vector. Cultures were grown in SD- LEU

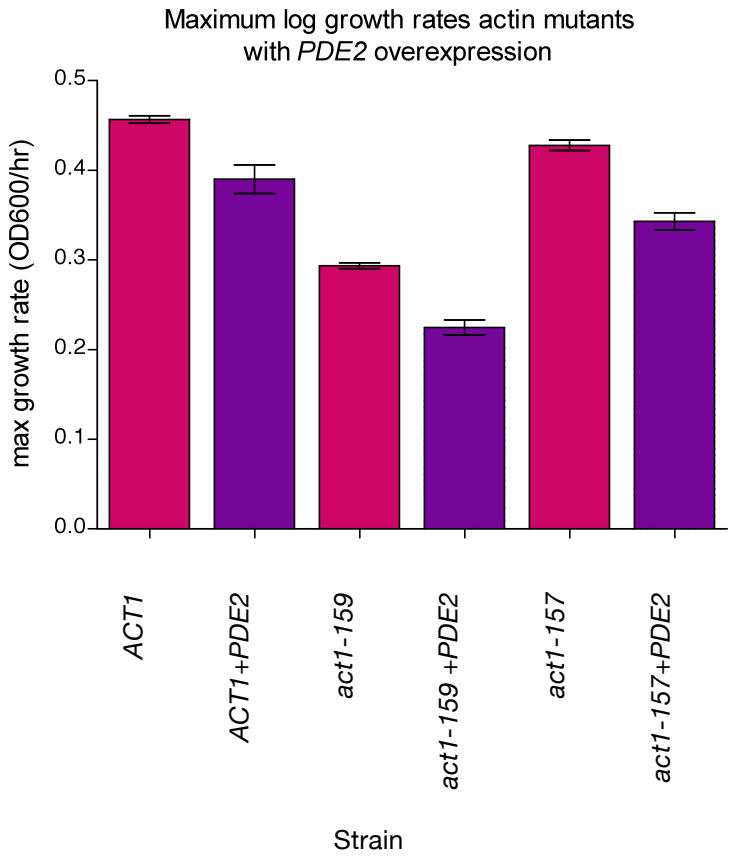

Figure 60. Maximum log growth rates from mean data of triplicate cultures of actin mutants and WT grown in SD- LEU and transformed with a plasmid expressing *PDE2* or an empty vector

5.10.2.2 Ste12p-Tec1p activity of actin mutants with *PDE2* overexpression

If the cAMP branch of Ras2 signaling is involved in the increased invasive growth signaling in actin mutants I would expect to see a decrease in expression of Ste12p-Tec1p targets when *PDE2* was overexpressed. Cultures were transformed with both the *PDE2* overexpression plasmid or empty vector and the Ste12p-Tec1p *lacZ* reporter pCG394 and grown on X-gal agar (Figure 61). Increased Pde2p levels did not affect wild-type or mutant cells in this assay, as the activity levels remain similar. This result suggests that cAMP signaling does not activate Ste12p-Tec1p in cells with altered actin dynamics.

Genotype	X-gal colonies
ACT1	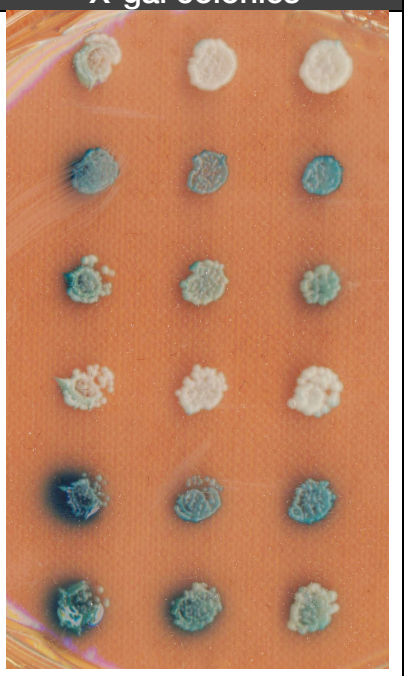
act1-159	
act1-157	
ACT1 +PDE2	
act1-159 +PDE2	
act1-157 +PDE2	

Figure 61. Ste12p-Tec1p activity in actin mutants transformed with *PDE2* overexpression plasmid pCG194 or empty vector pCG393 and *lacZ* reporter pCG394 were grown on SD-LEU-URA X-gal agar.

5.10.3 Active Ras2p-GFP localisation in actin mutants

I investigated if changes to Ras2 signaling in actin mutants might result in any differences in sub-cellular localisation. A plasmid which labels active GTP-bound Ras2p (pCG347), described in Leadsham et al. 2009 was transformed into cells to obtain the fluorescence micrographs in Figure 62. Images of wild-type cells show active Ras2p was present along the membrane and nucleus, and *act1-157* cells also had a similar phenotype, although there may have been a reduction in membrane Ras2p activity. The localisation was very different in *act1-159* cells. Active Ras2p appeared in small dots which moved slightly and were likely to be endosomes, and there was uneven distribution of activity at the membrane. Additionally active Ras2p did not usually appear in the nucleus in these stabilised cytoskeleton mutants.

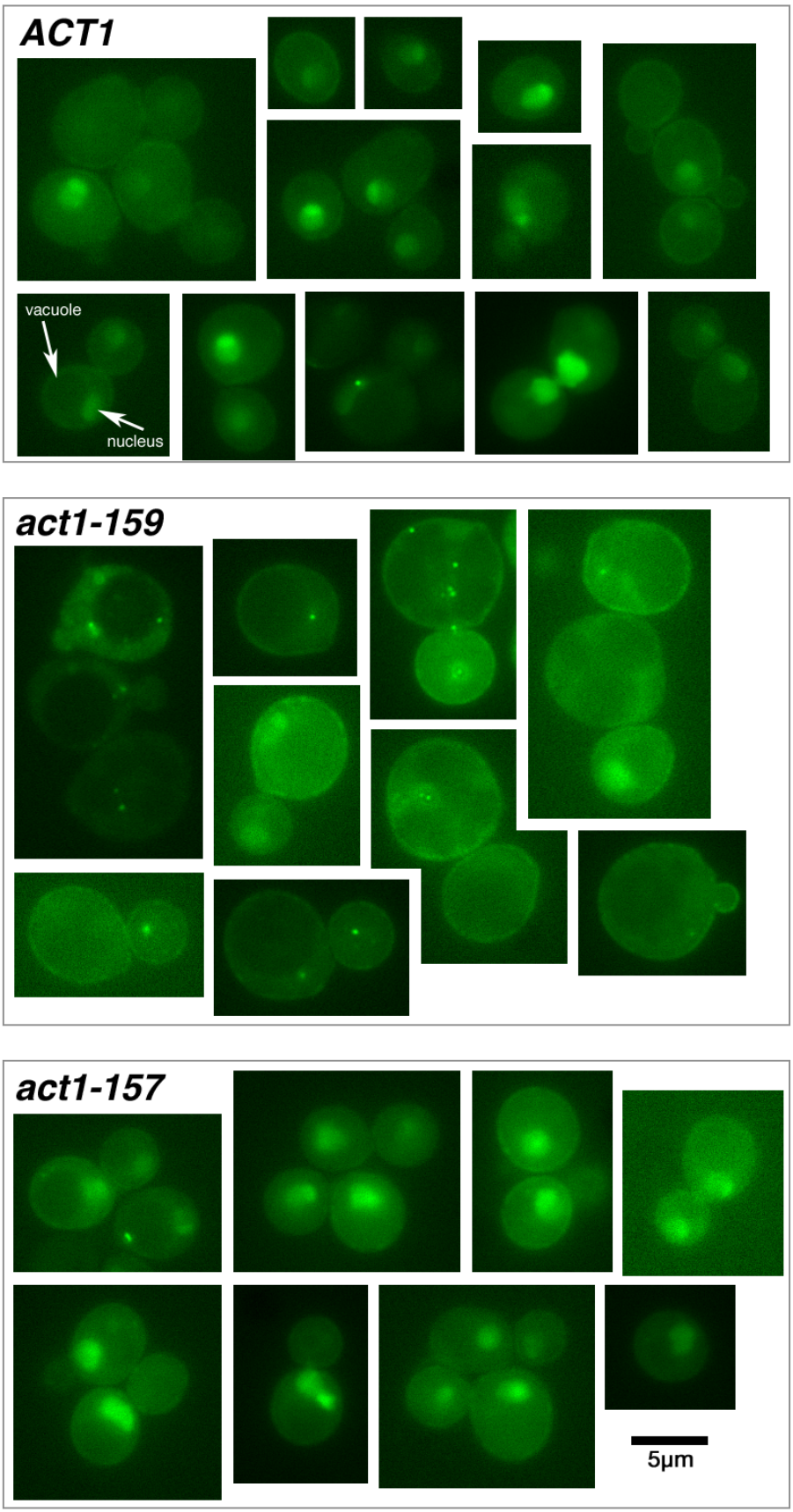

Figure 62. Fluorescence micrographs of actin mutants and wild-type expressing a GFP reporter for active GTP-bound Ras2p.

The micrographs show that Ras2p localisation was disrupted when there was a reduction of actin dynamics. It has been reported recently that active Ras2p localising to the nucleus is required for invasive growth (Broggi et al. 2013). Considering this it is unexpected that active Ras2p was not seen in the nucleus in *act1-159* cells, which have increased expression of invasive growth targets.

5.11 Chapter summary

A reduction in actin dynamics has been shown to clearly affect the activity both the Ste12p complexes which control expression in response to mating factor, and the Ste12p-Tec1p complexes which control filamentous/invasive growth. The observation that both transcription complexes are active simultaneously is interesting as despite the significant number of signaling components which are shared these pathways signal discretely in normal cells. Deletion of *FUS3* did not affect this phenotype, while deletion of *STE12* abolishes the Ste12p-Tec1p activity. Further to this, deletion of *FUS3* with wild-type actin resulted in activation of Ste12p-Tec1p. The response of actin mutants to the presence of mating factor has shown that they are able to respond and that following a growth arrest they have an increased ability to recover and divide rapidly.

Investigating the Ste12p-Tec1p activity in a library of strains with actin-interacting genes deleted has yielded information implicating the functions of actin structures at the cortical patches in controlling signaling activity. Of the deletions tested there was a high proportion of genes which are known to be involved in organising the cortical patches and regulating the events of endocytosis and membrane receptor recycling,

including Sla1p. Further analysis of Sla1p was carried out including investigation into which domains of this protein are required to produce wild-type levels of activity of Ste12p-Tec1p. I showed that a protein interaction with SH3 domain 3 may be important and also that the SHD1 domain was required for low Ste12-Tec1p activity. The localisation of the membrane receptor for the mating pathway was found to be altered in *act1-159* cells with more present at the cell membrane and less evidence of recycling processes.

Ras/cAMP/PKA signaling appears to contribute to the filamentous/invasive growth pathway as constitutive Ras2p activity induced Ste12p-Tec1p activity. Inhibition of the cAMP branch of Ras1p signaling did not reduce Ste12p-Tec1p activity in actin mutants. Ras2p activity was localised to the nucleus in wild-type cells but this was absent in *act1-159* cells.

I have also seen that increased actin dynamics as in the *act1-157* mutant produces some phenotypes which are similar to those of cells with reduced actin dynamics, such as increased Ste12p-Tec1p activity. Other phenotypes parallel the increased actin dynamics, including the increased respiratory capacity, while the growth rate and Ras2p localisation were is very similar to wild type. Additionally it was observed that there is vacuolar fragmentation in this strain, which is not seen in *act1-159* cells.

6 Discussion

It is clear now that further to the crucial roles played by actin remodeling in regulating cytokinesis, morphogenesis and establishing cell polarity, the cytoskeleton participates in a wide range of cellular events and pathways that are essential for a cell to control adaptability, functionality and cell survival. In this study I have further investigated the roles for a dynamic actin cytoskeleton in the regulation of processes including endocytosis, mitochondrial respiration, and signal transduction.

6.1 Stress-induced actin remodeling has protective functions

Previous studies have shown that cytoskeleton is a key target of pathways in response to diverse environmental changes, and that adapting to these changes often requires actin remodeling. Nutrient stress can lead to actin remodeling through the Ras/cAMP/PKA pathway, the filamentous/invasive growth MAPK pathway and TOR signaling via TORC1. Actin is also crucially involved in the morphological changes required for mating and as such is a target of the mating pathway. Osmotic stress results in rapid actin filament disassembly which requires HOG signaling for recovery (Yuzyuk et al. 2002), and oxidative stress induces a loss of actin dynamics as filaments collapse into large stable bodies (Farah et al. 2011). Cell wall integrity is closely linked to actin through roles in polarised growth, as well as being activated in response to cytoskeletal depolarization (Levin 2011). There is considerable potential for crosstalk between these signaling pathways, and furthermore many of them also depend upon the actin cytoskeleton for the activity and localisation of multiple components (Figure 63). Actin is therefore central to a cells ability to adapt and respond to their environment.

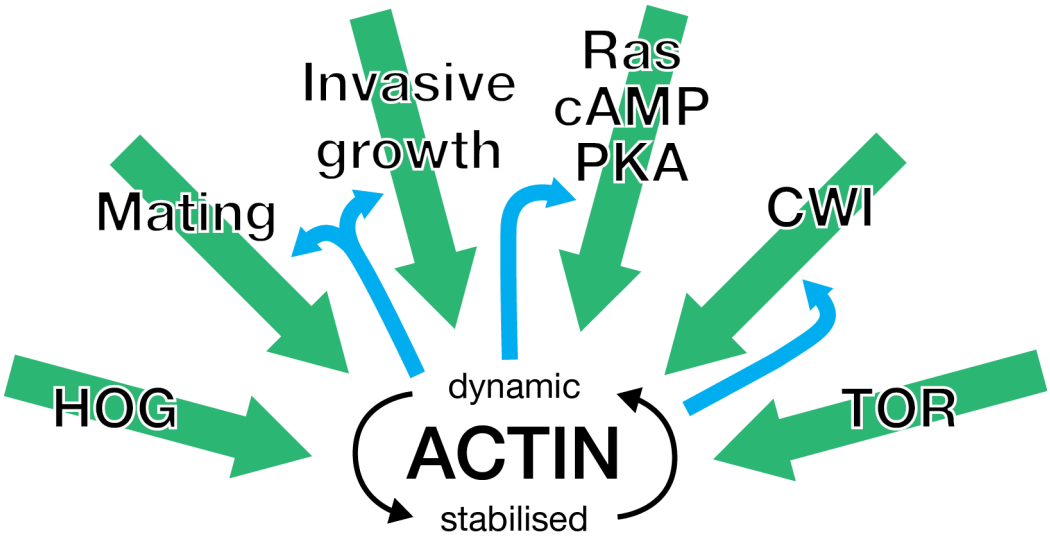

Figure 63. A diagram outlining the signaling pathways which target actin and the roles played by actin in regulating signaling along these pathways.

A reduction in actin dynamics and reorganization of the cytoskeleton is observed in response to acute oxidative stress (Farah et al. 2011). The cysteine residues which are modified in this process are well conserved in eukaryotes, suggesting that this response provides a selective advantage. The formation of clumped actin structures appears to protect actin or actin-regulating proteins facilitating recovery when the stress is removed. Additionally the loss of actin dynamics prevents division and endocytosis. Stabilisation of actin can also induce an apoptotic program through Ras/cAMP/PKA signaling (Gourlay & Ayscough 2006). The existence of apoptosis in unicellular organisms is interesting, as it illustrates that under certain conditions cells act to protect the health of the population by preventing proliferation of unhealthy individuals. In both of these examples, actin responds to environmental changes and promotes behaviour which benefits the population.

Close links between actin dynamics and environmental sensing pathways leave it well positioned for a role as a biosensor. The reduction in actin dynamics observed in ageing and in stressed cells therefore may be used to gauge intra- and extra-cellular conditions to protect the population by preventing mating and cell division when it is unfavourable. I have found further evidence of the involvement of actin in signaling pathways. I propose that further to being a downstream target of signaling pathways, actin dynamics is fundamentally involved in signal transduction, and under stress conditions changes in actin dynamics have an evolutionarily conserved role in altering cellular responses.

6.2 Actin dynamics regulates signaling in the filamentous/invasive growth and mating response MAPK pathways

The results presented here reveal that stabilised actin leads to activation of the Ste12p-Tec1p transcription factor complex associated with the filamentous/invasive growth response to nutrient starvation. I also saw the same activation using the *act1-157* mutant in which there is increased actin turnover. Further to the activation of Ste12p-Tec1p-mediated transcription, our reporter assay showed that the activity of Ste12 mediated transcription associated with the mating pathway was also increased by reduced actin dynamics. These pathways share a considerable proportion of their transduction pathways, including most of the MAPK cascade module. Where they differ is in the input signal to the MAPK module, and the terminal MAPK in the cascade. These differences are normally sufficient to elicit distinct transcription programs from Ste12p and Ste12p-Tec1p activity. Our observation that with actin stabilisation there is transcriptional activity from both pathways under conditions which would not normally stimulate either indicates that there is both an aberrant

activation, and also a loss of the signaling specificity which keeps the pathways distinct.

Our results suggest the terminal MAPKs in both pathway, Kss1p and Fus3p, are important for these phenotypes. I observed that deletion of Fus3p was sufficient to activate Ste12p-Tec1p activity in an *ACT1* background, whilst it did not abolish the elevated activity in the altered actin dynamics mutants. There is functional redundancy between the two MAPKs, and cells are still competent to induce a mating response in the absence of Fus3p via the activity of Kss1p (Elion et al. 1991). However the specificity of the signals is apparently dependent on the Fus3p/Kss1p system, and under normal conditions Fus3p will inhibit invasive growth. Kss1p appears to only become significantly involved in the mating pathway signal when Fus3p is absent, possibly due to a lower affinity for Fus3p targets. As I have shown that both pathways are active in *act1-159* cells it may be the case that with stabilised actin filaments there is a reduction in normal Fus3p activity, and that Kss1p is responsible for the activities of both Ste12p and Ste12p-Tec1p complexes.

This might be explained by the roles for actin in the mating pathway. As discussed earlier, Fus3p requires dynamic localisation for normal mating pathway signaling, and it must associate with the scaffold Ste5p to be activated. Ste5p localisation is dependent on actin via an interaction with the formin Bni1p (Qi & Elion 2007). The loss of actin dynamics then may result in failure to correctly localise Ste5p, which in turn causes Fus3p to be incompetent to transduce signal. In our screen of a library of strains with gene deletions, I observed that *Δbni1* colonies have increased Ste12p-

Tec1p activity compared to wild-type, and this may be due to this mutant having a similar effect on Ste5p due to abnormal actin organisation.

An alternative possibility is that the interaction of actin with Ste5p complexes depends on rapid depolymerisation, and with stabilised filaments the signaling complexes themselves become stabilised. This corresponds with reports that tethering of Fus3p to the plasma membrane by fusion to a lipid motif results in cells which hyperactivate Ste12p, while remaining competent to respond to pheromone (Chen et al. 2010). However given that Fus3p activity inhibits filamentous/invasive growth response (Conte & Curcio 2000) this model does not fit with the observed hyperactivation of Ste12p-Tec1p.

Attempts to mate *act1-159* cells for genetic studies have had very low success, and I have not observed cells forming the mating projections characteristic of a mating response (data not shown). This would suggest that the activation of the mating response when there is actin stabilisation is not fully realised and therefore may represent a short-circuited signal transduction pathway. A possibility is that the interactions between actin and components of the cascade have evolved a protective function for the population in preventing mating when actin damage has occurred.

6.3 Disruption of cortical patches activates filamentous/invasive growth

The increased activity of both the mating and filamentous growth pathways was observed during log growth when there is no nutrient starvation or mating pheromone

stimulus. Our observations suggest that altered cortical actin regulation may be involved in modulating signaling during actin damage. An increase in Ste12p-Tec1p activity was observed in a number of strains in which a single actin-regulating gene had been deleted. The most striking observation from this experiment was that the strains in which Ste12p-Tec1p activity was highest have important documented roles in cortical patch organisation and endocytosis.

In particular it was seen that loss of Sla1p caused a large increase in expression of Ste12p-Tec1p targets. While this protein has a key function in organisation of actin at cortical patches, it also is known to interact with NPFXD motifs to the targeting via of endocytic cargo molecules, including membrane receptors involved in detecting pheromone and cell wall stress. The NPFXD interaction occurs through the SHD1 domain of Sla1p. I found that cells expressing Sla1p with the SHD1 domain removed had increased Ste12p-Tec1p activity to the same extent as *Δsla1* cells, indicating that endocytic targeting of membrane receptors can modulate the activity of the pathway. Given that the recycling of receptors for the mating pathway occurs through this interaction, it is possible that the observed expression of filamentous/invasive growth targets occurs as a result of crosstalk between the pathways.

Further to this, microscopy indicated that reduced actin dynamics resulted in increased mating factor receptor fluorescence at the plasma membrane, whilst there was reduced fluorescence in endosomal vesicles. This may be a consequence of a recycling defect due to the requirement for dynamic actin filaments for endocytosis. It is likely that loss of actin dynamics through the *act1-159* mutation and loss of Sla1p result in similar defects in cortical patch organisation. It is not clear whether stabilised

actin disrupts the targeting of vesicles by Sla1p, or whether it occurs as a result of failure to generate the force for invagination of endocytic vesicles. Increased actin turnover, which also increases Ste12p-Tec1p activity, did not appear to affect membrane localisation of receptors, indicating that there may be another pathway inducing the activity.

It seems that *Δsla1* cells have mitochondrial function, while I observed that this is severely affected by loss of actin dynamics in *act1-159* cells. This was seen in the expression of retrograde response signals, and subsequently it was revealed that *act1-159* cells are effectively rho^0 and have no respiratory function. The activation of Ste12p-Tec1p activity is presumably a specific result of reduced cortical actin dynamics, which does not affect the maintenance of mitochondrial function.

Together, the data from the deletion library and the receptor localisation microscopy suggest that the activity in the MAPK pathways may occur as a result of increased membrane receptor levels. If actin dynamics influences crosstalk between the pathways the pheromone receptor may be leading to expression of filamentous/invasive growth targets. It is likely that other receptors that undergo actin-dependent endocytotic recycling would be similarly altered by reduced actin dynamics, which could be tested by deletion of *STE2* in *act1-159* and *act1-157* backgrounds.

6.4 Roles for HOG and Ras/cAMP/PKA signaling

Results from our microarray analysis indicated altered activity in the HOG pathway may occur with reduced actin dynamics. However microscopy of Hog1p-GFP did not

indicate that it affected translocation of this kinase to the nucleus where it accumulates during HOG activation, indicating that the pathway may not be active. Further work may reveal if the HOG pathway is involved in an altered signaling network with the other MAPK pathways with which it shares components. Inappropriate activation of Fus1p expression has been reported when there is disruption of HOG signaling (O'Rourke & Herskowitz 2002). This was shown to occur via the *SHO1* branch which shares Ste20p and Ste11p with both the mating and invasive growth pathways. The *SHO1* branch also involves the receptor Msb2p which is reported as a receptor for the invasive growth signal (Cullen et al. 2004). Actin is involved at multiple points in this signaling network, including multiple membrane receptors, the rho GTPases and the Ste5p scaffold. While these pathways can operate separately, there is clearly potential for crosstalk between them under different circumstances. This gives cells the ability to adapt their response to a stimulus by directing the signal to different pathways.

Ras2p signaling has diverse downstream effects including well documented connections to the filamentous/invasive growth pathway. Reduced actin dynamics induces Ras2p signaling via Srv2p/CAP and leads to apoptosis. I have shown that constitutive Ras2p activity increases expression of Ste12p-Tec1p targets, and that overexpression of Pde2p does not affect Ste12p-Tec1p activity in strains with reduced actin dynamics. In wild-type cells active Ras2p was detected in the nucleus, but in *act1-159* cells it was absent. It has been reported that for its role in activating filamentous/invasive growth targets Ras2p must localise to the nucleus (Broggi et al. 2013). This would suggest that Ste12p-Tec1p activity is not being induced by Ras2p signaling when actin dynamics is reduced. I have attempted to delete *RAS2* in the

act1-159 background but were unsuccessful, and this may indicate that Ras2p signaling has a role in maintenance of cells with actin damage.

6.5 Aberrant mating pathway activity does not prevent cell cycle arrest in response to pheromone

Treatment of *act1-159* cultures with pheromone showed that they are capable of responding to the signal by inducing cell cycle arrest. Treatment also demonstrated that they are capable of growing at rates comparable to wild-type. Therefore the reduced growth rate observed in cells expressing *act1-159* does not appear to be a direct result of the cytoskeleton failing to perform its normal cellular functions, but is due to a restriction imposed by altered signaling. The cells enact a growth arrest in response to pheromone much like wild-type cells, and are able to recover from it more effectively. The recovery from pheromone induced growth arrest is associated with Kss1p activity (Courchesne et al. 1989), and as the filamentous/invasive growth pathway is active in these mutants, it is likely that they are primed to activate a rapid recovery following degradation of pheromone. The activation of cell cycle arrest is associated with Far1p activation by Fus3p, but not Kss1p, which has a 10-fold lower affinity for Far1p (Breitkreutz et al. 2001). Since arrest was observed it is likely that Far1p does become phosphorylated in response to pheromone either by one or both of the MAPKs. Cell cycle arrest does not occur in *Δfus3* strains (Fujimura 1990).

For the observed growth arrest to occur via Far1p activity, either Kss1p must be sufficiently active to phosphorylate Far1p, or Fus3p may still be competent to perform this function. While I did not observe cells forming mating projections due to the

increased basal Ste12p activity, but considering that they are able to arrest growth in response to pheromone, it would be interesting to test if *act1-159* cells form mating projections in the presence of pheromone. The slow growth of untreated *act1-159* cultures might come as a result of low-level Far1p-induced cell cycle inhibition, which is then further activated in the presence of pheromone and subsequently is removed when pheromone is depleted.

6.6 A model for the effect of actin dynamics on mating and filamentous/invasive growth signaling

A model for the effect of actin dynamics on signaling in the mating and filamentous/invasive growth pathways is outlined in Figure 64. When actin dynamics is normal, the mating pathway is only activated in the presence of pheromone, and Fus3p inhibition maintains discrete pathways. When actin dynamics is reduced as occurs under stress or in aged cells, basal activity of the pathways increases through reduced endocytic recycling of receptors. Crosstalk between the pathways becomes possible as Fus3p becomes incompetent to signal, and Kss1p acts in its place, leading to expression of both mating and filamentous/invasive growth targets.

Several aspects of this hypothesis require further investigation. The role of Ras2p and HOG pathway signaling in activating Ste12p-Tec1p remains unclear, but it is possible that they have a role. The functionality of the mating pathway with reduced actin dynamics in the presence of pheromone also has not been established.

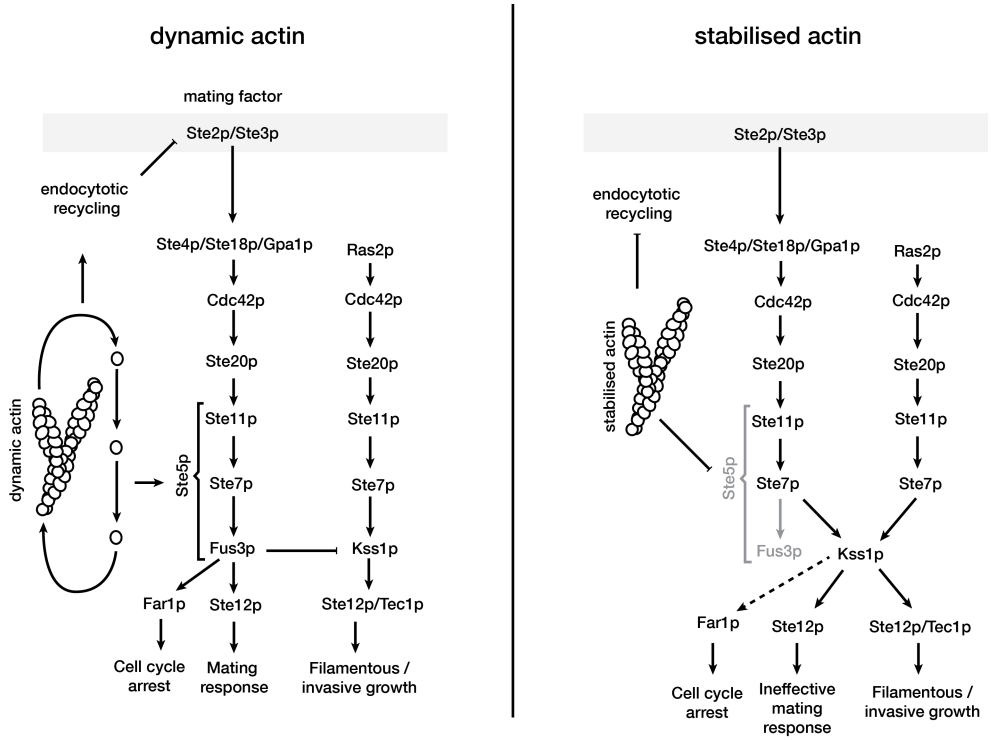

Figure 64. Model for the role of actin dynamics in modulating signaling in the mating and filamentous/invasive growth pathways. With wild-type, dynamic actin, endocytic recycling controls receptor levels at the plasma membrane and regulates Ste5p activity to allow Fus3p activation when pheromone is present. Under conditions which stabilise actin, endocytic function is lost and membrane receptor levels increase resulting in activation of signaling in the absence of pheromone. Ste5p is aberrantly localised preventing normal Fus3p activation, and the signal is diverted to Kss1p, which activates both Ste12p and Ste12p-Tec1p.

6.7 Conclusions

The results presented here support the theory that an altered environmental sensing network is active in cells under stress, and I have proposed a role for actin as a biosensor which controls this adaptation. The multiple interactions between actin and signal transduction cascades facilitate this adaptation, and facilitates responses which are protective to the cell population. This function may be conserved within eukaryotes as actin dynamics has been shown to regulate apoptotic responses in both plant and mammalian cells during stress and ageing (Franklin-Tong & Gourlay 2008;

Amberg et al. 2012). Further work in this area will uncover the extent to which cell fate decisions are influenced by the dynamic status of actin.

References

Adams, A.E. & Pringle, J.R., 1984. Relationship of actin and tubulin distribution to bud growth in wild-type and morphogenetic-mutant Saccharomyces cerevisiae. *The Journal of cell biology*, 98(3), pp.934–45.

Adler, C. & Errede, B., 1988. Identification of a Ty1 regulatory sequence responsive to STE7 and STE12. *Molecular and cellular biology*, 8(6).

Amatruda, J. et al., 1990. Disruption of the actin cytoskeleton in yeast capping protein mutants. *Nature*, 344(6264), pp.352–354 A.

Amatruda, J.F. et al., 1992. Effects of null mutations and overexpression of capping protein on morphogenesis, actin distribution and polarized secretion in yeast. *The Journal of cell biology*, 119(5), pp.1151–62.

Amberg, D. et al., 2012. Cellular ageing and the actin cytoskeleton. *Sub-cellular biochemistry*, 57, pp.331–52.

Amberg, D.C., 1998. Three-dimensional imaging of the yeast actin cytoskeleton through the budding cell cycle. *Molecular biology of the cell*, 9(12), pp.3259–62.

Andrin, C. et al., 2012. A requirement for polymerized actin in DNA double-strand break repair. *Nucleus (Austin, Tex.)*, 3(4), pp.384–95.

Ashburner, M. et al., 2000. Gene ontology: tool for the unification of biology. The Gene Ontology Consortium. *Nature genetics*, 25, pp.25–29.

Ayscough, K., 2000. Endocytosis and the development of cell polarity in yeast require a dynamic F-actin cytoskeleton. *Current Biology*, pp.1587–1590.

Ayscough, K.R., 2005. Coupling actin dynamics to the endocytic process in Saccharomyces cerevisiae. *Protoplasma*, 226(1-2), pp.81–8.

Ayscough, K.R. et al., 1999. Sla1p is a functionally modular component of the yeast cortical actin cytoskeleton required for correct localization of both Rho1p-GTPase and Sla2p, a protein with talin homology. *Molecular biology of the cell*, 10(4), pp.1061–75.

Ayscough, K.R. & Drubin, D.G., 1998. A role for the yeast actin cytoskeleton in pheromone receptor clustering and signalling. *Current Biology*, 8(16), pp.927–930.

Bandyopadhyay, S., Mehta, M. & Kuo, D., 2010. Rewiring of Genetic Networks in Response to DNA Damage. *Science*, 330(6009), pp.1385–1389.

Bao, M.Z. et al., 2004. Pheromone-dependent destruction of the Tec1 transcription factor is required for MAP kinase signaling specificity in yeast. *Cell*, 119(7), pp.991–1000.

Bardwell, L., 2004. A walk-through of the yeast mating pheromone response pathway. *Peptides*, 25(9), pp.1465–76.

Bardwell, L. et al., 1998. Differential regulation of transcription: repression by unactivated mitogen-activated protein kinase Kss1 requires the Dig1 and Dig2 proteins. *Proceedings of the National Academy of Sciences of the United States of America*, 95(26), pp.15400–5.

Bardwell, L. et al., 1998. Repression of yeast Ste12 transcription factor by direct binding of unphosphorylated Kss1 MAPK and its regulation by the Ste7 MEK. *Genes & Development*, 12(18), pp.2887–2898.

Bartholomew, B., 2013. Monomeric actin required for INO80 remodeling. *Nature structural & molecular biology*, 20(4), pp.405–7.

Bashkirov, V.I. et al., 2000. DNA repair protein Rad55 is a terminal substrate of the DNA damage checkpoints. *Molecular and cellular biology*, 20(12), pp.4393–404.

Belmont, L.D., Orlova, A, et al., 1999. A change in actin conformation associated with filament instability after Pi release. *Proceedings of the National Academy of Sciences of the United States of America*, 96(1), pp.29–34.

Belmont, L.D. & Drubin, D.G., 1998. The yeast V159N actin mutant reveals roles for actin dynamics in vivo. *The Journal of cell biology*, 142(5), pp.1289–99.

Belmont, L.D., Patterson, G.M. & Drubin, D.G., 1999. New actin mutants allow further characterization of the nucleotide binding cleft and drug binding sites. *Journal of cell science*, 112 (Pt 9, pp.1325–36.

Benchaar, S. et al., 2007. Mapping the interaction of cofilin with subdomain 2 on actin. *Biochemistry*, 46(1), pp.225–33.

Bi, E. et al., 1998. Involvement of an Actomyosin Contractile Ring in Saccharomyces cerevisiae Cytokinesis. *The Journal of cell biology*, 142(5), pp.1301–1312.

Boldogh, I.R. et al., 2001. Arp2/3 complex and actin dynamics are required for actin-based mitochondrial motility in yeast. *Proceedings of the National Academy of Sciences of the United States of America*, 98(6), pp.3162–7.

Boldogh, I.R. & Pon, L. a, 2006. Interactions of mitochondria with the actin cytoskeleton. *Biochimica et biophysica acta*, 1763(5-6), pp.450–62.

Bork, P., Sander, C. & Valencia, a, 1992. An ATPase domain common to prokaryotic cell cycle proteins, sugar kinases, actin, and hsp70 heat shock proteins. *Proceedings of the National Academy of Sciences of the United States of America*, 89(16), pp.7290–4.

Bose, I. et al., 2001. Assembly of scaffold-mediated complexes containing Cdc42p, the exchange factor Cdc24p, and the effector Cla4p required for cell cycle-regulated phosphorylation of Cdc24p. *The Journal of biological chemistry*, 276(10), pp.7176–86.

Brachmann, C.B., Davies, A., Cost, G.J., Caputo E., Li, J., Heiter, P., Boeke, J.D., 1998. Designer deletion strains derived from Saccharomyces cerevisiae S288C: a useful set of strains and plasmids for PCR-mediated gene disruption and other applications. *Yeast*, 14(2), 115-32.

Breitkreutz, A, Boucher, L. & Tyers, M., 2001. MAPK specificity in the yeast pheromone response independent of transcriptional activation. *Current biology : CB*, 11(16), pp.1266–71.

Bretscher, A., 2003. Polarized growth and organelle segregation in yeast: the tracks, motors, and receptors. *The Journal of cell biology*, 160(6), pp.811–6.

Brewster, J.L. & Gustin, M.C., 1994. Positioning of cell growth and division after osmotic stress requires a MAP kinase pathway. *Yeast*, 10, pp.425–439.

Broggi, S., Martegani, E. & Colombo, S., 2013. Nuclear Ras2-GTP controls invasive growth in Saccharomyces cerevisiae. *PloS one*, 8(11), p.e79274.

Brückner, S. et al., 2004. Differential regulation of Tec1 by Fus3 and Kss1 confers signaling specificity in yeast development. *Current Genetics*, 46, pp.331–342.

Butow, R.A. & Avadhani, N.G., 2004. Mitochondrial signaling: the retrograde response. *Molecular cell*, 14(1), pp.1–15.

Buzan, J.M. & Frieden, C., 1996. Yeast actin: polymerization kinetic studies of wild type and a poorly polymerizing mutant. *Proceedings of the National Academy of Sciences of the United States of America*, 93(1), pp.91–5.

Carmona-Gutierrez, D. et al., 2010. Apoptosis in yeast: triggers, pathways, subroutines. *Cell death and differentiation*, 17(5), pp.763–73.

Casella, J.F., Flanagan, M.D. & Lin, S., 1981. Cytochalasin D inhibits actin polymerization and induces depolymerization of actin filaments formed during platelet shape change. *Nature*, 293, pp.302–305.

Chang, M. et al., 2002. A genome-wide screen for methyl methanesulfonate-sensitive mutants reveals genes required for S phase progression in the presence of DNA damage. *Proceedings of the National Academy of Sciences of the United States of America*, 99(26), pp.16934–9.

Chaudhry, F. et al., 2013. Srv2/cyclase-associated protein forms hexameric shurikens that directly catalyze actin filament severing by cofilin. *Molecular biology of the cell*, 24(1), pp.31–41.

Chen, R.E. et al., 2010. Dynamic localization of Fus3 mitogen-activated protein kinase is necessary to evoke appropriate responses and avoid cytotoxic effects. *Molecular and cellular biology*, 30(17), pp.4293–307.

Cherkasova, V. a et al., 2003. A novel functional link between MAP kinase cascades and the Ras/cAMP pathway that regulates survival. *Current biology : CB*, 13(14), pp.1220–6.

Chou, S., Lane, S. & Liu, H., 2006. Regulation of mating and filamentation genes by two distinct Ste12 complexes in Saccharomyces cerevisiae. *Molecular and cellular biology*, 26(13), pp.4794–805.

Chowdhury, S., Smith, K.W. & Gustin, M.C., 1992. Osmotic stress and the yeast cytoskeleton: phenotype-specific suppression of an actin mutation. *The Journal of cell biology*, 118(3), pp.561–71.

Colombo, S. et al., 2004. Activation state of the Ras2 protein and glucose-induced signaling in Saccharomyces cerevisiae. *The Journal of biological chemistry*, 279(45), pp.46715–22.

Colombo, S. et al., 1998. Involvement of distinct G-proteins, Gpa2 and Ras, in glucose- and intracellular acidification-induced cAMP signalling in the yeast Saccharomyces cerevisiae. *The EMBO journal*, 17(12), pp.3326–41.

Coluccio, L.M. & Tilney, L.G., 1984. Phalloidin enhances actin assembly by preventing monomer dissociation. *The Journal of cell biology*, 99(2), pp.529–35.

Conte, D. & Curcio, M.J., 2000. Fus3 controls Ty1 transpositional dormancy through the invasive growth MAPK pathway. *Molecular microbiology*, 35(2), pp.415–27.

Courchesne, W.E., Kunisawa, R. & Thorner, J., 1989. A putative protein kinase overcomes pheromone-induced arrest of cell cycling in S. cerevisiae. *Cell*, 58, pp.1107–1119.

Cullen, P.J. et al., 2004. A signaling mucin at the head of the Cdc42- and MAPK-dependent filamentous growth pathway in yeast. *Genes & development*, 18(14), pp.1695–708.

Cullen, P.J. et al., 2000. Defects in protein glycosylation cause SHO1-dependent activation of a STE12 signaling pathway in yeast. *Genetics*, 155(3), pp.1005–18.

Cullen, P.J. & Sprague, G.F., 2000. Glucose depletion causes haploid invasive growth in yeast. *Proceedings of the National Academy of Sciences of the United States of America*, 97(25), pp.13619–24.

Desany, B. a. et al., 1998. Recovery from DNA replicational stress is the essential function of the S-phase checkpoint pathway. *Genes & Development*, 12(18), pp.2956–2970.

Desrivieres, S., 1998. MSS4, a Phosphatidylinositol-4-phosphate 5-Kinase Required for Organization of the Actin Cytoskeleton in Saccharomyces cerevisiae. *Journal of Biological Chemistry*, 273(25), pp.15787–15793.

Drubin, D.G., Jones, H.D. & Wertman, K.F., 1993. Actin structure and function: roles in mitochondrial organization and morphogenesis in budding yeast and identification of the phalloidin-binding site. *Molecular biology of the cell*, 4(12), pp.1277–94.

Dulić, V. & Riezman, H., 1990. Saccharomyces cerevisiae mutants lacking a functional vacuole are defective for aspects of the pheromone response. *Journal of cell science*, 97 (Pt 3), pp.517–25.

Eitzen, G. et al., 2002. Remodeling of organelle-bound actin is required for yeast vacuole fusion. *The Journal of cell biology*, 158(4), pp.669–79.

Elion, E. a, 2001. The Ste5p scaffold. *Journal of cell science*, 114(Pt 22), pp.3967–78.

Elion, E. a, Brill, J. a & Fink, G.R., 1991. FUS3 represses CLN1 and CLN2 and in concert with KSS1 promotes signal transduction. *Proceedings of the National Academy of Sciences of the United States of America*, 88(21), pp.9392–6.

Elorza, M., Rico, H. & Sentandreu, R., 1983. Calcofluor White Alters the Assembly of Chitin Fibrils in Saccharomyces cerevisiae and Candida albicans Cells. *Journal of general ...*, 129(5), pp.1577–1582.

Elzinga, M. et al., 1973. Complete amino-acid sequence of actin of rabbit skeletal muscle. *Proceedings of the National Academy of Sciences of the United States of America*, 70(9), pp.2687–91.

Engqvist-Goldstein, A.E.Y. & Drubin, D.G., 2003. Actin assembly and endocytosis: from yeast to mammals. *Annual review of cell and developmental biology*, 19, pp.287–332.

Farah, M.E. et al., 2011. Diverse protective roles of the actin cytoskeleton during oxidative stress. *Cytoskeleton (Hoboken, N.J.)*, 68(6), pp.340–54.

Featherstone, C. & Jackson, S.P., 1999. DNA double-strand break repair. *Current biology : CB*, 9(20), pp.R759–61.

Fehrenbacher, K.L. et al., 2002. Endoplasmic Reticulum Dynamics, Inheritance, and Cytoskeletal Interactions in Budding Yeast. *Molecular biology of the cell*, 13(March), pp.854–865.

Fehrenbacher, K.L. et al., 2004. Live Cell Imaging of Mitochondrial Movement along Actin Cables in Budding Yeast. , 14, pp.1996–2004.

Feliciano, D. & Di Pietro, S.M., 2012. SLAC, a complex between Sla1 and Las17, regulates actin polymerization during clathrin-mediated endocytosis. *Molecular biology of the cell*, 23(21), pp.4256–72.

Ferrigno, P. et al., 1998. Regulated nucleo/cytoplasmic exchange of HOG1 MAPK requires the importin beta homologs NMD5 and XPO1. *The EMBO journal*, 17(19), pp.5606–14.

Fox, T.D. et al., 1991. Analysis and manipulation of yeast mitochondrial genes. *Methods Enzymol.*, (194), pp.149–165.

Franklin-Tong, V.E. & Gourlay, C.W., 2008. A role for actin in regulating apoptosis/programmed cell death: evidence spanning yeast, plants and animals. *The Biochemical journal*, 413(3), pp.389–404.

Frederick, R.L. et al., 2004. Yeast Miro GTPase, Gem1p, regulates mitochondrial morphology via a novel pathway. *The Journal of cell biology*, 167(1), pp.87–98.

Fuchs, B.B. & Mylonakis, E., 2009. Our paths might cross: the role of the fungal cell wall integrity pathway in stress response and cross talk with other stress response pathways. *Eukaryotic cell*, 8(11), pp.1616–25.

Fujimura, H. aki, 1990. Molecular cloning of the DAC2/FUS3 gene essential for pheromone-induced G1-arrest of the cell cycle in Saccharomyces cerevisiae. *Current Genetics*, 18, pp.395–400.

Gabriely, G., Kama, R. & Gerst, J.E., 2007. Involvement of specific COPI subunits in protein sorting from the late endosome to the vacuole in yeast. *Molecular and cellular biology*, 27(2), pp.526–40.

Gancedo, J.M., 2001. Control of pseudohyphae formation in Saccharomyces cerevisiae. *FEMS microbiology reviews*, 25(1), pp.107–23.

Garcia-Rodriguez, L., Duran, A. & Roncero, C., 2000. Calcofluor Antifungal Action Depends on Chitin and a Functional High-Osmolarity Glycerol Response (HOG) Pathway: Evidence for a Physiological Role of the Saccharomyces cerevisiae HOG Pathway under Noninducing Conditions. *Journal of bacteriology*, 182(9), pp.2428–2437.

Gardiner, F.C., Costa, R. & Ayscough, K.R., 2007. Nucleocytoplasmic trafficking is required for functioning of the adaptor protein Sla1p in endocytosis. *Traffic (Copenhagen, Denmark)*, 8(4), pp.347–58.

Garinis, G. a et al., 2005. Transcriptome analysis reveals cyclobutane pyrimidine dimers as a major source of UV-induced DNA breaks. *The EMBO journal*, 24(22), pp.3952–62.

Gartner, A., Nasmyth, K. & Ammerer, G., 1992. Signal transduction in Saccharomyces cerevisiae requires tyrosine and threonine phosphorylation of FUS3 and KSS1. *Genes & development*, 6, pp.1280–1292.

Geli, M.I. & Riezman, H., 1998. Endocytic internalization in yeast and animal cells: similar and different. *Journal of cell science*, 111 (Pt 8, pp.1031–7.

Geli, M.I. & Riezman, H., 1996. Role of type I myosins in receptor-mediated endocytosis in yeast. *Science (New York, N.Y.)*, 272, pp.533–535.

Giannattasio, S. et al., 2005. Retrograde response to mitochondrial dysfunction is separable from TOR1/2 regulation of retrograde gene expression. *Journal of Biological Chemistry*, 280, pp.42528–42535.

Goffeau, A. et al., 1996. Life with 6000 genes. *Science (New York, N.Y.)*, 274, pp.546, 563–567.

Goode, B.L., Drubin, D.G. & Lappalainen, P., 1998. Regulation of the cortical actin cytoskeleton in budding yeast by twinfilin, a ubiquitous actin monomer-sequestering protein. *The Journal of cell biology*, 142(3), pp.723–33.

Gourlay, C.W. et al., 2004. A role for the actin cytoskeleton in cell death and aging in yeast. *The Journal of cell biology*, 164(6), pp.803–9.

Gourlay, C.W. & Ayscough, K.R., 2005a. A role for actin in aging and apoptosis. *Biochemical Society transactions*, 33(Pt 6), pp.1260–4.

Gourlay, C.W. & Ayscough, K.R., 2006. Actin-induced hyperactivation of the Ras signaling pathway leads to apoptosis in Saccharomyces cerevisiae. *Molecular and cellular biology*, 26(17), pp.6487–501.

Gourlay, C.W. & Ayscough, K.R., 2005b. Identification of an upstream regulatory pathway controlling actin-mediated apoptosis in yeast. *Journal of cell science*, 118(Pt 10), pp.2119–32.

Gueldener, U. et al., 2002. A second set of loxP marker cassettes for Cre-mediated multiple gene knockouts in budding yeast. *Nucleic acids research*, 30(6), p.e23.

Guo, S. et al., 2009. A MAP kinase dependent feedback mechanism controls Rho1 GTPase and actin distribution in yeast. *PloS one*, 4(6), p.e6089.

Gustin, M.C. et al., 1998. MAP kinase pathways in the yeast Saccharomyces cerevisiae. *Microbiology and molecular biology reviews : MMBR*, 62(4), pp.1264–300.

Von der Haar, T., 2007. Optimized protein extraction for quantitative proteomics of yeasts. *PloS one*, 2(10), p.e1078.

Haarer, B.K. et al., 1990. Purification of Profilin from Saccharomyces cerevisiae And Analysis of Profilin-deficient Cells. , 110(January).

Hagen, D.C., Mccaffrey, G. & Sprague, G.F., 1991. Pheromone Response Elements Are Necessary and Sufficient for Basal and Pheromone-Induced Transcription of the FUS] Gene of Saccharomyces cerevisiae.

Hagen, D.C. & Sprague, G.F., 1984. Induction of the yeast alpha-specific STE3 gene by the peptide pheromone a-factor. *Journal of molecular biology*, 178, pp.835–852.

Harrison, J.C. et al., 2001. A role for the Pkc1p/Mpk1p kinase cascade in the morphogenesis checkpoint. *Nature cell biology*, 3(4), pp.417–20.

Heeren, G. et al., 2004. The role of respiration, reactive oxygen species and oxidative stress in mother cell-specific ageing of yeast strains defective in the RAS signalling pathway. *FEMS yeast research*, 5(2), pp.157–67.

Heise, B. et al., 2010. The TEA transcription factor Tec1 confers promoter-specific gene regulation by Ste12-dependent and -independent mechanisms. *Eukaryotic cell*, 9(4), pp.514–31.

Helliwell, S.B. et al., 1998. The Rho1 effector Pkc1, but not Bni1, mediates signalling from Tor2 to the actin cytoskeleton. *Current biology : CB*, 8(22), pp.1211–4.

Herbert, A.P. et al., 2012. NMR structure of Hsp12, a protein induced by and required for dietary restriction-induced lifespan extension in yeast. *PloS one*, 7(7), p.e41975.

Herskowitz, I., 1995. MAP kinase pathways in yeast: for mating and more. *Cell*, 80(2), pp.187–97.

Higuchi, R. et al., 2013. Actin Dynamics Affect Mitochondrial Quality Control and Aging in Budding Yeast. *Current Biology*, pp.1–6.

Hill, K.L., Catlett, N.L. & Weisman, L.S., 1996. Actin and myosin function in directed vacuole movement during cell division in Saccharomyces cerevisiae. *The Journal of cell biology*, 135, pp.1535–1549.

Hirschman, J.E. & Jenness, D.D., 1999. Dual Lipid Modification of the Yeast G γ Subunit Ste18p Determines Membrane Localization of G β γ Dual Lipid Modification of the Yeast G ⁄ Subunit Ste18p Determines Membrane Localization of G ␣. , 19(11).

Hohmann, S., 2009. Control of high osmolarity signalling in the yeast Saccharomyces cerevisiae. *FEBS letters*, 583(24), pp.4025–9.

Hohmann, S., 2002. Osmotic Stress Signaling and Osmoadaptation in Yeasts Osmotic. *Microbiology and Molecular Biology Reviews*, 66(2).

Holmes, K. et al., 1990. Atomic model of the actin filament. *Nature*, 347, pp.44–49.

Holmes, K.C. et al., 2003. Electron cryo-microscopy shows how strong binding of myosin to actin releases nucleotide. *Nature*, 425(6956), pp.423–7.

Holtzman, D., Yang, S. & Drubin, D., 1993. Synthetic-lethal interactions identify two novel genes, SLA1 and SLA2, that control membrane cytoskeleton assembly in Saccharomyces cerevisiae. *The Journal of cell biology*, 122(3), pp.635–644.

Howard, J.P. et al., 2002. Sla1p serves as the targeting signal recognition factor for NPFX(1,2)D-mediated endocytosis. *The Journal of cell biology*, 157(2), pp.315–26.

Hu, Y. et al., 2010. The localization and concentration of the PDE2-encoded high-affinity cAMP phosphodiesterase is regulated by cAMP-dependent protein kinase A in the yeast Saccharomyces cerevisiae. *FEMS yeast research*, 10(2), pp.177–87.

Irizarry, R. a et al., 2003. Exploration, normalization, and summaries of high density oligonucleotide array probe level data. *Biostatistics (Oxford, England)*, 4(2), pp.249–64.

Iwahashi, H. et al., 1998. Evidence for the interplay between trehalose metabolism and Hsp104 in yeast. *Applied and environmental microbiology*, 64(11), pp.4614–7.

Jazayeri, A., 2004. Saccharomyces cerevisiae Sin3p facilitates DNA double-strand break repair. *Proceedings of the National Academy of Sciences of the United States of America*, 101(6), pp.1644–1649.

Kabsch, W. et al., 1990. Atomic structure of the actin:DNase I complex. *Nature*, 347, pp.37–44.

Kabsch, W. & Holmes, K., 1995. The actin fold. *The FASEB Journal*, 9, pp.167–174.

Kaksonen, M., Sun, Y. & Drubin, D.G., 2003. A pathway for association of receptors, adaptors, and actin during endocytic internalization. *Cell*, 115(4), pp.475–87.

Kamada, Y. et al., 1995. The protein kinase C-activated MAP kinase pathway of Saccharomyces cerevisiae mediates a novel aspect of the heat shock response. *Genes & Development*, 9(13), pp.1559–1571.

Kapoor, P. et al., 2013. Evidence for monomeric actin function in INO80 chromatin remodeling. *Nature structural & molecular biology*, 20(4), pp.426–32.

Karpova, T.S. et al., 2008. Depolarization of the actin cytoskeleton is a specific phenotype in Saccharomyces cerevisiae. , 111(Pt 17), pp.2689–2696.

Kelly, D.E., Lamb, D.C. & Kelly, S.L., 2001. Genome-wide generation of yeast gene deletion strains. *Comparative and functional genomics*, 2(4), pp.236–42.

Kilmartin, J. V & Adams, a E., 1984. Structural rearrangements of tubulin and actin during the cell cycle of the yeast Saccharomyces. *The Journal of cell biology*, 98(3), pp.922–33.

Kim, K. et al., 2004. Capping protein binding to actin in yeast: biochemical mechanism and physiological relevance. *The Journal of cell biology*, 164(4), pp.567–80.

Klamt, F. et al., 2009. Oxidant-induced apoptosis is mediated by oxidation of the actin-regulatory protein cofilin. *Nature cell biology*, 11(10), pp.1241–6.

Klein, S., Reuveni, H. & Levitzki, a, 2000. Signal transduction by a nondissociable heterotrimeric yeast G protein. *Proceedings of the National Academy of Sciences of the United States of America*, 97(7), pp.3219–23.

Klis, F.M., Boorsma, A. & De Groot, P.W.J., 2006. Cell wall construction in Saccharomyces cerevisiae. *Yeast (Chichester, England)*, 23(3), pp.185–202.

Korn, E.D., Carlier, M.F. & Pantaloni, D., 1987. Actin polymerization and ATP hydrolysis. *Science (New York, N.Y.)*, 238, pp.638–644.

Kornmann, B., Osman, C. & Walter, P., 2011. The conserved GTPase Gem1 regulates endoplasmic reticulum-mitochondria connections. *Proceedings of the National Academy of Sciences of the United States of America*, 108(34), pp.14151–6.

Kotiadis, V. et al., 2012. Identification of new surfaces of Cofilin that link mitochondrial function to the control of multi-drug resistance. *Journal of Cell ...*, 125(May 1), pp.2288–2299.

Kotiadis, V.N. et al., 2012. Identification of new surfaces of cofilin that link mitochondrial function to the control of multi-drug resistance. *Journal of cell science*, 125(Pt 9), pp.2288–99.

Lamson, R., Winters, M. & Pryciak, P., 2002. Cdc42 regulation of kinase activity and signaling by the yeast p21-activated kinase Ste20. *Molecular and cellular ...*, 22(9).

Lappalainen, P. et al., 1998. The ADF homology (ADF-H) domain: a highly exploited actin-binding module. *Molecular biology of the cell*, 9(8), pp.1951–9.

Lappalainen, P. & Drubin, D., 1997. Cofilin promotes rapid actin filament turnover in vivo. *Nature*, 389(September), pp.1–6.

Laun, P. et al., 2001. Aged mother cells of Saccharomyces cerevisiae show markers of oxidative stress and apoptosis. *Molecular microbiology*, 39(5), pp.1166–73.

Leadsham, J.E. et al., 2013. Loss of Cytochrome c Oxidase Promotes RAS-Dependent ROS Production from the ER Resident NADPH Oxidase, Yno1p, in Yeast. *Cell metabolism*, 18(2), pp.279–86.

Leadsham, J.E. et al., 2009. Whi2p links nutritional sensing to actin-dependent Ras-cAMP-PKA regulation and apoptosis in yeast. *Journal of cell science*, 122(Pt 5), pp.706–15.

Leadsham, J.E. & Gourlay, C.W., 2010. cAMP/PKA signaling balances respiratory activity with mitochondria dependent apoptosis via transcriptional regulation. *BMC cell biology*, 11(1), p.92.

Leadsham, J.E. & Gourlay, C.W., 2008. Cytoskeletal induced apoptosis in yeast. *Biochimica et biophysica acta*, 1783(7), pp.1406–12.

Lederer, M., Jockusch, B.M. & Rothkegel, M., 2005. Profilin regulates the activity of p42POP, a novel Myb-related transcription factor. *Journal of cell science*, 118(Pt 2), pp.331–41.

Lee, P. et al., 2011. Regulation of yeast Yak1 kinase by PKA and autophosphorylation-dependent 14-3-3 binding. *Molecular microbiology*, 79(3), pp.633–46.

Leeuw, T. et al., 1995. Pheromone response in yeast: association of Bem1p with proteins of the MAP kinase cascade and actin. *Science (New York, N.Y.)*, 270(5239), pp.1210–3.

Levin, D.E., 2005. Cell Wall Integrity Signaling in Saccharomyces cerevisiae Cell Wall Integrity Signaling in Saccharomyces cerevisiae. *Microbiology and Molecular Biology Reviews*, 69(2), pp.262–291.

Levin, D.E., 2011. Regulation of cell wall biogenesis in Saccharomyces cerevisiae: the cell wall integrity signaling pathway. *Genetics*, 189(4), pp.1145–75.

Livas, D. et al., 2011. Transcriptional responses to glucose in Saccharomyces cerevisiae strains lacking a functional protein kinase A. *BMC genomics*, 12(1), p.405.

Loewith, R. & Hall, M.N., 2011. Target of rapamycin (TOR) in nutrient signaling and growth control. *Genetics*, 189(4), pp.1177–201.

Lombardi, R. & Riezman, H., 2001. Rvs161p and Rvs167p, the two yeast amphiphysin homologs, function together in vivo. *The Journal of biological chemistry*, 276(8), pp.6016–22.

Lussier, M. et al., 1997. Large scale identification of genes involved in cell surface biosynthesis and architecture in Saccharomyces cerevisiae. *Genetics*, 147(2), pp.435–450.

Ma, D., Cook, J.G. & Thorner, J., 1995. Phosphorylation and localization of Kss1, a MAP kinase of the Saccharomyces cerevisiae pheromone response pathway. *Molecular biology of the cell*, 6(7), pp.889–909.

Madhani, H. & Fink, G., 1998. The riddle of MAP kinase signaling specificity. *Trends in Genetics*, 9525(98), pp.151–155.

Madhani, H.D. & Fink, G.R., 1997. Combinatorial Control Required for the Specificity of Yeast MAPK Signaling. *Science*, 275(5304), pp.1314–1317.

Maeda, T., Takekawa, M. & Saito, H., 1995. Activation of yeast PBS2 MAPKK by MAPKKKs or by binding of an SH3-containing osmosensor. *Science (New York, N.Y.)*, 269, pp.554–558.

Mahadev, R.K. et al., 2007. Structure of Sla1p homology domain 1 and interaction with the NPFxD endocytic internalization motif. *The EMBO journal*, 26(7), pp.1963–71.

Mattison, C.P. & Ota, I.M., 2000. Two protein tyrosine phosphatases , Ptp2 and Ptp3 , modulate the subcellular localization of the Hog1 MAP kinase in yeast. , pp.1229–1235.

Mayer, B.J. & Eck, M.J., 1995. SH3 domains: Minding your p's and q's. *Current Biology*, 5(4), pp.364–367.

McKinney, J.S. et al., 2013. A multistep genomic screen identifies new genes required for repair of DNA double-strand breaks in Saccharomyces cerevisiae. *BMC genomics*, 14, p.251.

Merrill, B.J. & Holm, C., 1999. A requirement for recombinational repair in Saccharomyces cerevisiae is caused by DNA replication defects of mec1 mutants. *Genetics*, 153(2), pp.595–605.

Miermont, A. et al., 2011. The Dynamical Systems Properties of the HOG Signaling Cascade. *Journal of signal transduction*, 2011, p.930940.

Miralles, F. & Visa, N., 2006. Actin in transcription and transcription regulation. *Current opinion in cell biology*, 18(3), pp.261–6.

Mizuguchi, G. et al., 2004. ATP-driven exchange of histone H2AZ variant catalyzed by SWR1 chromatin remodeling complex. *Science (New York, N.Y.)*, 303(5656), pp.343–8.

Moriyama, K. & Yahara, I., 2002. Human CAP1 is a key factor in the recycling of cofilin and actin for rapid actin turnover. *Journal of cell science*, 115(Pt 8), pp.1591–601.

Morton, W.M., Ayscough, K.R. & McLaughlin, P.J., 2000. Latrunculin alters the actin-monomer subunit interface to prevent polymerization. *Nature cell biology*, 2(6), pp.376–8.

Mösch, H.-U. et al., 1999. Crosstalk between the Ras2p-controlled mitogen-activated protein kinase and cAMP pathways during invasive growth of Saccharomyces cerevisiae. *Molecular biology of the cell*, 10(5), pp.1325–35.

Mösch, H.U., Roberts, R.L. & Fink, G.R., 1996. Ras2 signals via the Cdc42/Ste20/mitogen-activated protein kinase module to induce filamentous growth in Saccharomyces cerevisiae. *Proceedings of the National Academy of Sciences of the United States of America*, 93(11), pp.5352–6.

Moseley, J.B. et al., 2006. Twinfilin is an actin-filament-severing protein and promotes rapid turnover of actin structures in vivo. *Journal of cell science*, 119(Pt 8), pp.1547–57.

Moseley, J.B. & Goode, B.L., 2006. The yeast actin cytoskeleton: from cellular function to biochemical mechanism. *Microbiology and molecular biology reviews : MMBR*, 70(3), pp.605–45.

Moseley, J.B., Maiti, S. & Goode, B.L., 2006. Formin proteins: Purification and measurement of effects on actin assembly. *Methods in Enzymology*, 406, pp.215–234.

Mulholland, J. et al., 1999. Visualization of receptor-mediated endocytosis in yeast. *Molecular biology of the cell*, 10(3), pp.799–817.

Nakayama, N., Miyajima, a & Arai, K., 1985. Nucleotide sequences of STE2 and STE3, cell type-specific sterile genes from Saccharomyces cerevisiae. *The EMBO journal*, 4(10), pp.2643–8.

Nakayama, N., Miyajima, A. & Arai, K., 1987. Common signal transduction system shared by STE2 and STE3 in haploid cells of Saccharomyces cerevisiae : autocrine cell-cycle arrest results from forced expression of STE2 Q-N Y : STE3 Y : STE2 A : a-factor o : a-factor. , 6(1), pp.249–254.

Nelson, B. et al., 2004. Fus1p interacts with components of the Hog1p mitogen-activated protein kinase and Cdc42p morphogenesis signaling pathways to control cell fusion during yeast mating. *Genetics*, 166(1), pp.67–77.

Nkosi, P.J. et al., 2013. Hof1 and Rvs167 have redundant roles in actomyosin ring function during cytokinesis in budding yeast. *PloS one*, 8(2), p.e57846.

Noma, A. et al., 2011. Actin-binding protein ABP140 is a methyltransferase for 3-methylcytidine at position 32 of tRNAs in Saccharomyces cerevisiae. *RNA (New York, N.Y.)*, 17(6), pp.1111–9.

Novick, P., Osmond, B.C. & Botstein, D., 1989. Suppressors of yeast actin mutations. *Genetics*, 121(4), pp.659–74.

O'Rourke, S. & Herskowitz, I., 2002. A Third Osmosensing Branch in Saccharomyces cerevisiae Requires the Msb2 Protein and Functions in Parallel with the Sho1 Branch. *Molecular and cellular biology*, 22(13), pp.4739–4749.

Oh, Y. & Bi, E., 2011. Septin structure and function in yeast and beyond. *Trends in cell biology*, 21(3), pp.141–148.

Olave, I. a, Reck-Peterson, S.L. & Crabtree, G.R., 2002. Nuclear actin and actin-related proteins in chromatin remodeling. *Annual review of biochemistry*, 71, pp.755–81.

Otterbein, L.R., Graceffa, P. & Dominguez, R., 2001. The crystal structure of uncomplexed actin in the ADP state. *Science (New York, N.Y.)*, 293(5530), pp.708–11.

Ozaki-Kuroda, K. et al., 2001. Dynamic Localization and Function of Bni1p at the Sites of Directed Growth in Saccharomyces cerevisiae. , 21(3), pp.827–839.

Palmgren, S. et al., 2001. Interactions with PIP2, ADP-actin monomers, and capping protein regulate the activity and localization of yeast twinfilin. *The Journal of cell biology*, 155(2), pp.251–60.

Papamichos-Chronakis, M., Krebs, J.E. & Peterson, C.L., 2006. Interplay between Ino80 and Swr1 chromatin remodeling enzymes regulates cell cycle checkpoint adaptation in response to DNA damage. *Genes & development*, 20(17), pp.2437–49.

Pegg, A., 1984. Methylation of the O6 position of guanine in DNA is the most likely initiating event in carcinogenesis by methylating agents. *Cancer Invest.*, 2(3), pp.223–231.

Perrin, B.J. & Ervasti, J.M., 2010. The actin gene family: function follows isoform. *Cytoskeleton (Hoboken, N.J.)*, 67(10), pp.630–4.

Peter, M. & Herskowitz, I., 1994. Direct inhibition of the yeast cyclin-dependent kinase Cdc28-Cln by Far1. *Science (New York, N.Y.)*, 265, pp.1228–1231.

Pfeifer, G.P., You, Y.-H. & Besaratina, A., 2005. Mutations induced by ultraviolet light. *Biological Effects of Ultraviolet Radiation*, 571(1-2), pp.19–31.

Philip, B. & Levin, D.E., 2001. Wsc1 and Mid2 Are Cell Surface Sensors for Cell Wall Integrity Signaling That Act through Rom2 , a Guanine Nucleotide Exchange Factor for Rho1 Wsc1 and Mid2 Are Cell Surface Sensors for Cell Wall Integrity Signaling That Act through Rom2 , a Guanine Nucle.

Piao, H.L., Machado, I.M.P. & Payne, G.S., 2007. NPFXD-mediated Endocytosis Is Required for Polarity and Function of a Yeast Cell Wall Stress Sensor. *Molecular biology of the cell*, 18(January), pp.57–65.

Di Pietro, S.M. et al., 2010. Regulation of clathrin adaptor function in endocytosis: novel role for the SAM domain. *The EMBO journal*, 29(6), pp.1033–44.

Pinto, I.M. et al., 2012. Actin Depolymerization Drives Actomyosin Ring Contraction during Budding Yeast Cytokinesis. *Developmental cell*, 22(6), pp.1247–1260.

Pollard, T.D., 2007. Regulation of actin filament assembly by Arp2/3 complex and formins. *Annual review of biophysics and biomolecular structure*, 36, pp.451–77.

Pollard, T.D. & Borisy, G.G., 2003. Cellular motility driven by assembly and disassembly of actin filaments. *Cell*, 112(4), pp.453–65.

Posas, F. et al., 1996. Yeast HOG1 MAP kinase cascade is regulated by a multistep phosphorelay mechanism in the SLN1-YPD1-SSK1 "two-component" osmosensor. *Cell*, 86(6), pp.865–75.

Posas, F. & Saito, H., 1998. Activation of the yeast SSK2 MAP kinase kinase kinase by the SSK1 two-component response regulator. *The EMBO journal*, 17(5), pp.1385–94.

Posas, F., Takekawa, M. & Saito, H., 1998. Signal transduction by MAP kinase cascades in budding yeast. *Current opinion in microbiology*, 1(2), pp.175–82.

Prakash, L. & Prakash, S., 1977. Isolation and characterization of mms-sensitive mutants of Saccharomyces cerevisiae. *Genetics*, pp.33–55.

Prinz, W.A. et al., 2000. Mutants affecting the structure of the cortical endoplasmic reticulum in Saccharomyces cerevisiae. *The Journal of cell biology*, 150(3), pp.461–74.

Pruyne, D. et al., 2004. Mechanisms of polarized growth and organelle segregation in yeast. *Annual review of cell and developmental biology*, 20, pp.559–91.

Qi, M. & Elion, E. a., 2007. Formin-induced actin cables are required for polarized recruitment of the Ste5 scaffold and high level activation of MAPK Fus3. *Journal of Cell Science*, 120(4), pp.712–712.

Quintero-monzon, O. et al., 2005. Structural and Functional Dissection of the Abp1 ADFH Actin-binding Domain Reveals Versatile In Vivo Adapter Functions □. , 16(July), pp.3128–3139.

Raitt, D.C., Posas, F. & Saito, H., 2000. Yeast Cdc42 GTPase and Ste20 PAK-like kinase regulate Sho1-dependent activation of the Hog1 MAPK pathway. *The EMBO journal*, 19(17), pp.4623–31.

Rajavel, M. & Philip, B., 1999. Mid2 Is a Putative Sensor for Cell Integrity Signaling in Saccharomyces cerevisiae. ... *and cellular biology*, 19(6).

Raths, S. et al., 1993. end3 and end4: two mutants defective in receptor-mediated and fluid-phase endocytosis in Saccharomyces cerevisiae. *The Journal of cell biology*, 120(1), pp.55–65.

Reiser, V., Raitt, D.C. & Saito, H., 2003. Yeast osmosensor Sln1 and plant cytokinin receptor Cre1 respond to changes in turgor pressure. *The Journal of cell biology*, 161(6), pp.1035–40.

Reiser, V., Salah, S.M. & Ammerer, G., 2000. Polarized localization of yeast Pbs2 depends on osmostress, the membrane protein Sho1 and Cdc42. *Nature cell biology*, 2(9), pp.620–7.

Dos Remedios, C.G. et al., 2003. Actin binding proteins: regulation of cytoskeletal microfilaments. *Physiological reviews*, 83(2), pp.433–73.

Rep, M. et al., 1999. Osmotic Stress-Induced Gene Expression in Saccharomyces cerevisiae Requires Msn1p and the Novel Nuclear Factor Hot1p Osmotic Stress-Induced Gene Expression in Saccharomyces cerevisiae Requires Msn1p and the Novel Nuclear Factor Hot1p.

Ringnér, M., 2008. What is principal component analysis? *Nature biotechnology*, 26(3), pp.303–4.

Roberts, C.J., 2000. Signaling and Circuitry of Multiple MAPK Pathways Revealed by a Matrix of Global Gene Expression Profiles. *Science*, 287(5454), pp.873–880.

Roberts, R.L. & Fink, G.R., 1994. Elements of a single MAP kinase cascade in Saccharomyces cerevisiae mediate two developmental programs in the same cell type: mating and invasive growth. *Genes & Development*, 8(24), pp.2974–2985.

Roberts, R.L., Mösch, H.U. & Fink, G.R., 1997. 14-3-3 proteins are essential for RAS/MAPK cascade signaling during pseudohyphal development in S. cerevisiae. *Cell*, 89(7), pp.1055–65.

Rodal, A.A. et al., 2003. Negative Regulation of Yeast WASp by Two SH3 Domain-Containing Proteins. , 13, pp.1000–1008.

Rodríguez-Peña, J.M. et al., 2010. The high-osmolarity glycerol (HOG) and cell wall integrity (CWI) signalling pathways interplay: a yeast dialogue between MAPK routes. *Yeast (Chichester, England)*, 27(8), pp.495–502.

Roncero, C. et al., 1988. Isolation and characterization of Saccharomyces cerevisiae mutants resistant to Calcofluor white. *Journal of bacteriology*, 170(4), pp.1950–4.

Roncero, C. & Sánchez, Y., 2010. Cell separation and the maintenance of cell integrity during cytokinesis in yeast : the assembly of a septum. *Yeast*, (May), pp.521–530.

De Rosier, D.J., 1990. The changing shape of actin. *Nature*, 347, pp.21–22.

Scherens, B. & Goffeau, A., 2004. The uses of genome-wide yeast mutant collections. *Genome biology*, 5(7), p.229.

Schmidt, A. et al., 1997. The Yeast Phosphatidylinositol Kinase Homolog TOR2 Activates RHO1 and RHO2 via the Exchange Factor ROM2. *Cell*, 88, pp.531–542.

Schott, D.H., Collins, R.N. & Bretscher, A., 2002. Secretory vesicle transport velocity in living cells depends on the myosin-V lever arm length. *The Journal of cell biology*, 156(1), pp.35–9.

Sept, D. & McCammon, J. a, 2001. Thermodynamics and kinetics of actin filament nucleation. *Biophysical journal*, 81(2), pp.667–74.

Shortle, D., Haber, J.E. & Botstein, D., 1982. Lethal disruption of the yeast actin gene by integrative DNA transformation. *Science (New York, N.Y.)*, 217, pp.371–373.

Simon, M.N. et al., 1995. Role for the Rho-family GTPase Cdc42 in yeast mating-pheromone signal pathway. *Nature*, 376(6542), pp.702–5.

Sit, S.-T. & Manser, E., 2011. Rho GTPases and their role in organizing the actin cytoskeleton. *Journal of cell science*, 124(Pt 5), pp.679–83.

Sivadon, P., Crouzet, M. & Aigle, M., 1997. Functional assessment of the yeast Rvs161 and Rvs167 protein domains. *FEBS Letters*, 417(1), pp.21–27.

Slaughter, B. et al., 2009. Dual modes of cdc42 recycling fine-tune polarized morphogenesis. *Developmental cell*, 17(6), pp.823–835.

Smethurst, D.G.J., Dawes, I.W. & Gourlay, C.W., 2013. Actin - a biosensor that determines cell fate in yeasts. *FEMS yeast research*, 14, pp.89–95.

Smith, M.G., Swamy, S.R. & Pon, L. a, 2001. The life cycle of actin patches in mating yeast. *Journal of cell science*, 114(Pt 8), pp.1505–13.

Smyth, G., 2005. limma: Linear Models for Microarray Data. In *Bioinformatics and Computational Biology Solutions Using R and Bioconductor*. pp. 397–420.

Spink, B.J. et al., 2008. Long single alpha-helical tail domains bridge the gap between structure and function of myosin VI. *Nature structural & molecular biology*, 15(6), pp.591–7.

Staleva, L., Hall, A. & Orlow, S.J., 2004. Oxidative Stress Activates FUS1 and RLM1 Transcription in the Yeast Saccharomyces cerevisiae in an Oxidant- dependent Manner □. , 15(December), pp.5574–5582.

Stergiou, L. et al., 2011. NER and HR pathways act sequentially to promote UV-C-induced germ cell apoptosis in Caenorhabditis elegans. *Cell death and differentiation*, 18(5), pp.897–906.

Straub, F., 1942. Actin. *Studies from the Institute of Medical Chemistry University Szeged*, 2, pp.1–15.

Sunada, R. et al., 2005. The nuclear actin-related protein Act3p/Arp4p is involved in the dynamics of chromatin-modulating complexes. *Yeast (Chichester, England)*, 22(10), pp.753–68.

Symington, L.S., 2002. Role of RAD52 Epistasis Group Genes in Homologous Recombination and Double-Strand Break Repair Role of RAD52 Epistasis Group Genes in Homologous Recombination and Double-Strand Break Repair. , 66(4).

Tan, P., Howard, J. & Payne, G., 1996. The Sequence NPFXD Defines a New Class of Endocytosis Signal in Saccharomyces cerevisiae. *The Journal of cell biology*, 135(6), pp.1789–1800.

Tanaka, K. et al., 2014. Yeast osmosensors Hkr1 and Msb2 activate the Hog1 MAPK cascade by different mechanisms. *Science signaling*, 7, p.ra21.

Tang, H.Y., Xu, J. & Cai, M., 2000. Pan1p, End3p, and S1a1p, three yeast proteins required for normal cortical actin cytoskeleton organization, associate with each other and play essential roles in cell wall morphogenesis. *Molecular and cellular biology*, 20(1), pp.12–25.

Tatebayashi, K. et al., 2007. Transmembrane mucins Hkr1 and Msb2 are putative osmosensors in the SHO1 branch of yeast HOG pathway. *The EMBO journal*, 26(15), pp.3521–33.

Tedford, K. et al., 1997. Regulation of the mating pheromone and invasive growth responses in yeast by two MAP kinase substrates. *Current biology : CB*, 7, pp.228–238.

Teixeira, M.C. et al., 2014. The YEASTRACT database: an upgraded information system for the analysis of gene and genomic transcription regulation in Saccharomyces cerevisiae. *Nucleic acids research*, 42(Database issue), pp.D161–6.

Thevelein, J.M. et al., 2005. Nutrient sensing systems for rapid activation of the protein kinase A pathway in yeast. *Biochemical Society transactions*, 33(Pt 1), pp.253–6.

Thevelein, J.M. & de Winde, J.H., 1999. Novel sensing mechanisms and targets for the cAMP-protein kinase A pathway in the yeast Saccharomyces cerevisiae. *Molecular microbiology*, 33(5), pp.904–18.

Truman, A.W., Kim, K.-Y. & Levin, D.E., 2009. Mechanism of Mpk1 mitogen-activated protein kinase binding to the Swi4 transcription factor and its regulation by a novel caffeine-induced phosphorylation. *Molecular and cellular biology*, 29(24), pp.6449–61.

Varela, J.C. et al., 1995. The Saccharomyces cerevisiae HSP12 gene is activated by the high-osmolarity glycerol pathway and negatively regulated by protein kinase A. *Molecular and cellular biology*, 15(11), pp.6232–45.

Vartiainen, M.K. et al., 2007. Nuclear actin regulates dynamic subcellular localization and activity of the SRF cofactor MAL. *Science (New York, N.Y.)*, 316(5832), pp.1749–52.

Verna, J. et al., 1997. A family of genes required for maintenance of cell wall integrity and for the stress response in Saccharomyces cerevisiae. *Proceedings of the National Academy of Sciences of the United States of America*, 94(25), pp.13804–9.

Vilella, F. et al., 2005. Pkc1 and the upstream elements of the cell integrity pathway in Saccharomyces cerevisiae, Rom2 and Mtl1, are required for cellular responses to oxidative stress. *The Journal of biological chemistry*, 280(10), pp.9149–59.

Vinod, P.K. et al., 2008. Integration of global signaling pathways, cAMP-PKA, MAPK and TOR in the regulation of FLO11. *PloS one*, 3(2), p.e1663.

Visegrády, B. et al., 2004. The effect of phalloidin and jasplakinolide on the flexibility and thermal stability of actin filaments. *FEBS letters*, 565(1-3), pp.163–6.

Wang, H., Robinson, R.C. & Burtnick, L.D., 2010. The structure of native G-actin. *Cytoskeleton*, 67(7), pp.456–465.

Wang, Y. et al., 2004. Ras and Gpa2 mediate one branch of a redundant glucose signaling pathway in yeast. *PLoS biology*, 2(5), p.E128.

Warren, D.T. et al., 2002. Sla1p couples the yeast endocytic machinery to proteins regulating actin dynamics. *Journal of cell science*, 115(Pt 8), pp.1703–15.

Water, R., Pringle, J. & Kleinsmith, L., 1980. Identification of an Actin-Like Protein and of Its Messenger Ribonucleic Acid in Saccharomyces cerevisiae. *Journal of bacteriology*, 144(3), pp.1143–1151.

Wertman, K., Drubin, D. & Botstein, D., 1992. Systematic Mutational Analysis of the Yeast ACTl Gene Kenneth. *Genetics*, 132, pp.337–350.

Wesp, a et al., 1997. End4p/Sla2p interacts with actin-associated proteins for endocytosis in Saccharomyces cerevisiae. *Molecular biology of the cell*, 8(11), pp.2291–306.

Westermann, B. & Neupert, W., 2000. Mitochondria-targeted green fluorescent proteins: convenient tools for the study of organelle biogenesis in Saccharomyces cerevisiae. *Yeast (Chichester, England)*, 16(15), pp.1421–7.

Whitacre, J. et al., 2001. Generation of an isogenic collection of yeast actin mutants and identification of three interrelated phenotypes. *Genetics*, 157(2), pp.533–43.

Winder, S.J., Jess, T. & Ayscough, K.R., 2003. SCP1 encodes an actin-bundling protein in yeast. *The Biochemical journal*, 375(Pt 2), pp.287–95.

Winkler, A. et al., 2002. Heat Stress Activates the Yeast High-Osmolarity Glycerol Mitogen-Activated Protein Kinase Pathway , and Protein Tyrosine Phosphatases Are Essential under Heat Stress. , 1(2), pp.163–173.

Winter, D. et al., 1997. The complex containing actin-related proteins Arp2 and Arp3 is required for the motility and integrity of yeast actin patches. *Current biology : CB*, 7(7), pp.519–29.

Wloka, C. & Bi, E., 2012. Mechanisms of cytokinesis in budding yeast. *Cytoskeleton (Hoboken, N.J.)*, 69(10), pp.710–26.

Wolven, A.K. et al., 2000. In vivo importance of actin nucleotide exchange catalyzed by profilin. *The Journal of cell biology*, 150(4), pp.895–904.

Wong Sak Hoi, J. & Dumas, B., 2010. Ste12 and Ste12-like proteins, fungal transcription factors regulating development and pathogenicity. *Eukaryotic cell*, 9(4), pp.480–5.

Wu, Z. et al., 2004. A Model-Based Background Adjustment for Oligonucleotide Expression Arrays. *Journal of the American Statistical Association*, 99(468), pp.909–917.

Yang, H.-C. & Pon, L. a, 2002. Actin cable dynamics in budding yeast. *Proceedings of the National Academy of Sciences of the United States of America*, 99(2), pp.751–6.

Yuzyuk, T., Foehr, M. & Amberg, D., 2002. The MEK kinase Ssk2p promotes actin cytoskeleton recovery after osmotic stress. *Molecular biology of the cell*, 13(August), pp.2869–2880.

Zdanov, S., Klamt, F. & Shacter, E., 2010. Importance of cofilin oxidation for oxidant-induced apoptosis. *Cell cycle (Georgetown, Tex.)*, 9(9), pp.1675–7.